

Supplementary Materials for

Enhanced Ligand Discovery through Generative AI and Latent-Space Exploration: Application to the Mizoroki-Heck Reaction

Wenxin Lu^{1†}, Haote Li^{1†}, Jan Paul Menzel¹, Abbigayle E. Cuomo¹, Andrea M. Nikolic¹, H. Ray Kelly^{1,2}, Yu Shee¹, Sanil Sreekumar², Frederic Buono², Jinhua J. Song², Robert H. Crabtree¹, Victor S. Batista^{1*}, and Timothy R. Newhouse^{1*}

Corresponding authors: timothy.newhouse@yale.edu, victor.batista@yale.edu

Table of Contents:

General Information.....	2
Phosphine Ligand Sources.....	3
Additional Training and Model Specifications.....	4
Additional Optimization of Reaction Conditions	6
General Experimental Procedure for Pd-Catalyzed Mizoroki-Heck Reaction	7
Characterization of Products.....	8
Comparison of Different Methods for the Synthesis of N-Containing <i>t</i> -Butyl Acrylates	15
Unsuccessful Examples for Pd-Catalyzed Mizoroki-Heck Reaction	16
Computational Benchmarking	16
Computational Coordinates	17
NMR Spectra	20
References.....	57

General Information

General Experimental Procedures: All reactions were carried out under an inert nitrogen atmosphere with dry solvents under anhydrous conditions unless otherwise stated. All reactions were capped with a rubber septum or Teflon-coated silicon microwave cap unless otherwise stated. Stainless steel cannulas or syringes were used to transfer solvent, and air- and moisture-sensitive liquid reagents. Reactions were monitored by thin-layer chromatography (TLC) and carried out on 0.25 mm Merck silica gel plates (60F-254) using UV light as the visualizing agent. A basic solution of KMnO₄ was used as a developing reagent which was accompanied by 30–60 seconds of heating. SiliaFlash® P60 (40–63 µm, 230–400 mesh) silica gel purchased from SiliCycle Inc. was used for flash column chromatography.

Materials: All anhydrous reaction solvents were purchased from MilliporeSigma or taken from solvent purification system. MachinePhos A (**L1**) was prepared following a literature-reported procedure (42), and all of the other catalysts and ligands were purchased from Strem Chemicals or MilliporeSigma. *t*-Butyl acrylate (**2a**) and all aryl bromides were purchased from MilliporeSigma, TCI Chemicals, Fischer Scientific, or AmBeed. Unless otherwise stated, all reagents were used as received without further purification.

Instrumentation: All new compounds were characterized with ¹H NMR, ¹³C NMR, FT-IR (thin film), and HR-MS. Relevant ¹H and ¹³C NMR spectra can be found at the end of each experimental procedure. NMR spectra were recorded using Agilent DD2 400 MHz NMR spectrometer, Agilent DD2 500 MHz NMR spectrometer, or Agilent DD2 600 MHz NMR spectrometer. All ¹H NMR data are reported in δ units, parts per million (ppm), and were calibrated relative to the signals for residual chloroform (7.26 ppm) or tetramethylsilane (0.00 ppm) in deuteriochloroform (CDCl₃). All ¹³C NMR data are reported in ppm relative to CDCl₃ (77.2 ppm) and were obtained with proton decoupling unless otherwise stated. The following abbreviations or combinations thereof were used to explain the multiplicities: s = singlet, d = doublet, t = triplet, q = quartet, m = multiplet, and a = apparent. All IR spectra were taken on an FT-IR/Raman Thermo Nicolet 6700. High resolution mass spectra (HR-MS) were recorded on a Shimadzu 9030 Quadrupole Time-of-Flight mass spectrometer using ESI-TOF (electrospray ionization-time of flight).

Computational Details: All density functional theory (DFT) calculations were performed using the Gaussian 16 suite of programs (revision A3, 51). The B3LYP functional was used to investigate reaction pathways (52). Geometry optimizations for the ground states, transition states and products were performed with the LANL2DZ pseudopotential for palladium (Pd, 53), the 6-31G(d,p) (54) basis set for all other atoms and GD3 empirical dispersion (55). The stationary points are characterized via calculations of the analytical gradients and Hessians. Intermediates and transition states were identified by the observation of the correct number of imaginary eigenvalues in the Hessian matrix: zero (0) and one (1) respectively. To refine the results, single point energy calculations were performed on the gas-phase optimized structures. This was performed using the ωB97X-D (56) functional with the LANL2DZ pseudopotential for Pd and the 6-311++G(d,p) basis set for all other atoms. All quoted free energies are reported at 298.15 K in THF (ε(0) = 7.43, ε(∞) = 1.41) and were calculated via the SMD (57) continuum solvation model.

Data Processing and Training Procedure for KAE: In the initial procedure for dataset preparation for our Kernel-Elastic Autoencoder (KAE), each SMILES string underwent preprocessing whereby it was encapsulated between special start-of-sequence token "<SOS>" and end-of-sequence token "?". These tokens serve as indicators during model testing to signal the completion of translation. Subsequently, all characters within the training data were extracted and cataloged into a character-to-token dictionary, facilitating conversions from characters to tokens. A padding token was added to ensure uniformity in sequence lengths. A token-to-character

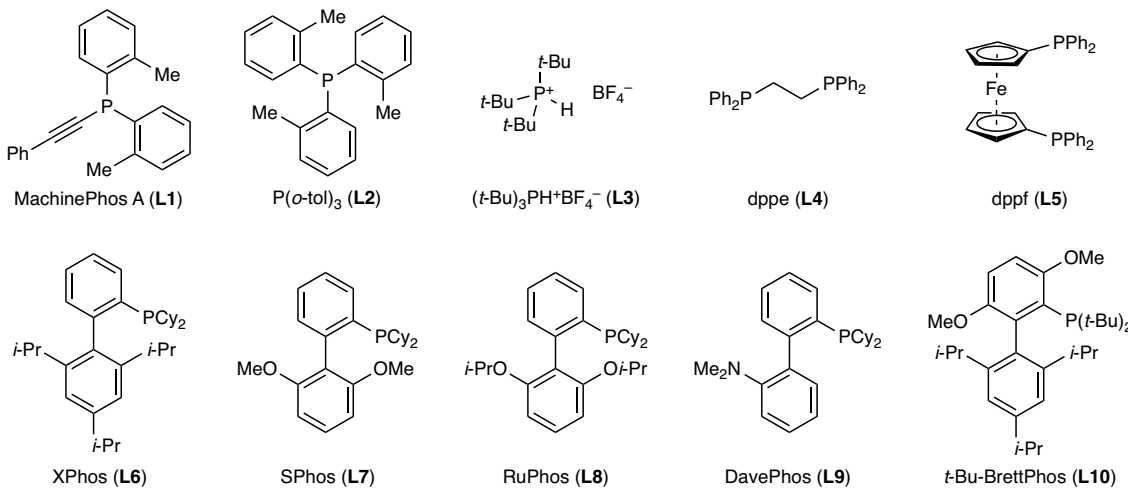
dictionary was generated to aid in the interpretation of model outputs. Leveraging the character-to-token dictionary, all SMILES representations were converted into their corresponding tokens. Given the Transformer architecture employed, uniformity in model inputs for batch training was ensured by applying padding to all sequences.

Post-padding, all sequences were standardized to a consistent length. Numerical values representing $\%V_{\text{bur}}$ and charge conditions were appended to the tokenized SMILES, thereby augmenting the sequence length with two additional dimensions. Subsequently, the tokenized dataset was partitioned into batches of size 128.

During training, molecules were randomly selected to form batches in each iteration. To mitigate biases and enhance model robustness, molecule sampling was re-normalized to ensure a balanced distribution of $\%V_{\text{bur}}$ conditions throughout training, particularly in regions with limited training data. Though molecules may be drawn repeatedly within the same epoch, the number of updates in one epoch is still defined as the number of data instances divided by the training batch size.

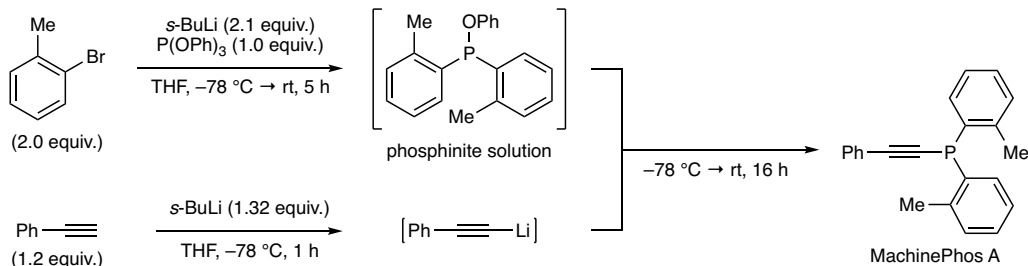
Our KAE model employs 128-dimensional embedding vectors, 1280 latent dimensions, 32 multi-head dimensions, 6-layers of encoders and decoders, a dropout rate of 0.1, and the ADAM optimizer with a learning rate of 0.0002. Training was conducted over 150 epochs to sufficiently capture the intricacies of the dataset and optimize relevant model performance.

Phosphine Ligand Sources



L2–L10: purchased from Strem Chemicals or MilliporeSigma and used as received.

MachinePhos A (L1): prepared according to a literature-reported procedure (42) with slight modification as follows.

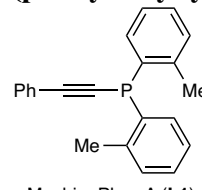


A flame-dried 100-mL round-bottomed flask was charged with a magnetic stir bar, connected to the manifold, and placed under a nitrogen atmosphere. After the flask was cooled to room temperature, 2-bromotoluene (1.2 mL, 10 mmol, 2.0 equiv.) and anhydrous THF (20 mL) were

added. The mixture was cooled to -78°C (dry ice/acetone bath), and *s*-butyllithium (1.4 M in cyclohexane, 7.5 mL, 10.5 mmol, 2.1 equiv.) was added dropwise. The cloudy yellow suspension was allowed to stir at -78°C for 1 hour, followed by the dropwise addition of triphenyl phosphite (1.3 mL, 5.0 mmol, 1.0 equiv.), which caused the solution to gradually turn orange and transparent. The mixture was warmed to room temperature over 5 hours.

To another flame-dried 100-mL round-bottomed flask charged with a magnetic stir bar was added phenylacetylene (0.66 mL, 6.0 mmol, 1.2 equiv.) and anhydrous THF (15 mL). The mixture was cooled to -78°C (dry ice/acetone bath), and *s*-butyllithium (1.4 M in cyclohexane, 4.7 mL, 6.6 mmol, 1.32 equiv.) was added dropwise. The brown suspension was allowed to stir at -78°C for 1 hour, followed by addition of the above-prepared phosphinite solution at -78°C . The resulting reaction mixture was warmed to room temperature, stirred for 16 hours, and quenched with water (*H₂* generated during the initial stages) followed by 4.0 M NaOH (5.0 mL, to remove phenol). The mixture was washed with diethyl ether (2 \times 20 mL), and the combined organic layers were washed with brine and dried over anhydrous Na₂SO₄. The organic solution was concentrated *in vacuo* to provide an amber oil, which was purified by flash column chromatography on silica gel (100% hexanes to 50:1 hexanes/CH₂Cl₂) to afford MachinePhos A (**L1**) as a colorless oil (1.02 g, 65% yield), which solidified to form a white solid after long-term standing.

(phenylethynyl)di-*o*-tolylphosphane (MachinePhos A, **L1**)


White solid. Yield: 65%. **R_f**: 0.47 (5:1 hexanes/CH₂Cl₂).
IR (neat): 3052 (m), 2920 (m), 2858 (w), 2155 (m), 1587 (m), 1486 (m), 1465 (m), 1273 (m), 1200 (m), 1129 (m), 1025 (m), 748 (s) cm⁻¹.
¹H NMR (400 MHz, CDCl₃): δ 7.63 – 7.56 (m, 2H), 7.54 – 7.48 (m, 2H), 7.36 – 7.31 (m, 3H), 7.31 – 7.27 (m, 2H), 7.22 (t, *J* = 6.8 Hz, 4H), 2.52 (s, 6H).
¹³C NMR (100 MHz, CDCl₃): δ 142.1 (d, *J* = 26.9 Hz), 133.2 (d, *J* = 6.0 Hz), 133.1 (d, *J* = 3.4 Hz), 131.9 (d, *J* = 1.8 Hz), 130.4 (d, *J* = 5.2 Hz), 129.4, 128.8, 128.4, 126.4 (d, *J* = 2.3 Hz), 123.2, 108.1 (d, *J* = 4.4 Hz), 85.4 (d, *J* = 7.2 Hz), 21.3 (d, *J* = 20.7 Hz).
³¹P NMR (162 MHz, CDCl₃): δ –47.3.
HRMS (ESI⁺) [M+H]⁺: Calc'd for C₂₂H₂₀P⁺: 315.1297 m/z, found: 315.1292 m/z.

Additional Training and Model Specifications

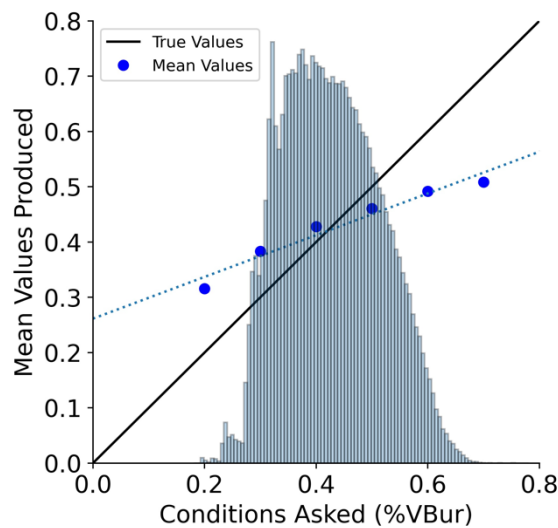


Fig. S1.

$\%V_{\text{bur}}$ -varying ligand generation with mean charge condition using KAE. At each asked condition, 1000 latent vectors were sampled. Only the unique (non-repeating) and novel (not in the training dataset) candidates were kept for further evaluation. These candidates were then optimized by GFN2-xTB to obtain their $\%V_{\text{bur}}$ the same way as the dataset was prepared. The figure shows correlation of the mean values of the obtained $\%V_{\text{bur}}$ vs the asked values.

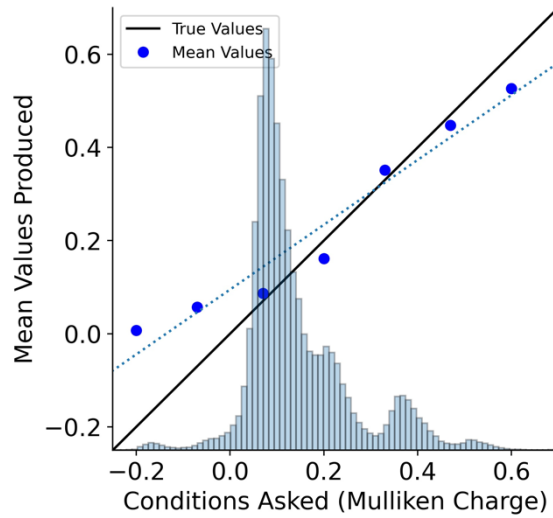


Fig. S2.

Charge-varying ligand generation with mean $\%V_{\text{bur}}$ condition using KAE. At each asked condition, 1000 latent vectors were sampled. Only the unique (non-repeating) and novel (not in the training dataset) candidates were kept for further evaluation. These candidates were then optimized by GFN2-xTB to obtain their Mulliken Charge. The figure shows correlation of the mean values of the calculated Mulliken Charge vs the asked values.

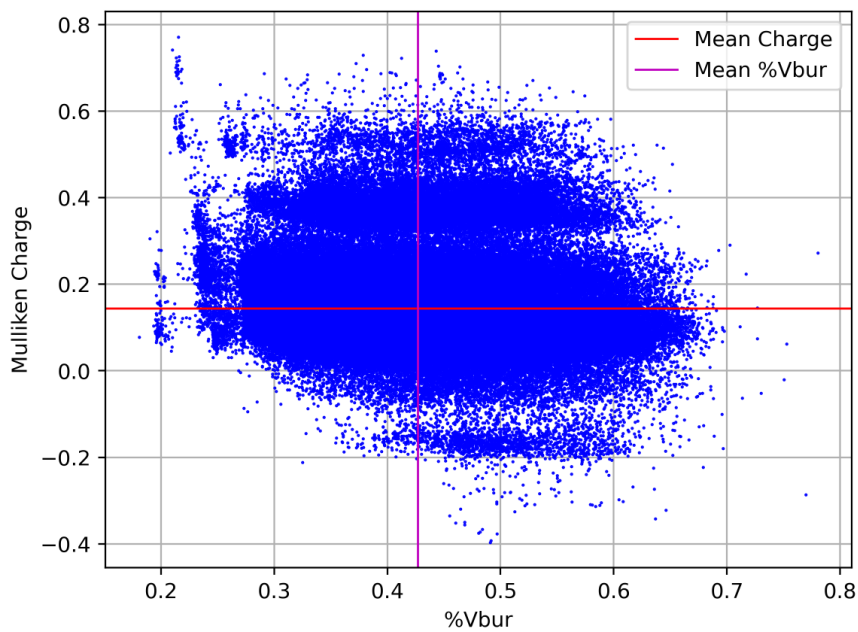
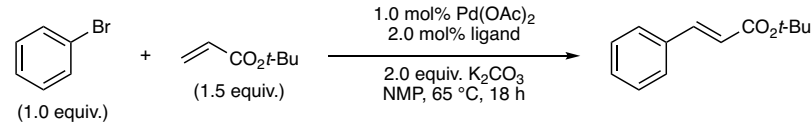


Fig. S3.

Mulliken Charge vs. $\%V_{bur}$ for each training data point. The mean charge and mean $\%V_{bur}$ values are labeled by red and magenta lines on the plot. The distribution shows less abundant data in the region for small charge and low $\%V_{bur}$ and for big charge with big $\%V_{bur}$.

Additional Optimization of Reaction Conditions

Table S1. Ligand screen. $^1\text{H-NMR}$ yield was determined using CH_2Br_2 as internal standard.



Entry	Ligand	Conversion of bromide	NMR yield
1	L1	25%	18%
2	L2	20%	13%
3	L3	11%	4%
4	L4	8%	2%
5	L5	5%	2%
6	L6	21%	10%
7	L7	12%	2%
8	L8	15%	10%
9	L9	<2%	trace
10	L10	11%	3%
11*	L1	60%	52%
12*†	L1	51%	trace
13*‡	L1	47%	trace

* 5.0 mol% of Pd(OAc)₂ and 10 mol% of **L1** were used as precatalyst.

† 1.0 equiv. AgNO₃ as additive.

‡ 1.0 equiv. AgOAc as additive.

Table S2. Base screen. ¹H-NMR yield was determined using CH₂Br₂ as internal standard.

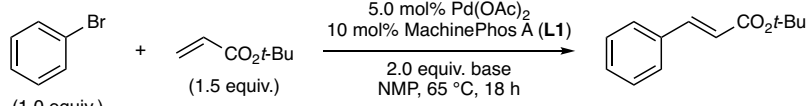
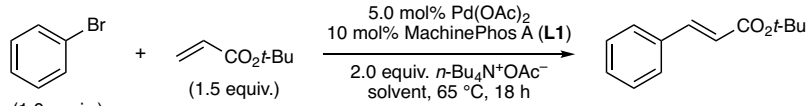
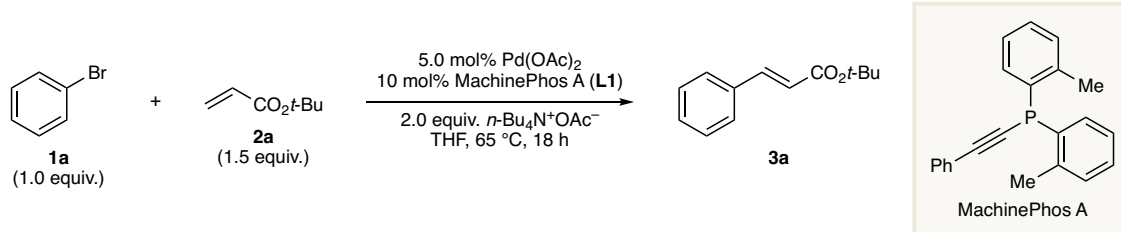
			
Entry	Base	Conversion of bromide	NMR yield
1	Na ₂ CO ₃	33%	11%
2	NaHCO ₃	40%	5%
3	KHCO ₃	26%	19%
4	Cs ₂ CO ₃	50%	3%
5	HCO ₂ Na	44%	21%
6	NaOAc	19%	8%
7	PhCO ₂ Na	23%	19%
8	NaOt-Bu	<2%	trace
9	NaOTMS	<2%	trace
10	Et ₃ N	30%	10%
11	DIPEA (Hünig's base)	35%	6%
12	<i>n</i> -Bu ₄ N ⁺ OAc ⁻	61%	58%

Table S3. Solvent screen. ¹H-NMR yield was determined using CH₂Br₂ as internal standard.

			
Entry	Solvent	Conversion of bromide	NMR yield
1	NMP	61%	58%
2	Toluene	58%	44%
3	THF	79%	64%
4	DME	51%	44%
5	1,4-Dioxane	53%	40%
6	MeCN	77%	20%
7	DMF	75%	51%

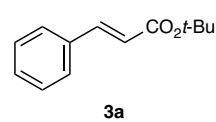
General Experimental Procedure for Pd-Catalyzed Mizoroki-Heck Reaction



To a flame-dried 10-mL microwave vial equipped with a magnetic stir bar was added Pd(OAc)₂ (1.1 mg, 0.005 mmol, 5.0 mol%), MachinePhos A (3.1 mg, 0.01 mmol, 10 mol%), and tetrabutylammonium acetate (60.3 mg, 0.2 mmol, 2.0 equiv.). The vial was capped, evacuated, and backfilled with N₂ (repeated three times). THF (0.5 mL) was added via syringe, and the solution was allowed to stir at room temperature for 20 min. A THF solution (0.5 mL) of bromobenzene **1a** (15.7 mg, 0.1 mmol, 1.0 equiv.) and *t*-butyl arylate **2a** (19.2 mg, 0.15 mmol, 1.5 equiv.) were added to the vial sequentially under N₂. The reaction vial was placed into a pre-heated 65 °C oil bath and allowed to stir for 18 hours. Upon completion, the reaction was quenched by addition of sat. aq. NH₄Cl (1.0 mL), diluted with diethyl ether (2.0 mL), and stirred at room temperature for 30 min. The mixture was passed through a short plug of celite, then eluted with Et₂O (3 × 8.0 mL). The combined eluent was dried over anhydrous Na₂SO₄ and concentrated *in vacuo* to a provide yellow oil, which was purified by flash column chromatography on silica gel (hexanes:ethyl acetate = 60:1) to afford **3a** as yellow oil (13.1 mg, 64% yield).

Characterization of Products

tert-Butyl cinnamate (**3a**)



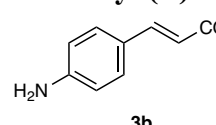
Yellow oil. Yield: 64%. R_f : 0.45 (20:1 hexanes/ethyl acetate).

¹H NMR (400 MHz, CDCl₃): δ 7.59 (d, *J* = 16.0 Hz, 1H), 7.54 – 7.47 (m, 2H), 7.39 – 7.34 (m, 3H), 6.37 (d, *J* = 16.0 Hz, 1H), 1.54 (s, 9H).

¹³C NMR (100 MHz, CDCl₃): δ 166.4, 143.7, 134.8, 130.1, 128.9, 128.1, 120.3, 80.6, 28.3.

The NMR data are consistent with the reported literature (58).

tert-Butyl (E)-3-(4-aminophenyl)acrylate (**3b**)



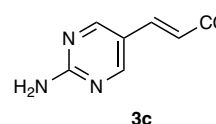
Brown solid. Yield: 66%. R_f : 0.54 (3:1 hexanes/ethyl acetate).

¹H NMR (400 MHz, CDCl₃): δ 7.49 (d, *J* = 16.0 Hz, 1H), 7.36 – 7.27 (m, 2H), 6.66 – 6.58 (m, 2H), 6.16 (d, *J* = 16.0 Hz, 1H), 3.94 (s, 2H), 1.52 (s, 9H).

¹³C NMR (100 MHz, CDCl₃): δ 167.2, 148.6, 143.9, 129.8, 125.0, 115.7, 114.9, 80.1, 28.4.

The NMR data are consistent with the reported literature (59).

tert-Butyl (E)-3-(2-aminopyrimidin-5-yl)acrylate (**3c**)



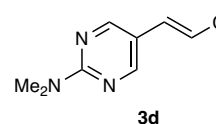
Pale yellow solid. Yield: 60%. R_f : 0.32 (1:1 hexanes/ethyl acetate).

¹H NMR (400 MHz, CDCl₃): δ 8.44 (s, 2H), 7.39 (d, *J* = 16.0 Hz, 1H), 6.27 (d, *J* = 16.0 Hz, 1H), 5.58 (br s, 2H), 1.51 (s, 9H).

¹³C NMR (100 MHz, CDCl₃): δ 166.1, 163.1, 157.9, 137.3, 119.1, 118.4, 80.9, 28.3.

The NMR data are consistent with the reported literature (60).

tert-Butyl (E)-3-(2-(dimethylamino)pyrimidin-5-yl)acrylate (**3d**)



Pale yellow solid. Yield: 68%. R_f : 0.47 (4:1 hexanes/ethyl acetate).

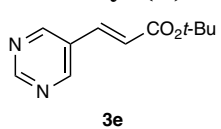
IR (neat): 2966 (m), 2928 (m), 1692 (s), 1609 (m), 1536 (m), 1363 (m), 1322 (m), 1143 (s) cm⁻¹.

¹H NMR (400 MHz, CDCl₃): δ 8.42 (s, 2H), 7.36 (d, *J* = 16.0 Hz, 1H), 6.18 (d, *J* = 16.0 Hz, 1H), 3.20 (s, 6H), 1.50 (s, 9H).

¹³C NMR (100 MHz, CDCl₃): δ 166.5, 162.1, 157.3, 138.2, 116.3, 116.2, 80.5, 37.3, 28.3.

HRMS (ESI⁺) [M+H]⁺: Calc'd for C₁₃H₂₀N₃O₂⁺: 250.1550 m/z, found: 250.1541 m/z.

tert-Butyl (E)-3-(pyrimidin-5-yl)acrylate (3e)

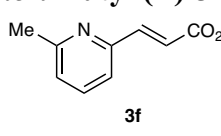

3e White solid. Yield: 51%. R_f : 0.45 (3:1 hexanes/ethyl acetate).
 $^1\text{H NMR}$ (400 MHz, CDCl_3): δ 9.15 (s, 1H), 8.84 (s, 2H), 7.48 (d, J = 16.0 Hz, 1H), 6.50 (d, J = 16.0 Hz, 1H), 1.51 (s, 9H).

$^{13}\text{C NMR}$ (100 MHz, CDCl_3): δ 165.0, 159.1, 155.6, 136.1, 128.7, 124.5, 81.6,

28.2.

The NMR data are consistent with the reported literature (61).

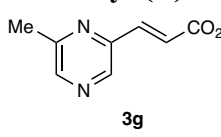
tert-Butyl (E)-3-(6-methylpyridin-2-yl)acrylate (3f)


3f Colorless oil. Yield: 62%. R_f : 0.48 (5:1 hexanes/ethyl acetate).
 $^1\text{H NMR}$ (400 MHz, CDCl_3): δ 7.56 (t, J = 7.6 Hz, 1H), 7.55 (d, J = 15.6 Hz, 1H), 7.21 (d, J = 7.6 Hz, 1H), 7.09 (d, J = 7.6 Hz, 1H), 6.79 (d, J = 15.6 Hz, 1H), 2.55 (s, 3H), 1.51 (s, 9H).

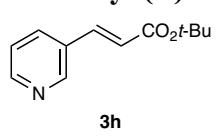
$^{13}\text{C NMR}$ (100 MHz, CDCl_3): δ 166.2, 158.9, 152.7, 142.7, 136.9, 124.2, 123.8, 121.0, 80.7, 28.3, 24.7.

The NMR data are consistent with the reported literature (62).

tert-Butyl (E)-3-(6-methylpyrazin-2-yl)acrylate (3g)

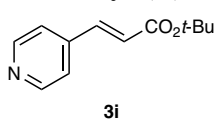

3g Colorless oil. Yield: 22%. R_f : 0.61 (2:1 hexanes/ethyl acetate).
IR (neat): 2976 (m), 2931 (m), 1705 (s), 1643 (m), 1393 (m), 1321 (m), 1140 (s), 1014 (m) cm^{-1} .
 $^1\text{H NMR}$ (400 MHz, CDCl_3): δ 8.44 (s, 1H), 8.39 (s, 1H), 7.55 (d, J = 15.6 Hz, 1H), 6.93 (d, J = 15.6 Hz, 1H), 2.57 (s, 3H), 1.53 (s, 9H).
 $^{13}\text{C NMR}$ (100 MHz, CDCl_3): δ 165.6, 154.1, 147.8, 144.9, 141.8, 138.9, 126.4, 81.2, 28.3, 21.8.
HRMS (ESI $^+$) [M+H] $^+$: Calc'd for $\text{C}_{12}\text{H}_{17}\text{N}_2\text{O}_2^+$: 221.1285 m/z, found: 221.1265 m/z.

tert-Butyl (E)-3-(pyridin-3-yl)acrylate (3h)


3h White solid. Yield: 63%. R_f : 0.44 (3:1 hexanes/ethyl acetate).
 $^1\text{H NMR}$ (400 MHz, CDCl_3): δ 8.69 (d, J = 2.4 Hz, 1H), 8.54 (dd, J = 4.8, 1.6 Hz, 1H), 7.78 (dt, J = 8.0, 2.0 Hz, 1H), 7.53 (d, J = 16.0 Hz, 1H), 7.28 (dd, J = 7.6, 4.4 Hz, 1H), 6.40 (d, J = 16.0 Hz, 1H), 1.50 (s, 9H).

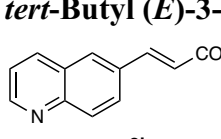
$^{13}\text{C NMR}$ (100 MHz, CDCl_3): 165.6, 150.7, 149.6, 139.8, 134.2, 130.5, 123.8, 122.5, 81.0, 28.2.
The NMR data are consistent with the reported literature (63).

tert-Butyl (E)-3-(pyridin-4-yl)acrylate (3i)


3i White solid. Yield: 60%. R_f : 0.32 (2:1 hexanes/ethyl acetate).
 $^1\text{H NMR}$ (400 MHz, CDCl_3): δ 8.64 – 8.57 (m, 2H), 7.47 (d, J = 16.0 Hz, 1H), 7.35 – 7.30 (m, 2H), 6.50 (d, J = 16.0 Hz, 1H), 1.52 (s, 9H).
 $^{13}\text{C NMR}$ (100 MHz, CDCl_3): δ 165.4, 150.5, 142.0, 140.7, 125.0, 121.9, 81.4, 28.2.

The NMR data are consistent with the reported literature (64).

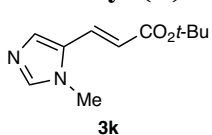
tert-Butyl (E)-3-(quinolin-6-yl)acrylate (3j)


3j Pale yellow solid. Yield: 78%. R_f : 0.28 (5:1 hexanes/ethyl acetate).
 $^1\text{H NMR}$ (400 MHz, CDCl_3): δ 8.88 (dd, J = 4.4, 1.6 Hz, 1H), 8.12 (dd, J = 8.4, 1.6 Hz, 1H), 8.05 (d, J = 8.8 Hz, 1H), 7.89 – 7.81 (m, 2H), 7.71 (d, J = 16.0 Hz, 1H), 7.38 (dd, J = 8.4, 4.4 Hz, 1H), 6.48 (d, J = 16.0 Hz, 1H), 1.53 (s, 9H).

^{13}C NMR (100 MHz, CDCl_3): δ 166.1, 151.2, 149.0, 142.6, 136.5, 133.0, 130.2, 129.0, 128.3, 127.4, 121.8, 121.7, 80.8, 28.3.

The NMR data are consistent with the reported literature (65).

tert-Butyl (*E*)-3-(1-methyl-1*H*-imidazol-5-yl)acrylate (3k)



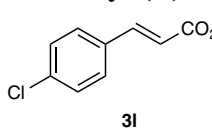
Pale yellow solid. Yield: 14%. R_f : 0.55 (15:1 $\text{CH}_2\text{Cl}_2/\text{MeOH}$).

^1H NMR (400 MHz, CDCl_3): δ 7.48 (s, 1H), 7.40 (d, $J = 16.0$ Hz, 1H), 7.40 (s, 1H), 6.18 (d, $J = 16.0$ Hz, 1H), 3.68 (s, 3H), 1.49 (s, 9H).

^{13}C NMR (100 MHz, CDCl_3): δ 166.4, 140.7, 131.9, 128.9, 128.6, 118.4, 80.8, 32.4, 28.2.

The NMR data are consistent with the reported literature (60).

tert-Butyl (*E*)-3-(4-chlorophenyl)acrylate (3l)



White solid. Yield: 94%. R_f : 0.50 (15:1 hexanes/ethyl acetate).

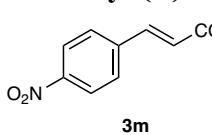
^1H NMR (400 MHz, CDCl_3): δ 7.52 (d, $J = 16.0$ Hz, 1H), 7.46 – 7.39 (m, 2H), 7.33 (d, $J = 8.4$ Hz, 2H), 6.33 (d, $J = 16.0$ Hz, 1H), 1.53 (s, 9H).

^{13}C NMR (100 MHz, CDCl_3): δ 166.2, 142.2, 135.9, 133.3, 129.2, 120.9,

80.8, 28.3.

The NMR data are consistent with the reported literature (66).

tert-Butyl (*E*)-3-(4-nitrophenyl)acrylate (3m)



Yellow solid. Yield: 87%. R_f : 0.41 (6:1 hexanes/ethyl acetate).

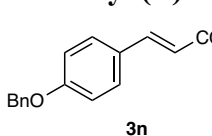
^1H NMR (400 MHz, CDCl_3): δ 8.26 – 8.19 (m, 2H), 7.67 – 7.63 (m, 2H), 7.60 (d, $J = 16.0$ Hz, 1H), 6.48 (d, $J = 16.0$ Hz, 1H), 1.54 (s, 9H).

^{13}C NMR (100 MHz, CDCl_3): δ 165.4, 148.5, 141.0, 140.7, 128.6, 124.7,

124.3, 81.5, 28.3.

The NMR data are consistent with the reported literature (67).

tert-Butyl (*E*)-3-(4-(benzyloxy)phenyl)acrylate (3n)



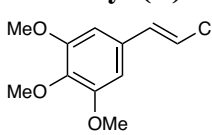
White solid. Yield: 35%. R_f : 0.54 (4:1 hexanes/ethyl acetate).

^1H NMR (400 MHz, CDCl_3): δ 7.55 (d, $J = 16.0$ Hz, 1H), 7.49 – 7.31 (m, 7H), 7.00 – 6.93 (m, 2H), 6.25 (d, $J = 16.0$ Hz, 1H), 5.09 (s, 2H), 1.54 (s, 9H).

^{13}C NMR (100 MHz, CDCl_3): δ 166.8, 160.4, 143.3, 136.6, 129.7, 128.8, 128.3, 127.7, 127.6, 117.9, 115.2, 80.4, 70.1, 28.3.

The NMR data are consistent with the reported literature (68).

tert-Butyl (*E*)-3-(3,4,5-trimethoxyphenyl)acrylate (3o)



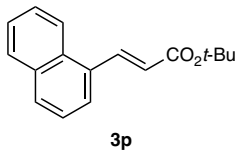
Light yellow solid. Yield: 23%. R_f : 0.36 (5:1 hexanes/ethyl acetate).

^1H NMR (400 MHz, CDCl_3): δ 7.48 (d, $J = 16.0$ Hz, 1H), 6.71 (s, 2H), 6.26 (d, $J = 16.0$ Hz, 1H), 3.86 (s, 9H), 1.52 (s, 9H).

^{13}C NMR (100 MHz, CDCl_3): δ 166.3, 153.4, 143.6, 139.8, 130.3, 119.5, 105.1, 80.6, 61.0, 56.2, 28.3.

The NMR data are consistent with the reported literature (69).

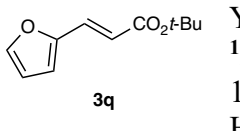
tert-Butyl (*E*)-3-(naphthalen-1-yl)acrylate (3p)



Pale yellow oil. Yield: 97%. R_f : 0.43 (20:1 hexanes/ethyl acetate).
 $^1\text{H NMR}$ (400 MHz, CDCl_3): δ 8.45 (d, $J = 15.6$ Hz, 1H), 8.24 – 8.18 (m, 1H), 7.91 – 7.85 (m, 2H), 7.77 – 7.72 (m, 1H), 7.61 – 7.50 (m, 2H), 7.48 (t, $J = 7.7$ Hz, 1H), 6.48 (d, $J = 15.6$ Hz, 1H), 1.60 (s, 9H).
 $^{13}\text{C NMR}$ (100 MHz, CDCl_3): δ 166.4, 140.7, 133.7, 132.1, 131.5, 130.3, 128.8, 126.8, 126.2, 125.6, 125.0, 123.6, 122.9, 80.7, 28.4.

The NMR data are consistent with the reported literature (63).

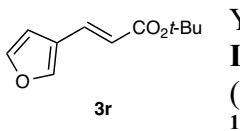
***tert*-Butyl (E)-3-(furan-2-yl)acrylate (3q)**



Yellow oil. Yield: 55%. R_f : 0.32 (20:1 hexanes/ethyl acetate).
 $^1\text{H NMR}$ (400 MHz, CDCl_3): δ 7.45 (d, $J = 1.6$ Hz, 1H), 7.32 (d, $J = 15.6$ Hz, 1H), 6.56 (d, $J = 3.2$ Hz, 1H), 6.44 (dd, $J = 3.2, 1.6$ Hz, 1H), 6.24 (d, $J = 15.6$ Hz, 1H), 1.51 (s, 9H).
 $^{13}\text{C NMR}$ (100 MHz, CDCl_3): δ 166.5, 151.3, 144.5, 130.2, 118.1, 114.2, 112.3, 80.5, 28.3.

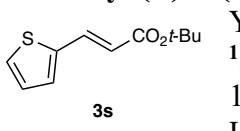
The NMR data are consistent with the reported literature (70).

***tert*-Butyl (E)-3-(furan-3-yl)acrylate (3r)**



Yellow oil. Yield: 70%. R_f : 0.28 (20:1 hexanes/ethyl acetate).
IR (neat): 2978 (w), 2933 (w), 1705 (s), 1640 (m), 1368 (m), 1253 (m), 1149 (s), 845 (m) cm^{-1} .
 $^1\text{H NMR}$ (400 MHz, CDCl_3): δ 7.63 – 7.59 (m, 1H), 7.46 (d, $J = 16.0$ Hz, 1H), 7.41 (d, $J = 2.0$ Hz, 1H), 6.56 (d, $J = 2.0$ Hz, 1H), 6.09 (d, $J = 16.0$ Hz, 1H), 1.51 (s, 9H).
 $^{13}\text{C NMR}$ (100 MHz, CDCl_3): δ 166.4, 144.4, 144.2, 133.6, 122.8, 120.1, 107.6, 80.5, 28.3.
HRMS (ESI $^+$) [M+H] $^+$: Calc'd for $\text{C}_{11}\text{H}_{15}\text{O}_3^+$: 195.1016 m/z, found: 195.1002 m/z.

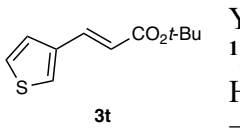
***tert*-Butyl (E)-3-(thiophen-2-yl)acrylate (3s)**



Yellow oil. Yield: 42%. R_f : 0.32 (20:1 hexanes/ethyl acetate).
 $^1\text{H NMR}$ (400 MHz, CDCl_3): δ 7.68 (d, $J = 15.6$ Hz, 1H), 7.33 (d, $J = 5.2$ Hz, 1H), 7.21 (d, $J = 3.6$ Hz, 1H), 7.03 (dd, $J = 5.2, 3.6$ Hz, 1H), 6.17 (d, $J = 15.6$ Hz, 1H), 1.52 (s, 9H).
 $^{13}\text{C NMR}$ (100 MHz, CDCl_3): δ 166.2, 139.9, 136.1, 130.5, 128.1, 128.1, 119.2, 80.6, 28.3.

The NMR data are consistent with the reported literature (71).

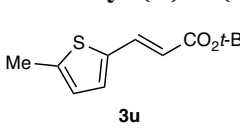
***tert*-Butyl (E)-3-(thiophen-3-yl)acrylate (3t)**



Yellow oil. Yield: 17%. R_f : 0.28 (20:1 hexanes/ethyl acetate).
 $^1\text{H NMR}$ (400 MHz, CDCl_3): δ 7.57 (d, $J = 16.0$ Hz, 1H), 7.45 (dd, $J = 2.8, 1.2$ Hz, 1H), 7.32 (dd, $J = 5.2, 2.8$ Hz, 1H), 7.27 (dd, $J = 5.2, 1.2$ Hz, 1H), 6.19 (d, $J = 16.0$ Hz, 1H), 1.52 (s, 9H).
 $^{13}\text{C NMR}$ (100 MHz, CDCl_3): δ 166.7, 137.9, 137.2, 127.6, 126.9, 125.3, 120.0, 80.6, 28.3.

The NMR data are consistent with the reported literature (71).

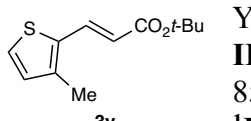
***tert*-Butyl (E)-3-(5-methylthiophen-2-yl)acrylate (3u)**



Pale yellow oil. Yield: 37%. R_f : 0.48 (15:1 hexanes/ethyl acetate).
 $^1\text{H NMR}$ (400 MHz, CDCl_3): δ 7.59 (d, $J = 15.6$ Hz, 1H), 7.00 (d, $J = 3.6$ Hz, 1H), 6.70 – 6.66 (m, 1H), 6.02 (d, $J = 15.6$ Hz, 1H), 2.48 (s, 3H), 1.51 (s, 9H).
 $^{13}\text{C NMR}$ (100 MHz, CDCl_3): δ 166.5, 143.5, 137.9, 136.6, 131.3, 126.5, 117.6, 80.4, 28.3, 15.9.

The NMR data are consistent with the reported literature (72).

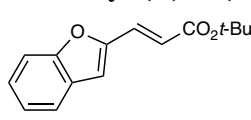
tert-Butyl (E)-3-(3-methylthiophen-2-yl)acrylate (3v)

 Yellow oil. Yield: 32%. R_f : 0.48 (15:1 hexanes/ethyl acetate).
IR (neat): 2977 (m), 2928 (w), 1698 (s), 1617 (s), 1366 (m), 1281 (m), 1141 (s), 851 (m) cm⁻¹.

3v **¹H NMR (400 MHz, CDCl₃):** δ 7.76 (d, J = 15.6 Hz, 1H), 7.22 (d, J = 5.2 Hz, 1H), 6.85 (d, J = 5.2 Hz, 1H), 6.11 (d, J = 15.6 Hz, 1H), 2.32 (s, 3H), 1.52 (s, 9H).

¹³C NMR (100 MHz, CDCl₃): δ 166.7, 140.9, 134.7, 133.9, 131.2, 126.6, 118.0, 80.5, 28.3, 14.2.
HRMS (EI⁺) [M]⁺: Calc'd for C₁₂H₁₆O₂S⁺: 224.0866 m/z, found: 224.0853 m/z.

tert-Butyl (E)-3-(benzofuran-2-yl)acrylate (3w)

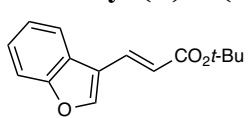
 White solid. Yield: 94%. R_f : 0.43 (20:1 hexanes/ethyl acetate).
IR (neat): 2931 (w), 1689 (s), 1637 (m), 1450 (m), 1370 (m), 1290 (m), 1236 (s), 1039 (m) cm⁻¹.

3w **¹H NMR (400 MHz, CDCl₃):** δ 7.60 – 7.55 (m, 1H), 7.49 – 7.41 (m, 2H), 7.37 – 7.31 (m, 1H), 7.26 – 7.20 (m, 1H), 6.89 (s, 1H), 6.53 (d, J = 15.6 Hz, 1H), 1.55 (s, 9H).

¹³C NMR (100 MHz, CDCl₃): δ 166.1, 155.6, 152.7, 130.4, 128.5, 126.3, 123.3, 121.8, 121.2, 111.5, 110.6, 80.8, 28.3.

HRMS (EI⁺) [M]⁺: Calc'd for C₁₅H₁₆O₃⁺: 244.1094 m/z, found: 244.1082 m/z.

tert-Butyl (E)-3-(benzofuran-3-yl)acrylate (3x)

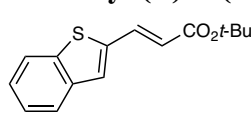
 Light yellow solid. Yield: 54%. R_f : 0.40 (20:1 hexanes/ethyl acetate).
IR (neat): 3136 (m), 1703 (s), 1638 (s), 1450 (s), 1316 (m), 1249 (s), 1140 (m), 1080 (m) cm⁻¹.

3x **¹H NMR (400 MHz, CDCl₃):** δ 7.89 – 7.82 (m, 2H), 7.69 (d, J = 16.0 Hz, 1H), 7.56 – 7.49 (m, 1H), 7.42 – 7.29 (m, 2H), 6.50 (d, J = 16.0 Hz, 1H), 1.55 (s, 9H).

¹³C NMR (100 MHz, CDCl₃): δ 166.6, 156.2, 147.6, 133.5, 125.4, 125.0, 123.8, 121.2, 120.5, 118.0, 112.1, 80.7, 28.4.

HRMS (EI⁺) [M]⁺: Calc'd for C₁₅H₁₆O₃⁺: 244.1094 m/z, found: 244.1081 m/z.

tert-Butyl (E)-3-(benzo[b]thiophen-2-yl)acrylate (3y)

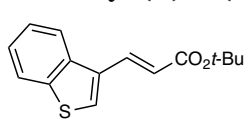
 White solid. Yield: 72%. R_f : 0.43 (20:1 hexanes/ethyl acetate).
IR (neat): 1708 (s), 1627 (s), 1364 (m), 1316 (m), 1299 (m), 1256 (m), 1141 (s), 978 (m) cm⁻¹.

3y **¹H NMR (400 MHz, CDCl₃):** δ 7.82 – 7.71 (m, 3H), 7.42 (s, 1H), 7.40 – 7.31 (m, 2H), 6.24 (d, J = 15.6 Hz, 1H), 1.55 (s, 9H).

¹³C NMR (100 MHz, CDCl₃): δ 165.9, 140.2, 139.9, 139.7, 136.7, 128.3, 126.1, 124.9, 124.4, 122.5, 121.6, 80.9, 28.3.

HRMS (EI⁺) [M]⁺: Calc'd for C₁₅H₁₆O₂S⁺: 260.0866 m/z, found: 260.0851 m/z.

tert-Butyl (E)-3-(benzo[b]thiophen-3-yl)acrylate (3z)

 Light yellow oil. Yield: 33%. R_f : 0.40 (20:1 hexanes/ethyl acetate).
IR (neat): 3050 (w), 2928 (w), 1698 (s), 1617 (s), 1366 (m), 1281 (m), 1141 (s), 851 (m) cm⁻¹.

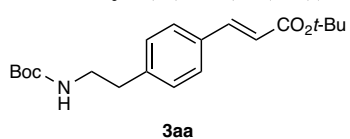
3z **¹H NMR (400 MHz, CDCl₃):** δ 8.05 – 7.99 (m, 1H), 7.92 – 7.84 (m, 2H), 7.71 (s, 1H), 7.49 – 7.43 (m, 1H), 7.42 – 7.37 (m, 1H), 6.48 (d, J = 16.0 Hz, 1H), 1.57 (s, 9H).

¹³C NMR (100 MHz, CDCl₃): δ 166.6, 140.6, 137.3, 135.4, 131.9, 127.6,

125.1, 125.0, 123.1, 122.2, 120.8, 80.7, 28.4.

The NMR data are consistent with the reported literature (60).

tert-Butyl (E)-3-(4-(2-((tert-butoxycarbonyl)amino)ethyl)phenyl)acrylate (3aa)



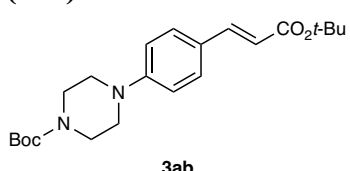
Pale yellow oil. Yield: 41%. R_f : 0.49 (4:1 hexanes/ethyl acetate).
IR (neat): 3362 (br), 2976 (m), 2933 (m), 1694 (s), 1635 (m), 1511 (m), 1366 (m), 1145 (m) cm⁻¹.

¹H NMR (400 MHz, CDCl₃): δ 7.55 (d, J = 16.0 Hz, 1H), 7.44 (d, J = 8.0 Hz, 2H), 7.19 (d, J = 8.0 Hz, 2H), 6.33 (d, J = 16.0 Hz, 1H), 4.57 (s, 1H), 3.37 (q, J = 6.8 Hz, 2H), 2.80 (t, J = 6.8 Hz, 2H), 1.52 (s, 9H), 1.42 (s, 9H).

¹³C NMR (100 MHz, CDCl₃): δ 166.5, 155.9, 143.4, 141.4, 133.0, 129.4, 128.3, 119.8, 80.6, 79.4, 41.7, 36.2, 28.5, 28.3.

HRMS (ESI⁺) [M+H]⁺: Calc'd for C₂₀H₃₀NO₄⁺: 348.2169 m/z, found: 348.2153 m/z.

tert-Butyl (E)-4-(4-(3-(tert-butoxy)-3-oxoprop-1-en-1-yl)phenyl)piperazine-1-carboxylate (3ab)



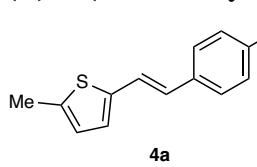
Light yellow solid. Yield: 12%. R_f : 0.50 (4:1 hexanes/ethyl acetate).
IR (neat): 2930 (w), 1687 (s), 1599 (s), 1478 (m), 1451 (m), 1364 (m), 1286 (m), 1141 (m) cm⁻¹.

¹H NMR (400 MHz, CDCl₃): δ 7.51 (d, J = 16.0 Hz, 1H), 7.45 – 7.38 (m, 2H), 6.91 – 6.82 (m, 2H), 6.21 (d, J = 16.0 Hz, 1H), 3.57 (t, J = 5.2 Hz, 4H), 3.22 (t, J = 5.2 Hz, 4H), 1.52 (s, 9H), 1.48 (s, 9H).

¹³C NMR (100 MHz, CDCl₃): δ 167.0, 154.8, 152.2, 143.5, 129.5, 125.9, 116.8, 115.5, 80.2, 80.2, 48.2, 43.4 (broad signal with low intensity due to Boc-rotamer), 28.5, 28.4.

HRMS (ESI⁺) [M+H]⁺: Calc'd for C₂₂H₃₃N₂O₄⁺: 389.2435 m/z, found: 389.2417 m/z.

(E)-2-(4-Methoxystyryl)-5-methylthiophene (4a)



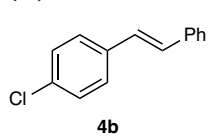
Pale yellow solid. Yield: 47%. R_f : 0.45 (6:1 hexanes/ethyl acetate).

¹H NMR (400 MHz, CDCl₃): δ 7.43 – 7.37 (m, 2H), 7.04 (d, J = 16.0 Hz, 1H), 6.93 – 6.87 (m, 2H), 6.83 (d, J = 3.6 Hz, 1H), 6.78 (d, J = 16.0 Hz, 1H), 6.66 (dd, J = 3.6, 1.2 Hz, 1H), 3.83 (s, 3H), 2.50 (s, 3H).

¹³C NMR (100 MHz, CDCl₃): δ 159.2, 141.3, 138.7, 130.1, 127.5, 126.8, 125.8, 125.8, 120.3, 114.2, 55.4, 15.7.

The NMR data are consistent with the reported literature (73).

(E)-1-Chloro-4-styrylbenzene (4b)



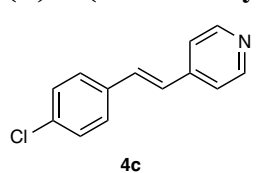
White solid. Yield: 47%. R_f : 0.61 (100% hexanes).

¹H NMR (400 MHz, CDCl₃): δ 7.51 (d, J = 7.6 Hz, 2H), 7.44 (d, J = 8.0 Hz, 2H), 7.41 – 7.24 (m, 5H), 7.07 (ABd, J_A = J_B = 16.4 Hz, 2H).

¹³C NMR (100 MHz, CDCl₃): δ 137.1, 136.0, 133.3, 129.4, 129.0, 128.9, 128.0, 127.8, 127.5, 126.7.

The NMR data are consistent with the reported literature (74).

(E)-4-(4-Chlorostyryl)pyridine (4c)



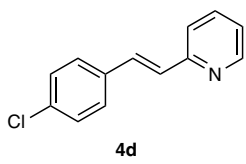
Yellow solid. Yield: 42%. R_f : 0.53 (3:1 hexanes/ethyl acetate).

¹H NMR (400 MHz, CDCl₃): δ 8.58 (d, J = 6.0 Hz, 2H), 7.50 – 7.44 (m, 2H), 7.39 – 7.33 (m, 4H), 7.25 (d, J = 16.4 Hz, 1H), 6.99 (d, J = 16.4 Hz, 1H).

¹³C NMR (100 MHz, CDCl₃): δ 150.3, 144.4, 134.8, 134.6, 132.0, 129.2, 128.3, 126.7, 121.0.

The NMR data are consistent with the reported literature (75).

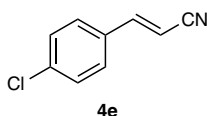
(E)-2-(4-Chlorostyryl)pyridine (4d)



Yellow solid. Yield: 80%. R_f : 0.45 (3:1 hexanes/ethyl acetate).
 $^1\text{H NMR}$ (400 MHz, CDCl_3): δ 8.63 – 8.56 (m, 1H), 7.65 (td, J = 7.6, 1.6 Hz, 1H), 7.59 (d, J = 16.0 Hz, 1H), 7.52 – 7.46 (m, 2H), 7.37 – 7.29 (m, 3H), 7.18 – 7.11 (m, 1H), 7.12 (d, J = 16.0 Hz, 1H).
 $^{13}\text{C NMR}$ (100 MHz, CDCl_3): δ 155.3, 149.8, 136.7, 135.3, 134.1, 131.5, 129.0, 128.6, 128.4, 122.4, 122.4.

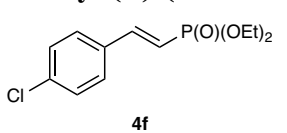
The NMR data are consistent with the reported literature (76).

(E)-3-(4-Chlorophenyl)acrylonitrile (4e)



Yellow solid. Yield: 74% (*E*-isomer). R_f : 0.58 (10:1 hexanes/ethyl acetate).
 $^1\text{H NMR}$ (400 MHz, CDCl_3): δ 7.42 – 7.32 (m, 5H), 5.86 (d, J = 16.4 Hz, 1H).
 $^{13}\text{C NMR}$ (100 MHz, CDCl_3): δ 149.2, 137.4, 132.1, 129.6, 128.7, 117.9, 97.1.
The NMR data are consistent with the reported literature (76).

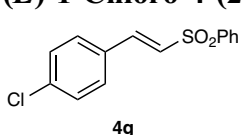
Diethyl (E)-(4-chlorostyryl)phosphonate (4f)



Colorless oil. Yield: 41%. R_f : 0.27 (1:1 hexanes/ethyl acetate).
 $^1\text{H NMR}$ (400 MHz, CDCl_3): δ 7.51 – 7.36 (m, 3H), 7.34 (d, J = 8.4 Hz, 2H), 6.22 (t, J = 17.2 Hz, 1H), 4.21 – 4.03 (m, 4H), 1.34 (t, J = 7.2 Hz, 6H).
 $^{13}\text{C NMR}$ (100 MHz, CDCl_3): δ 147.3 (d, J = 6.8 Hz), 136.2, 133.5 (d, J = 23.7 Hz), 129.2, 129.0, 114.9 (d, J = 191.6 Hz), 62.0 (d, J = 5.5 Hz), 16.5 (d, J = 6.5 Hz).
 $^{31}\text{P NMR}$ (162 MHz, CDCl_3): δ 18.9.

The NMR data are consistent with the reported literature (77).

(E)-1-Chloro-4-(2-(phenylsulfonyl)vinyl)benzene (4g)



White solid. Yield: 55%. R_f : 0.71 (2:1 hexanes/ethyl acetate).
 $^1\text{H NMR}$ (400 MHz, CDCl_3): δ 7.98 – 7.90 (m, 2H), 7.66 – 7.58 (m, 2H), 7.54 (dd, J = 8.4, 6.8 Hz, 2H), 7.43 – 7.37 (m, 2H), 7.34 (d, J = 8.4 Hz, 2H), 6.86 (d, J = 15.2 Hz, 1H).
 $^{13}\text{C NMR}$ (100 MHz, CDCl_3): δ 141.0, 140.5, 137.3, 133.6, 130.9, 129.8, 129.5, 129.4, 127.9, 127.7.

The NMR data are consistent with the reported literature (78).

Comparison of Different Methods for the Synthesis of N-Containing *t*-Butyl Acrylates

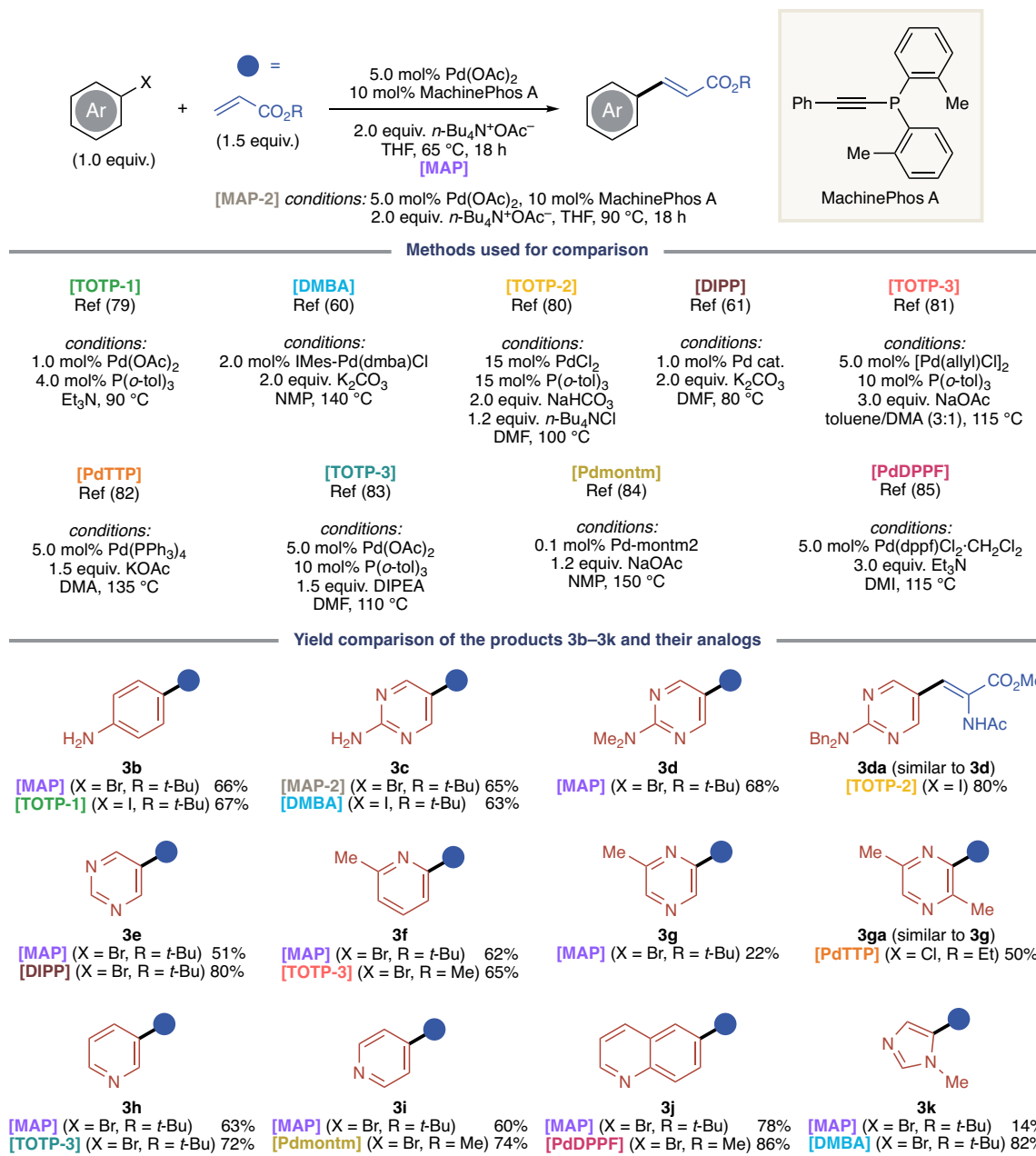


Fig. S4.

Select examples of aniline and *N*-containing heterocyclic substrates, whose yields are reported in literatures utilizing the Mizoroki-Heck reaction. Since there is no report on the synthesis of identical **3d** and **3g**, **3da** and **3ga** are shown as the products similar to **3d** and **3g**, respectively.

Unsuccessful Examples for Pd-Catalyzed Mizoroki-Heck Reaction

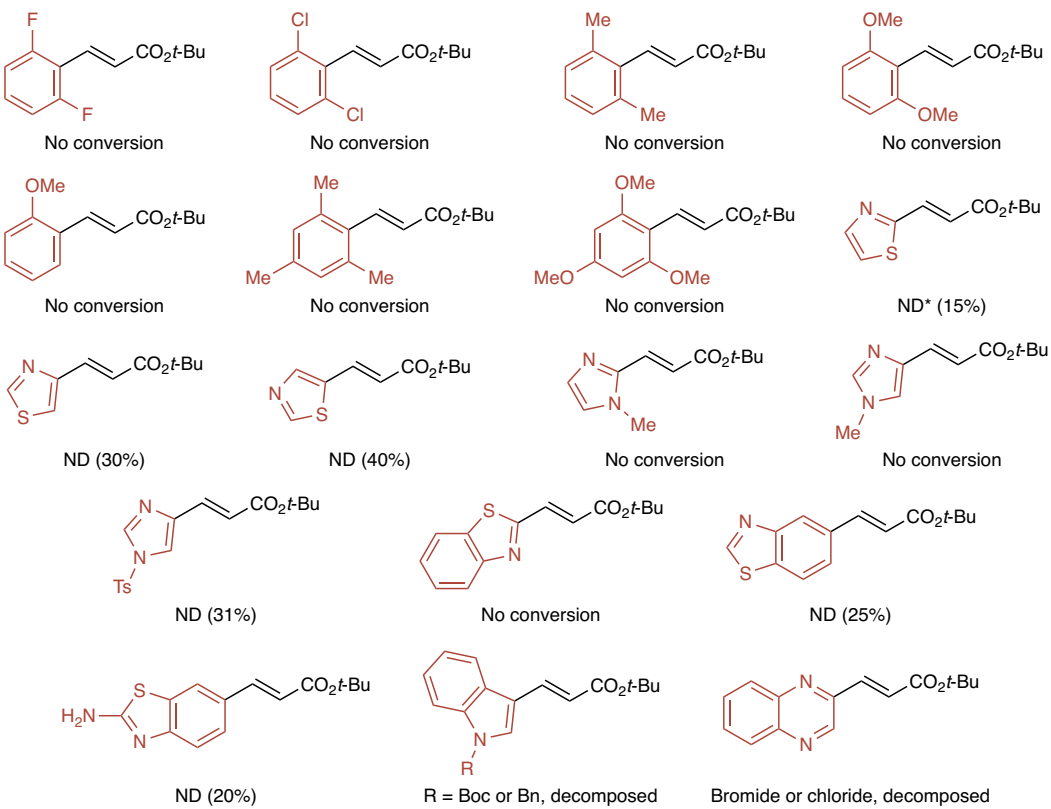


Fig. S5.

Select examples of aryl halides that failed to participate in the Mizoroki-Heck reaction to afford the products. Values in parentheses are conversion of halide determined by analysis of ^1H NMR spectra of unpurified mixtures, using CH_2Br_2 as the internal standard. *ND: The anticipated product is not detected by ^1H NMR in unpurified mixtures.

Computational Benchmarking

Calculations for the alkene associative adduct, migratory insertion transition state, and migratory insertion products were evaluated for a variety of functionals (B3LYP (52), PBE (86), PBE0 (87), M06 (52), M06-2X (52), and ω B97X-D (56)). The ΔG^\ddagger for the migratory TS, product energy, P–C–C bond angle of the alkyne in the TS and the product, as well as the Pd–C1(alkyne) and Pd–C2(alkyne) distance were compared in the product as well. All values for energy and geometry comparisons were relatively consistent across all of the test functionals. M06-D3 saw the largest variation when compared to the other functionals, and was therefore not considered further for this DFT study.

Table S4.

Geometry and energy comparisons of various DFT functionals and dispersion corrections for the alkene association adduct, migratory insertion TS, and migratory insertion product.

Functional	Basis Set (non-heavy)	Basis Set (Pd)	ΔG^\ddagger	Product Energy	P-C-C (TS)	P-C-C (Pdt)	Pd-C1 (Pdt)	Pd-C2 (Pdt)
B3LYP-D3BJ	6-31G(d,p)	LANL2DZ	11.70	-14.84	169.35	159.75	2.73	3.25
B3LYP-D3BJ	6-31G(d,p)	Def2TZVP	11.33	-14.62	169.66	160.10	2.71	3.24
B3LYP-D3BJ	Def2TZVP	Def2TZVP	11.90	-13.76	171.69	161.92	2.72	3.30
PBE-D2	6-31G(d,p)	LANL2DZ	11.69	-14.50	168.85	160.84	2.70	3.24
PBE0-D3BJ	6-31G(d,p)	LANL2DZ	11.32	-14.16	170.06	160.06	2.67	3.17
M06-D3	6-31G(d,p)	LANL2DZ	8.72	-16.94	169.87	158.71	2.68	3.16
M06-2X-D3	6-31G(d,p)	LANL2DZ	11.62	-13.46	169.06	159.86	2.70	3.17
ω B97-XD	6-31G(d,p)	LANL2DZ	10.46	-14.40	170.64	160.24	2.74	3.26

Computational Coordinates

Cationic Oxidative Addition Adduct

Zero-point correction = 0.424321 (Hartree/Particle)
 Zero-point correction = 0.430785 (Hartree/Particle)
 Thermal correction to Energy = 0.459768
 Thermal correction to Enthalpy = 0.460712
 Thermal correction to Gibbs Free Energy = 0.365169
 Sum of electronic and zero-point Energies = -1548.986750
 Sum of electronic and thermal Energies = -1548.957767
 Sum of electronic and thermal Enthalpies = -1548.956823
 Sum of electronic and thermal Free Energies= -1549.052366
 E(RwB97XD) = -1549.21572928

Pd	-0.64525700	0.48309500	-1.34590800
P	1.67119800	0.18218600	-0.47995500
C	2.62852000	-1.34477500	-0.66050600
C	2.99865800	-1.66682300	-1.97647300
C	3.00324600	-2.17338400	0.42332200
C	3.75486500	-2.80620500	-2.23787200
H	2.69513200	-1.01895600	-2.79370800
C	3.75946200	-3.31306200	0.12845000
C	4.13342300	-3.62923000	-1.17828400
H	4.04332500	-3.04673200	-3.25537100
H	4.06121800	-3.96434800	0.94324000
H	4.72244700	-4.52123200	-1.36616500
C	2.66316400	1.43282400	0.39444600
C	2.11627500	2.69835900	0.70743400
C	4.01094800	1.14969800	0.66295400
C	2.95306900	3.63476100	1.32215200
C	4.82241600	2.10534800	1.26925800
H	4.42542000	0.18420800	0.39527700
C	4.28879400	3.34845000	1.60402600
H	2.54854200	4.60985100	1.57641500
H	5.86289200	1.87778400	1.47509600
H	4.91219300	4.10082600	2.07606600
C	0.27323200	-0.22857900	0.53428600
C	-0.85176100	-0.46675200	1.00698400
C	-2.04322900	-0.85974600	1.66644000
C	-2.31912300	-2.23281500	1.82580500
C	-2.96285400	0.10592000	2.12125000
C	-3.50100400	-2.62774000	2.44272000
C	-4.13980600	-0.30371900	2.73223300
H	-2.75254300	1.15831900	1.96934900
C	-4.41018300	-1.66718800	2.89312900
H	-3.71547800	-3.68339500	2.57022600
H	-4.85213300	0.43649700	3.08029600
H	-5.33376300	-1.98057100	3.36884900
C	0.68262100	3.06288900	0.41285800
H	-0.01632900	2.49540000	1.03658000
H	0.50725600	4.12497400	0.59522900
H	0.42527200	2.86271500	-0.63666100
C	2.60599700	-1.88874900	1.84980600
H	2.74694400	-0.83800700	2.11630000
H	1.55098700	-2.13004700	2.02074400
H	3.19785000	-2.49265400	2.54050600
H	-1.60742500	-2.96739800	1.46461800
C	-2.62161100	0.51547400	-1.26093900
C	-3.19850100	1.78241500	-1.19748300
C	-3.37222800	-0.64768800	-1.40430400
H	-2.60260900	2.67360800	-1.01676300

H	-2.90815900	-1.62895500	-1.37596700
C	-4.75205400	-0.52269600	-1.59120600
H	-5.35558800	-1.41360100	-1.73452600
C	-4.58219300	1.88855400	-1.38766000
H	-5.05134300	2.86735700	-1.36789300
C	-5.35094500	0.73986100	-1.58038500
H	-6.42545300	0.82681000	-1.70531600

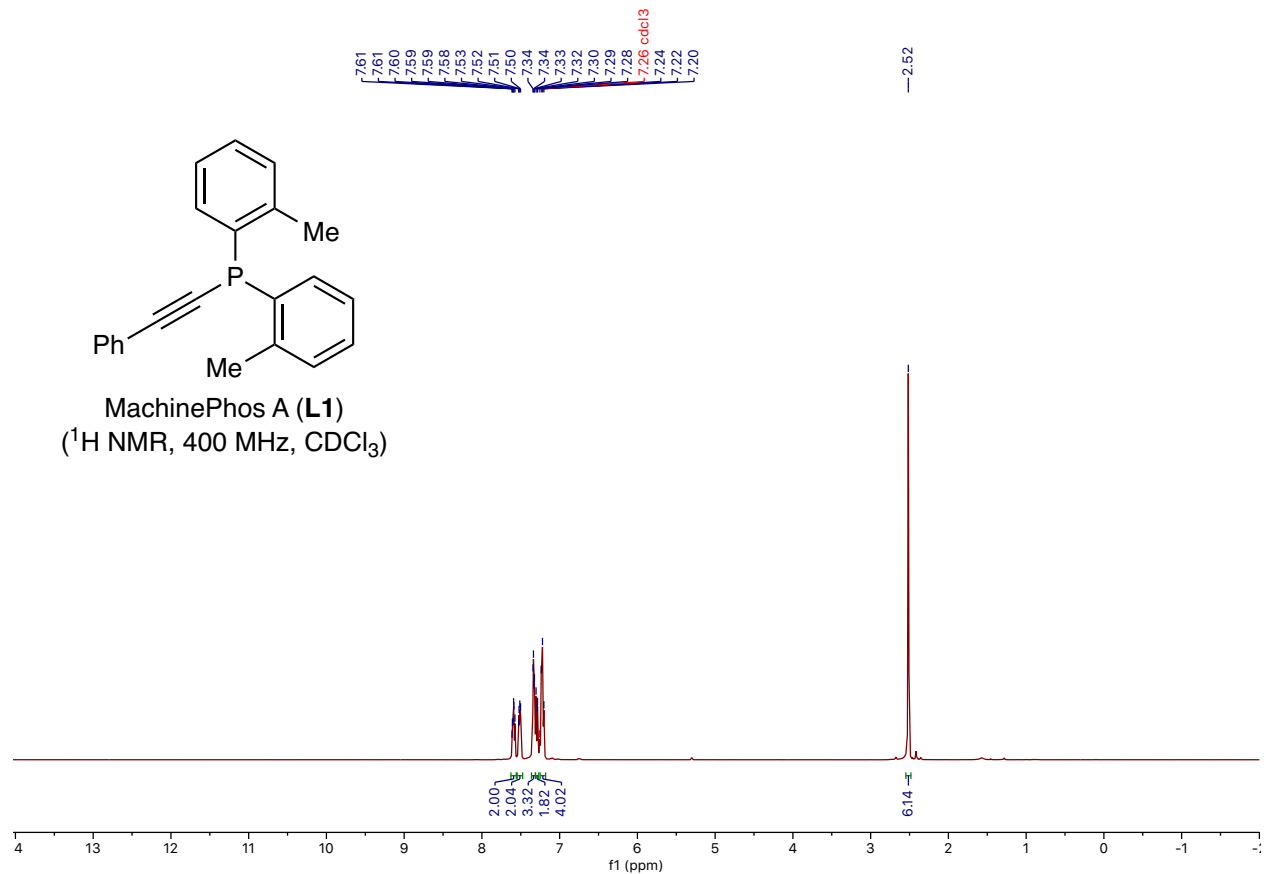
Neutral Oxidative Addition Adduct

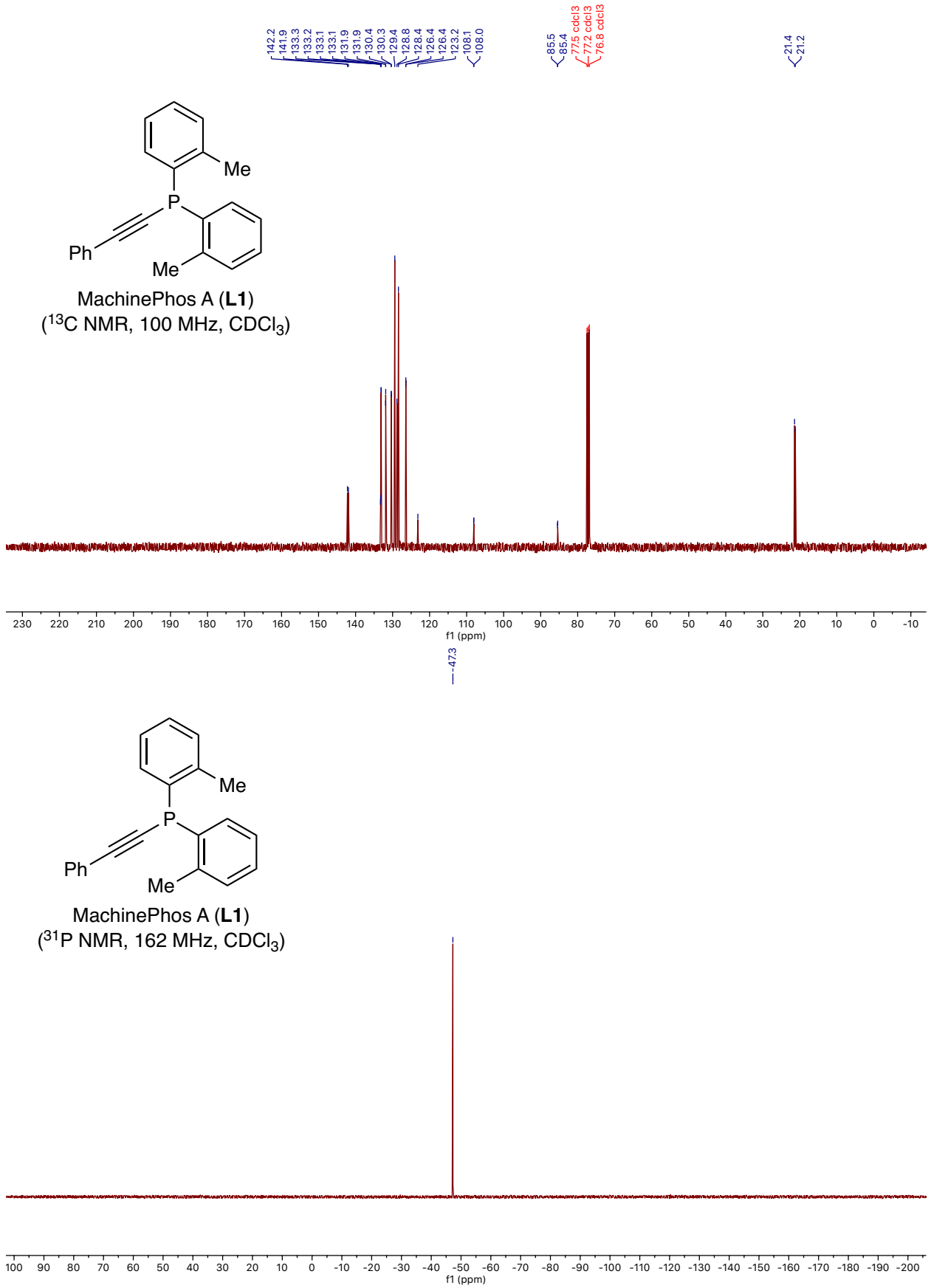
Zero-point correction = 0.433001 (Hartree/Particle)
 Thermal correction to Energy = 0.463689
 Thermal correction to Enthalpy = 0.464633
 Thermal correction to Gibbs Free Energy = 0.363800
 Sum of electronic and zero-point Energies = -4120.689617
 Sum of electronic and thermal Energies = -4120.658929
 Sum of electronic and thermal Enthalpies = -4120.657985
 Sum of electronic and thermal Free Energies= -4120.758818
 E(RwB97XD) = -4123.64820912

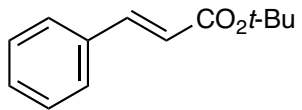
Pd	0.87161500	1.48574600	0.35881000
P	-0.22990300	-0.54170600	0.20537300
C	0.35186600	-1.56133700	-1.19554200
C	1.20026200	-2.64106000	-0.91707700
C	0.13789400	-1.15019600	-2.52882500
C	1.81308900	-3.34696600	-1.94841200
H	1.39672300	-2.91818500	0.11263700
C	0.75002500	-1.88909900	-3.54773000
C	1.57693000	-2.97550300	-3.27048800
H	2.47524600	-4.17494300	-1.71679800
H	0.58748700	-1.58643900	-4.57846700
H	2.04787800	-3.51826900	-4.08440900
C	-0.14726100	-1.57869400	1.71085800
C	-0.81382600	-2.81946900	1.85289400
C	0.59765800	-1.05239100	2.77606600
C	-0.66606300	-3.50089300	3.06642100
C	0.72358900	-1.74843200	3.97618300
H	1.06633200	-0.08043600	2.65747400
C	0.09416500	-2.98298100	4.11532600
H	-1.16816000	-4.45623600	3.19055200
H	1.30448300	-1.32676700	4.79001100
H	0.18350300	-3.54162900	5.04217400
C	-1.94508300	-0.26042800	-0.02413700
C	-3.11031400	0.07225000	-0.14850400
C	-4.47280600	0.44904400	-0.31103200
C	-5.38951200	-0.43874500	-0.90559100
C	-4.91241600	1.71612300	0.11696000
C	-6.71884600	-0.06156100	-1.06744700
C	-6.24468800	2.08189200	-0.04798000
H	-4.20206800	2.39755000	0.57270400
C	-7.14909700	1.19665500	-0.63934100
H	-7.42130200	-0.74954300	-1.52734700
H	-6.57813300	3.06003400	0.28380000
H	-8.18732400	1.48694000	-0.76688300
Br	1.86126800	3.70103500	0.57797100
C	2.51355900	0.53584500	-0.23267200
C	3.32124700	-0.12840800	0.68653100
C	2.80632100	0.51800600	-1.59458700
H	3.10506200	-0.09741100	1.74717900

H	2.18175600	1.04970800	-2.30244300	C	7.11319200	0.35246100	-0.83451500
C	-1.68062600	-3.41606200	0.77275000	H	6.36659500	2.34188400	-1.20409500
H	-1.11315100	-3.60985700	-0.14130500	H	7.56496200	-1.71289200	-0.40873600
H	-2.11701500	-4.35887900	1.11010100	H	8.14733000	0.61851300	-1.03180800
H	-2.49496500	-2.73674200	0.50454000	Br	1.13457900	2.47739000	-0.43523000
C	-0.67325100	0.07029500	-2.88248300	C	-2.65393200	-0.14761100	-1.18347600
H	-1.73899700	-0.07419400	-2.68571700	C	-3.45489000	-0.36715300	-0.04972700
H	-0.35863600	0.93955500	-2.29136200	C	-2.63356900	-1.10303100	-2.20704900
H	-0.54948400	0.31873500	-3.93913900	H	-3.52015900	0.40346200	0.71073700
H	-5.04586200	-1.41383000	-1.23430700	H	-2.03505100	-0.93151600	-3.09693600
C	3.90947100	-0.21126100	-2.04433300	C	0.74749400	-2.17305500	-2.48722000
H	4.13167900	-0.23738200	-3.10705800	H	1.80961300	-2.15486100	-2.22594300
C	4.71603100	-0.90286300	-1.13952400	H	0.64706400	-2.59313300	-3.49127900
H	5.56933700	-1.47250200	-1.49487900	H	0.41900800	-1.12784600	-2.51620000
C	4.42528600	-0.85315300	0.22289500	C	1.46728200	-2.55359100	2.73121500
H	5.05386800	-1.37784600	0.93702100	H	1.10818000	-3.22473600	1.94764200
				H	2.40050600	-2.11354500	2.36798100
				H	1.69042600	-3.15219100	3.61773700
				H	3.98667500	1.72181100	-0.75167900
				C	-2.93950300	1.74478100	-1.96061600
				C	-2.01818900	2.72117000	-1.50654000
				H	-1.32926500	3.20626300	-2.18817800
				H	-2.91073800	1.46154300	-3.00605200
				C	-2.32029700	3.39953200	-0.21885700
				O	-1.61622100	4.52342900	-0.08721400
				O	-3.11038100	2.94618200	0.60360800
				H	-3.91663600	1.73160700	-1.49651100
				C	-4.17687200	-1.55156500	0.07515500
Pd	-0.88010700	1.01567500	-0.81596900	C	-4.13627200	-2.51058400	-0.94219200
P	0.16353900	-0.80287200	0.28261100	C	-3.37194800	-2.28073100	-2.08568300
C	-0.14569000	-0.65537500	2.08365000	H	-3.33536400	-3.02345600	-2.87607400
C	-1.021178700	0.36847900	2.47572800	H	-4.69932600	-3.43331300	-0.84306300
C	0.46417800	-1.47695600	3.06214500	H	-4.77862700	-1.72391200	0.96295600
C	-1.32804900	0.57802600	3.81799500	C	-1.49263000	5.20494500	1.21425200
H	-1.45499900	1.01882300	1.72395200	C	-0.39976800	6.23497400	0.93572800
C	0.13421600	-1.24893000	4.40372600	H	-0.21097300	6.83353300	1.83173200
C	-0.75026200	-0.24047400	4.78518600	H	0.52243900	5.72676200	0.64340400
H	-2.00638600	1.37756400	4.09756700	H	-0.70123900	6.90483300	0.12534600
H	0.59223500	-1.87517300	5.16436200	C	-1.03520400	4.21498700	2.28873300
H	-0.97808600	-0.09281000	5.83676100	H	-1.83504000	3.52557600	2.55807300
C	-0.37398500	-2.48535300	-0.20916500	H	-0.17736300	3.64288700	1.92609900
C	-0.05301600	-2.97697800	-1.49432700	H	-0.73596700	4.77195800	3.18221300
C	-1.17115800	-3.24666300	0.65360200	C	-2.82416000	5.87120000	1.55988100
C	-0.50950900	-4.25225200	-1.84517500	H	-2.71470900	6.45829000	2.47744100
C	-1.62036100	-4.51105600	0.27903700	H	-3.13252800	6.54677500	0.75619000
H	-1.44007600	-2.84630600	1.62456400	H	-3.60107400	5.12077900	1.71151300
C	-1.27862000	-5.01970100	-0.97208600				
H	-0.26129600	-4.64212100	-2.82877200				
H	-2.23495300	-5.09015700	0.96122100				
H	-1.61879700	-6.00571500	-1.27452200				
C	1.90265700	-0.83330500	0.12139000				
C	3.08844900	-0.64821100	-0.07510200				
C	4.45199200	-0.33328500	-0.32647600				
C	4.78423500	0.98910900	-0.68178700				
C	5.46276400	-1.30639200	-0.22908200				
C	6.11177200	1.32234100	-0.93152100				
C	6.78641000	-0.95991500	-0.48413100				
H	5.19806100	-2.32225900	0.04551100				

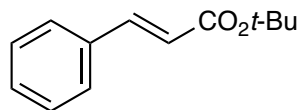
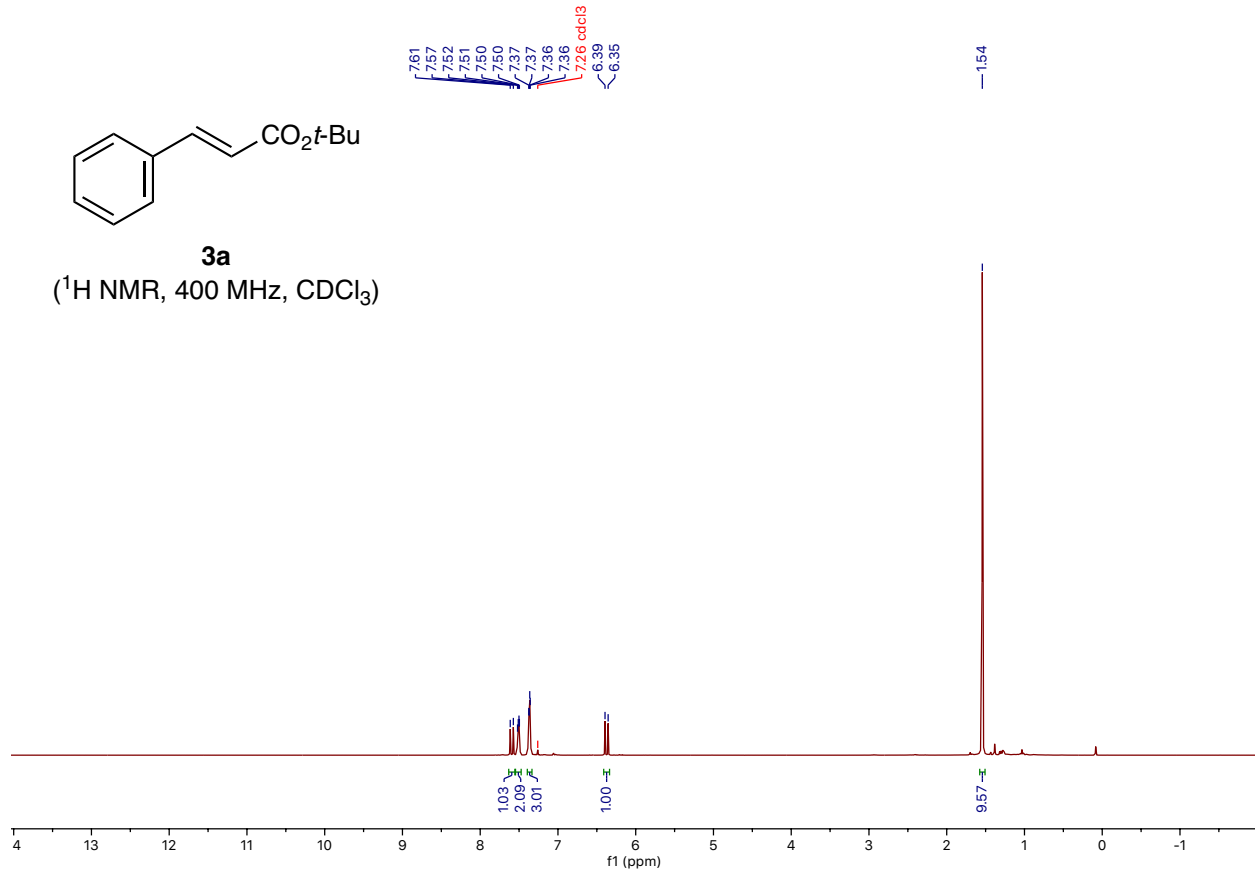
NMR Spectra



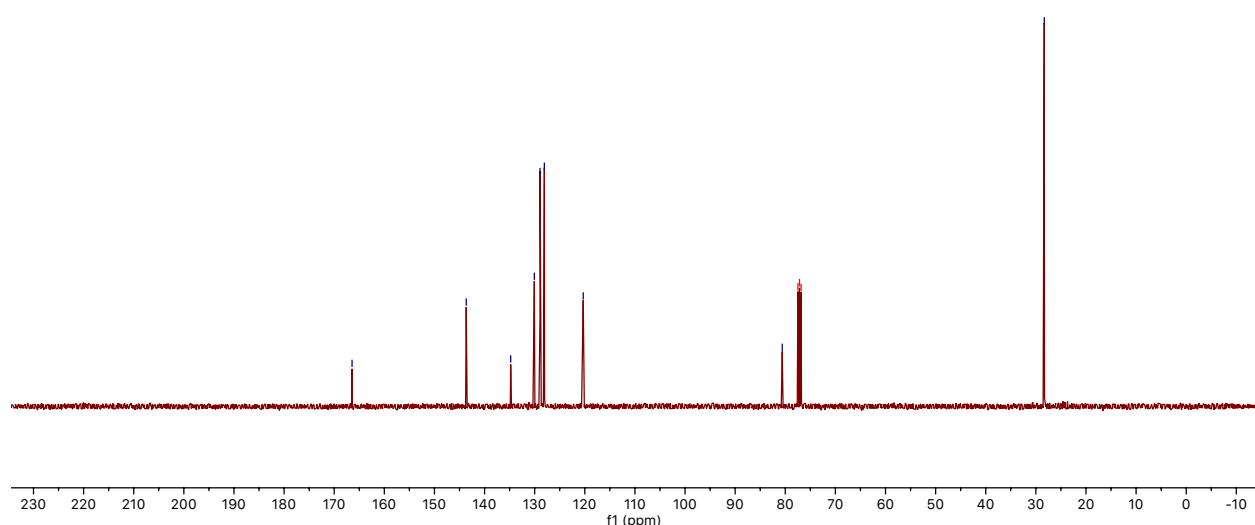


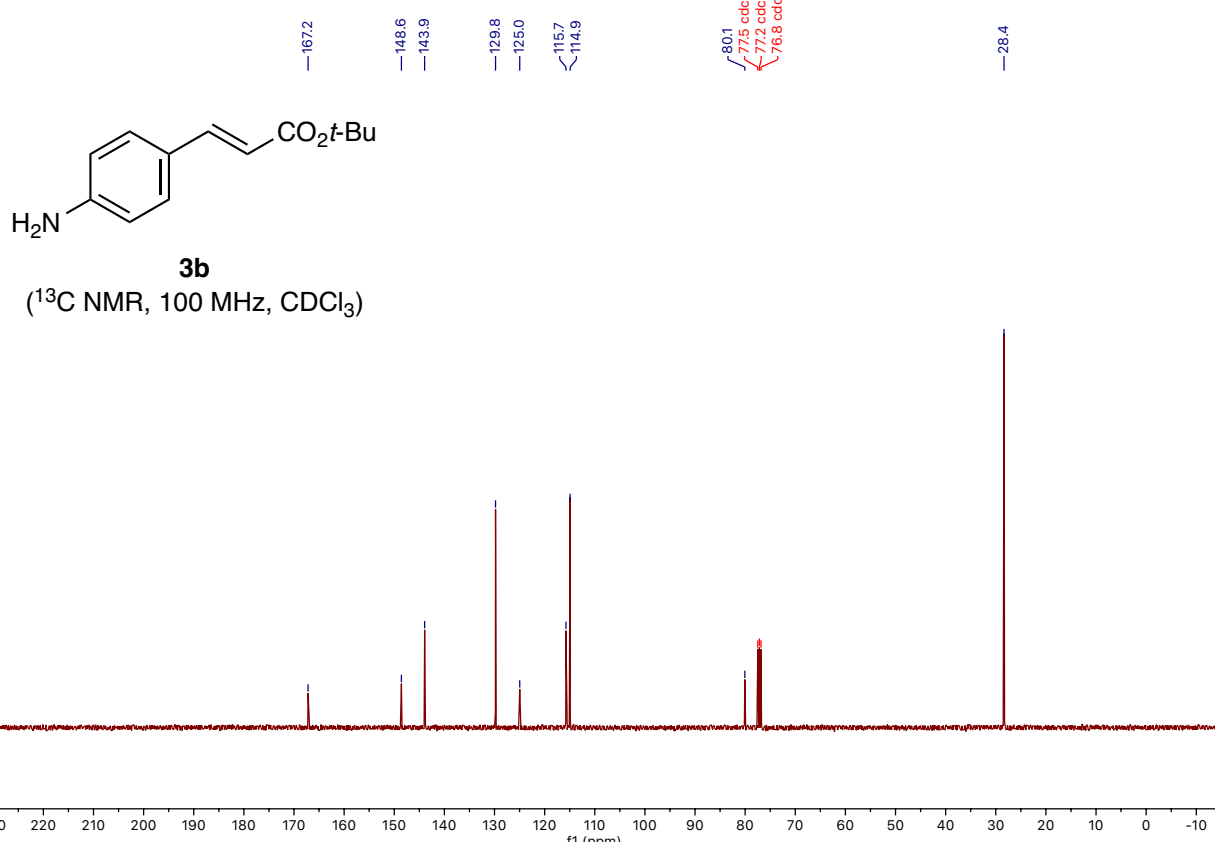
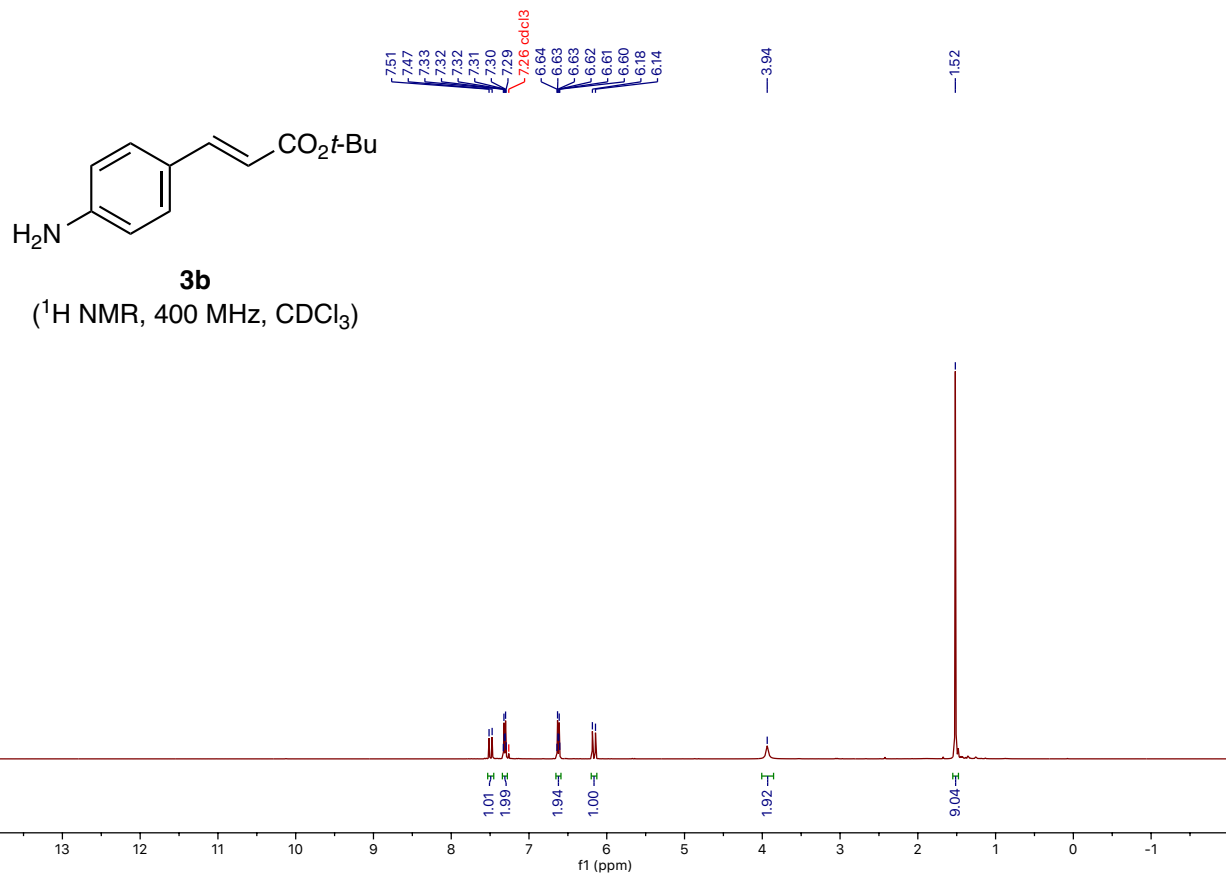


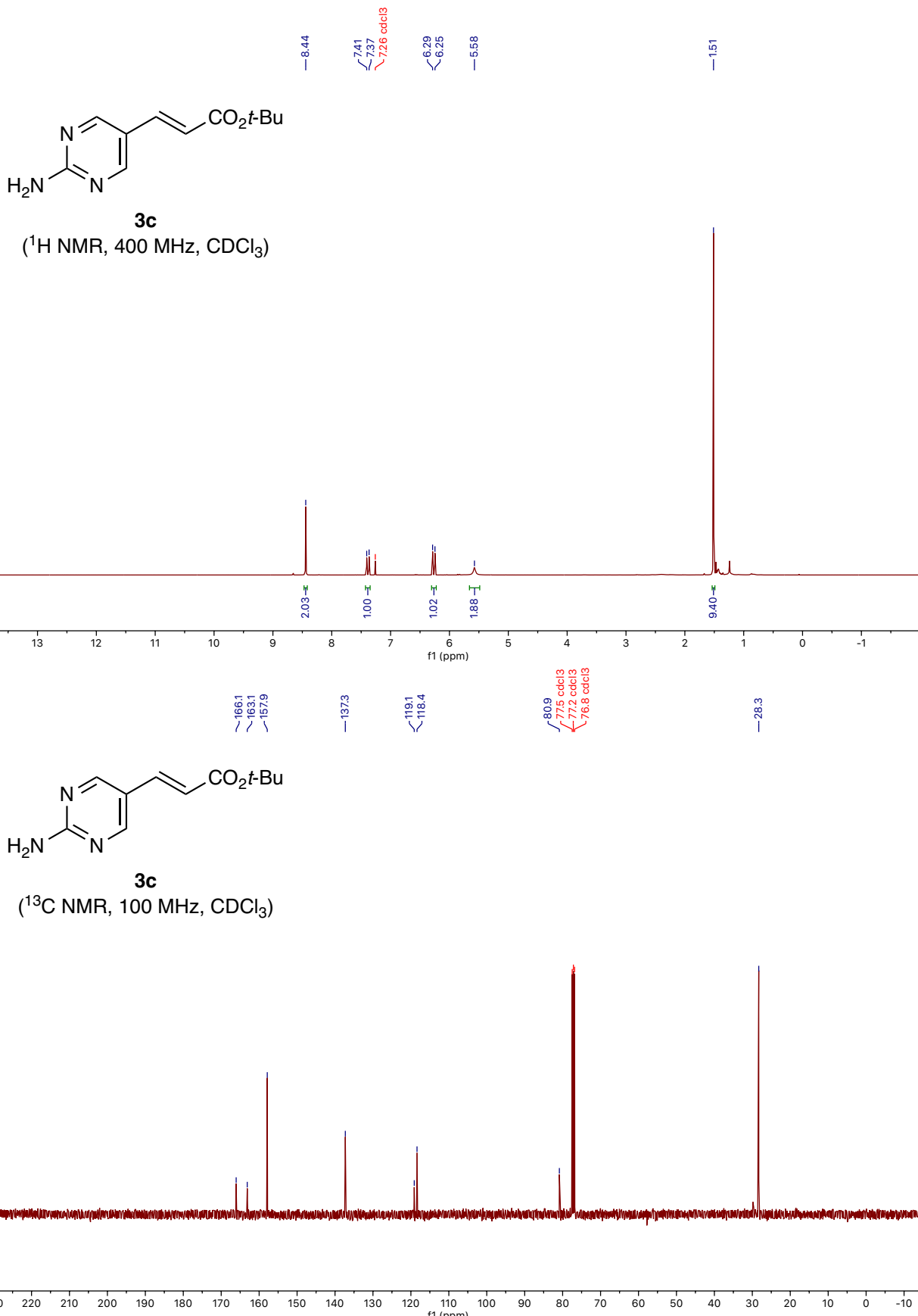
(^1H NMR, 400 MHz, CDCl_3)

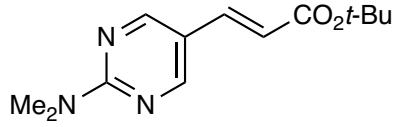


(^{13}C NMR, 100 MHz, CDCl_3)



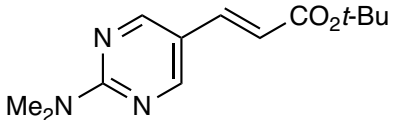
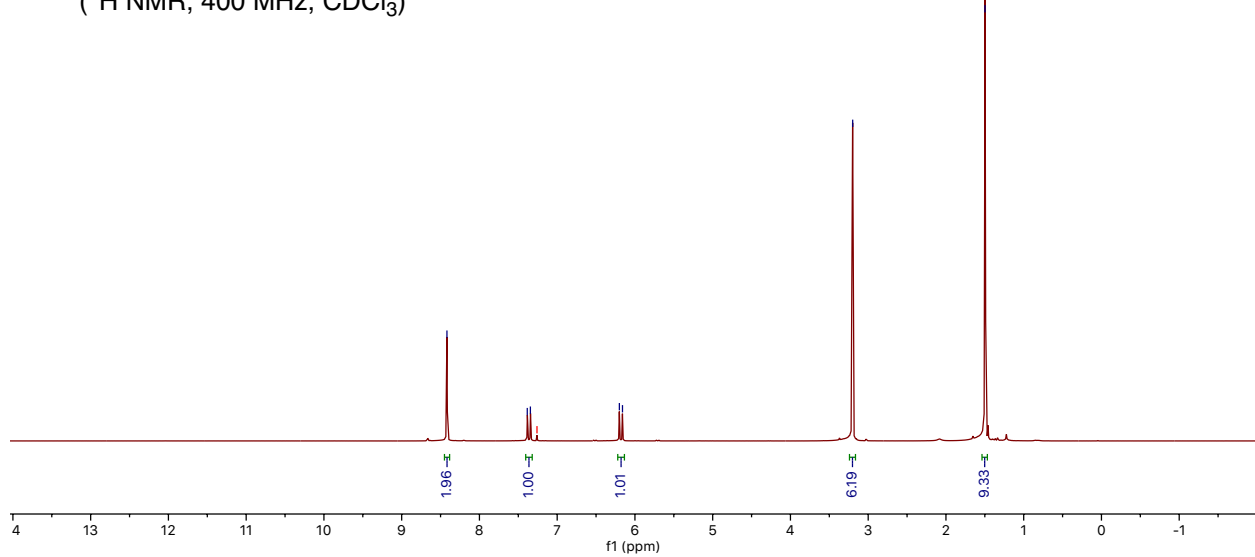






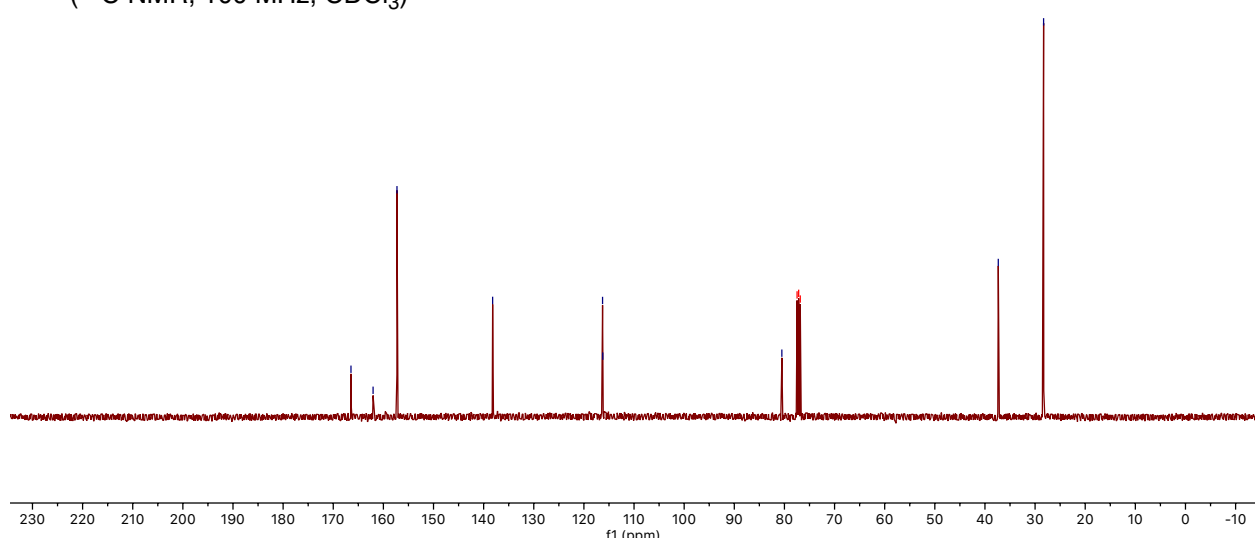
3d

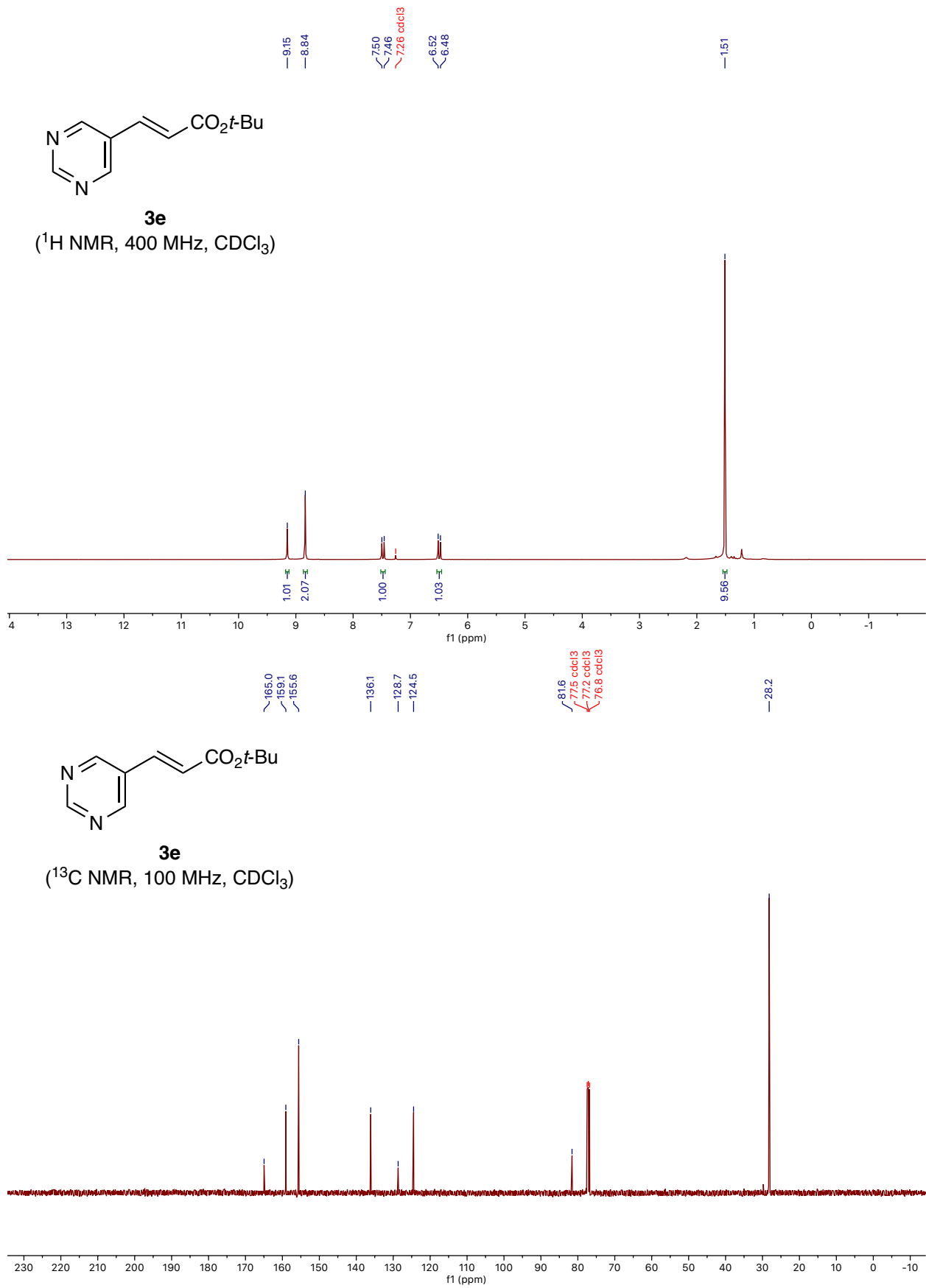
(^1H NMR, 400 MHz, CDCl_3)

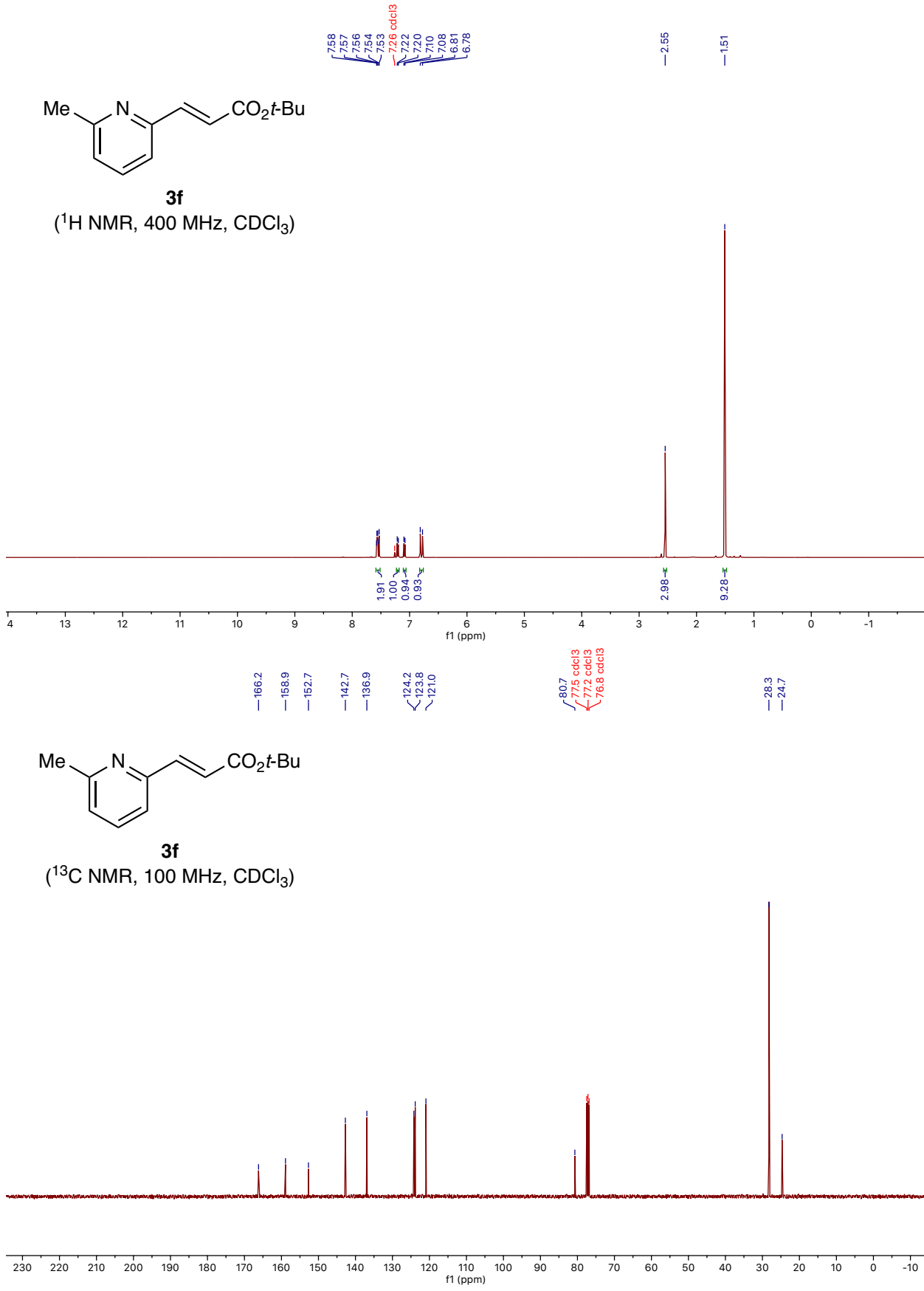


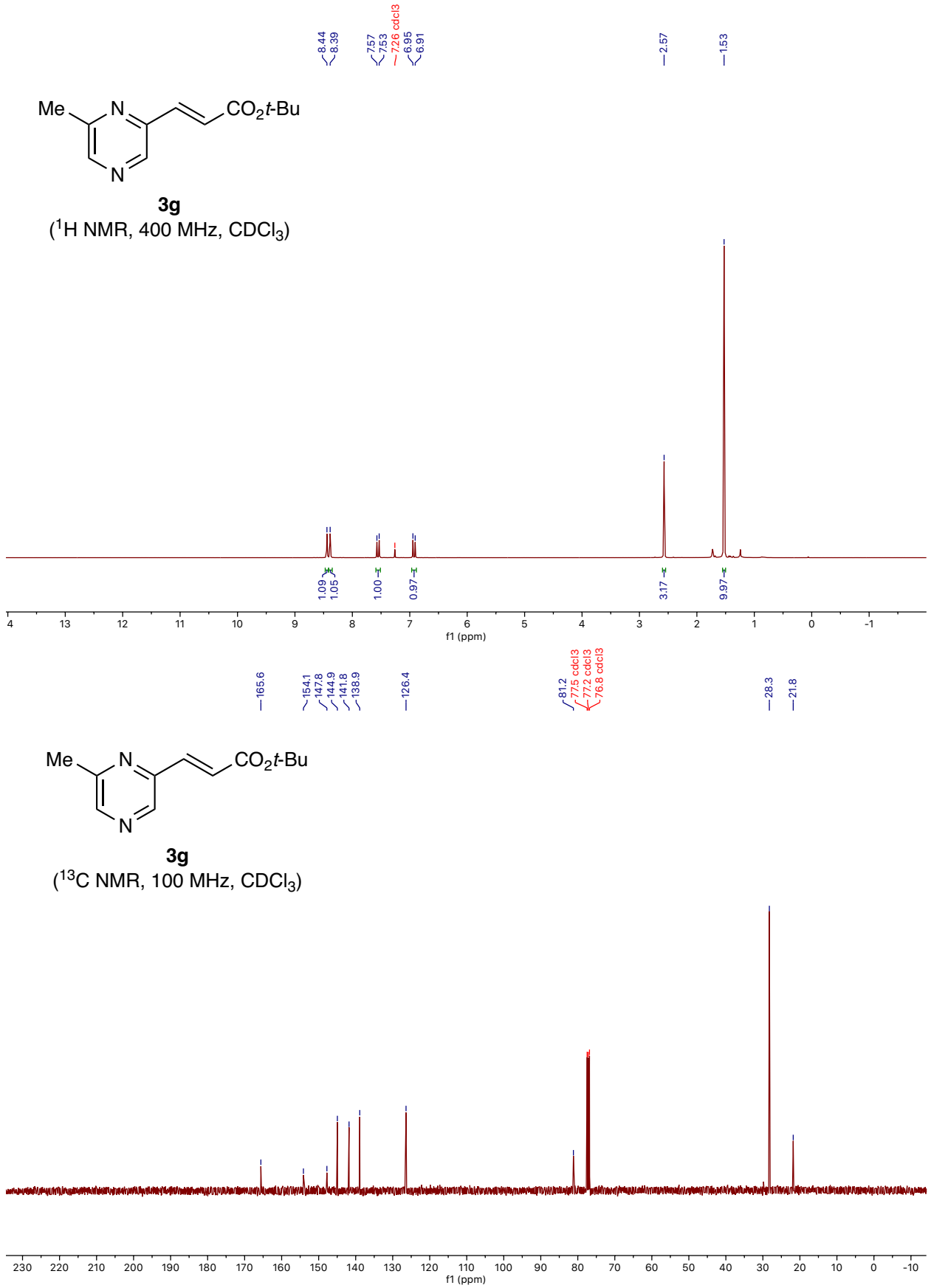
3d

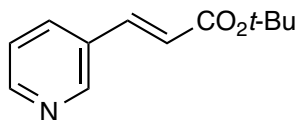
(^{13}C NMR, 100 MHz, CDCl_3)





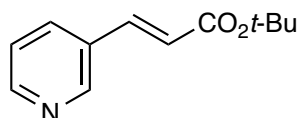
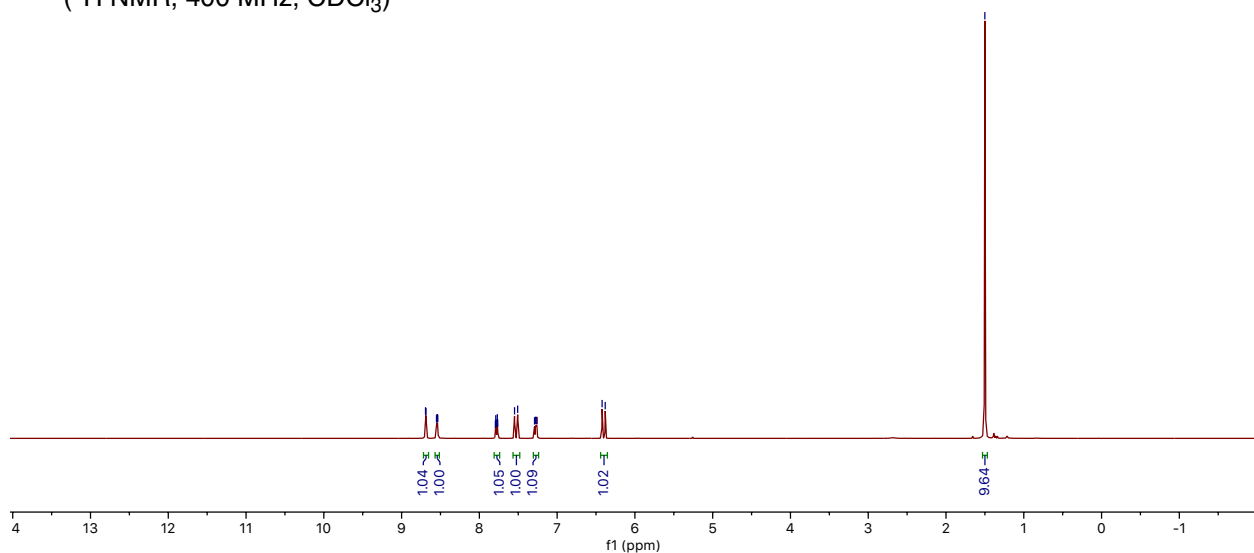






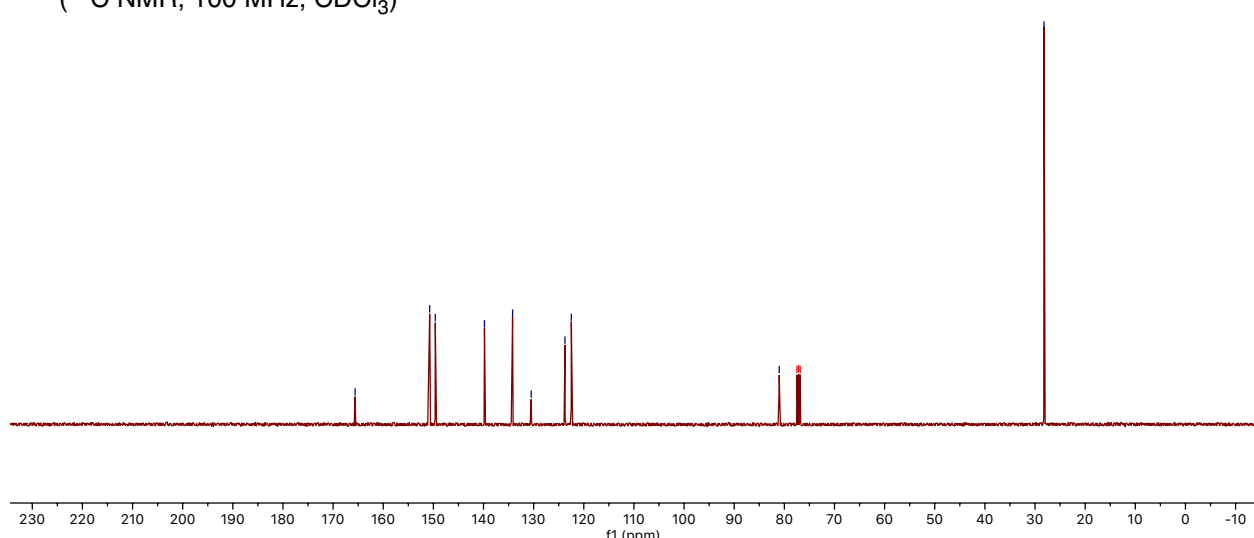
3h

(^1H NMR, 400 MHz, CDCl_3)



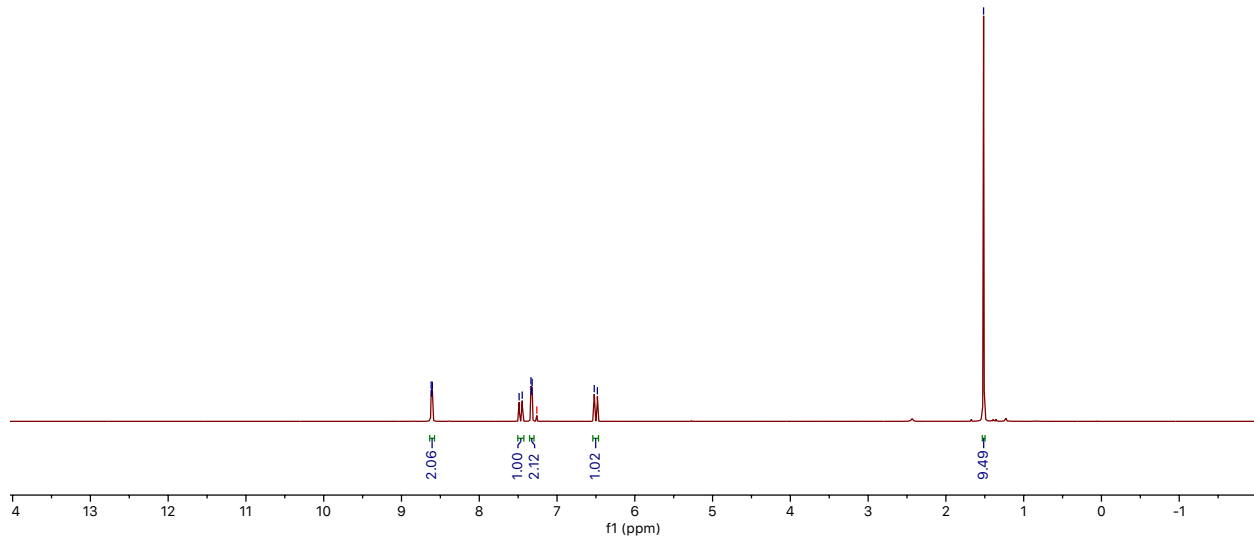
3h

(^{13}C NMR, 100 MHz, CDCl_3)

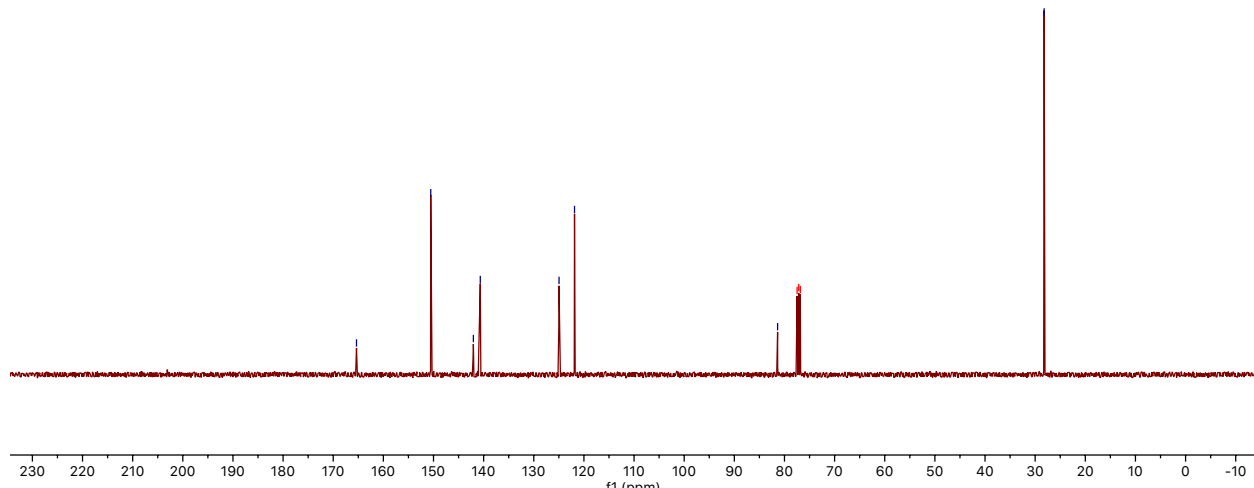


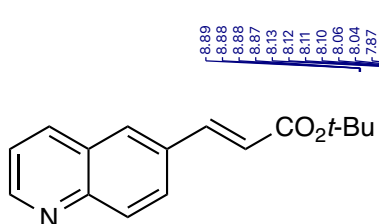


3i
(^1H NMR, 400 MHz, CDCl_3)

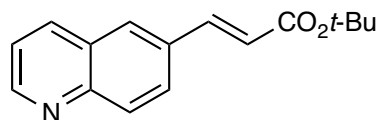
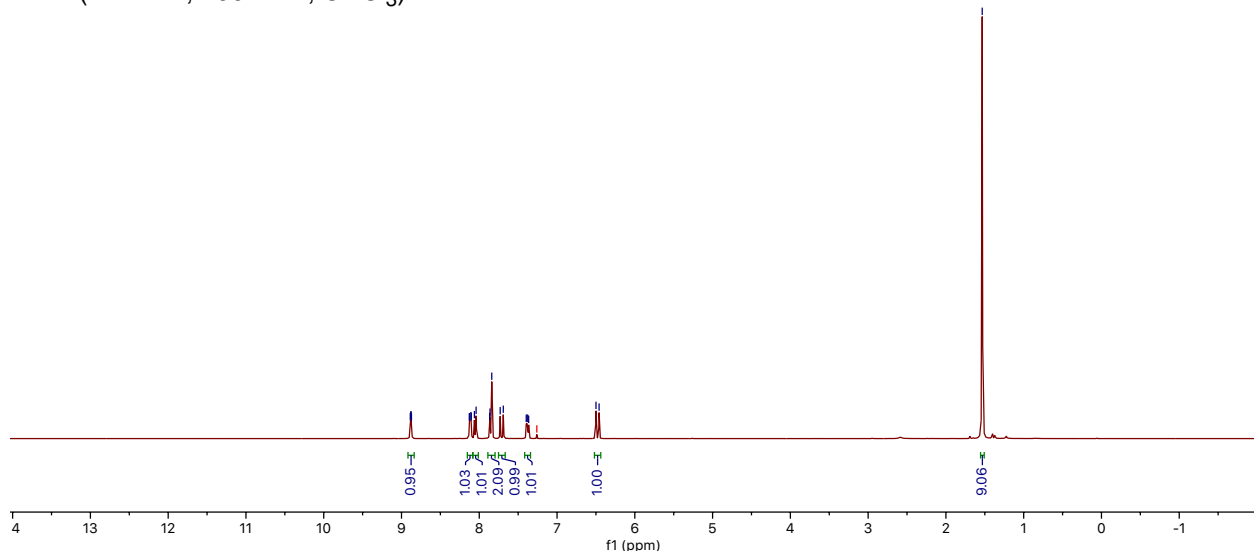


3i
(^{13}C NMR, 100 MHz, CDCl_3)

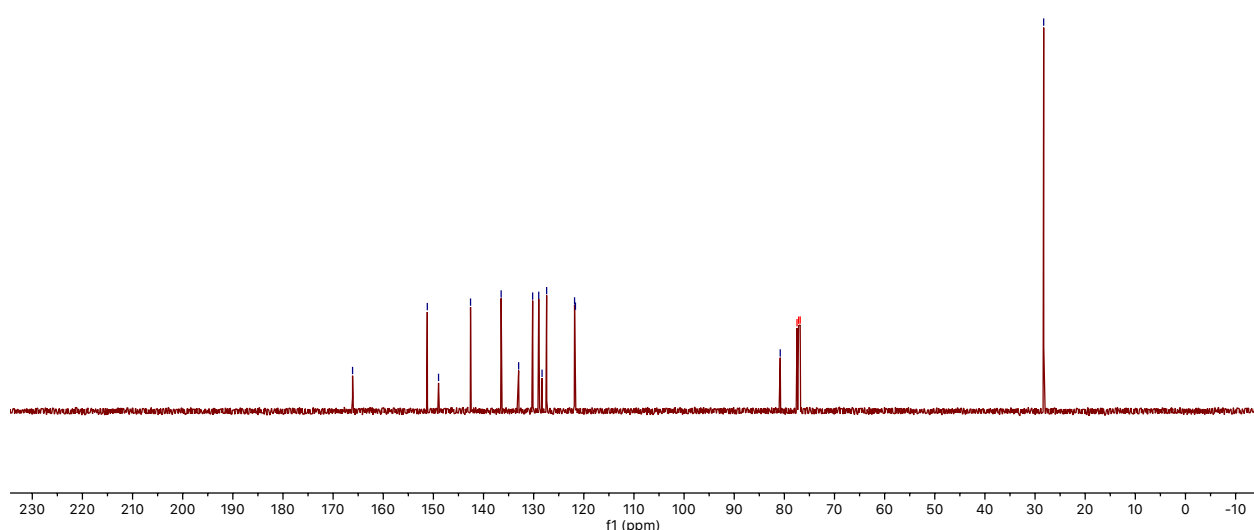


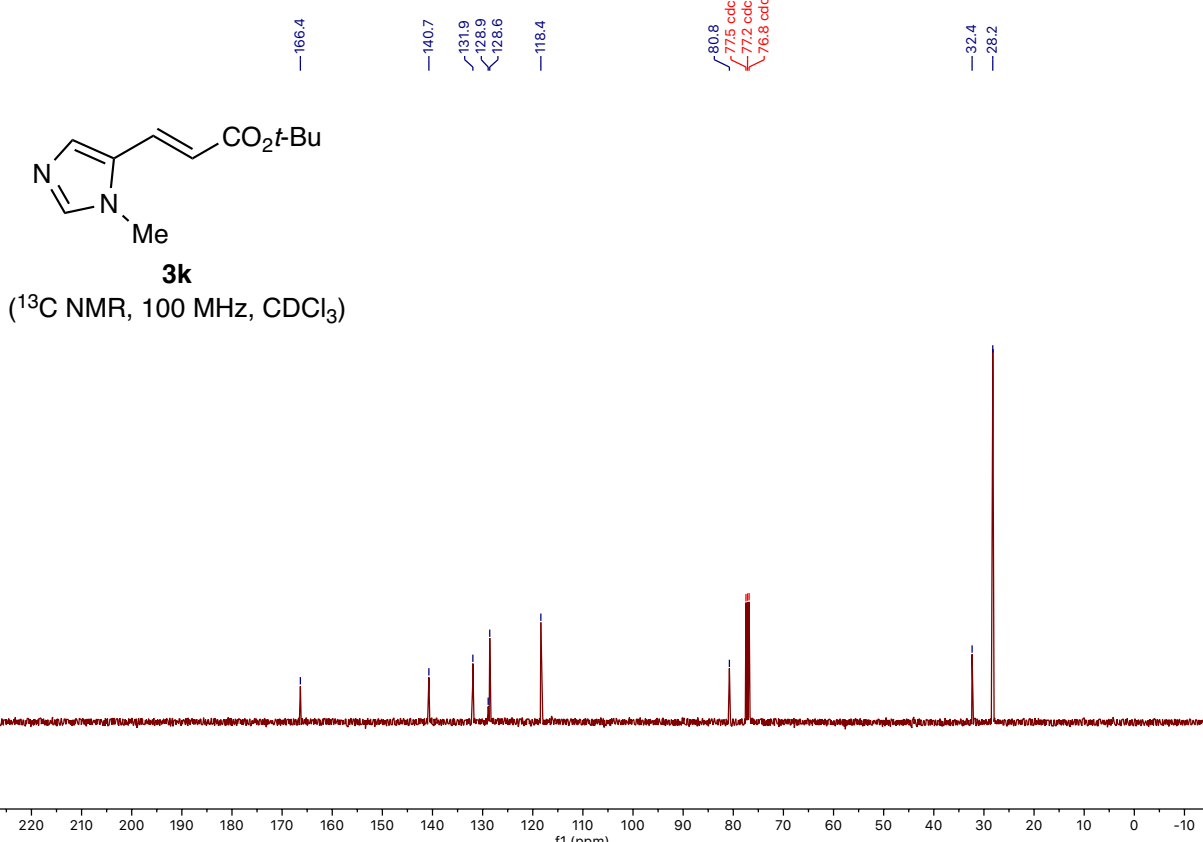
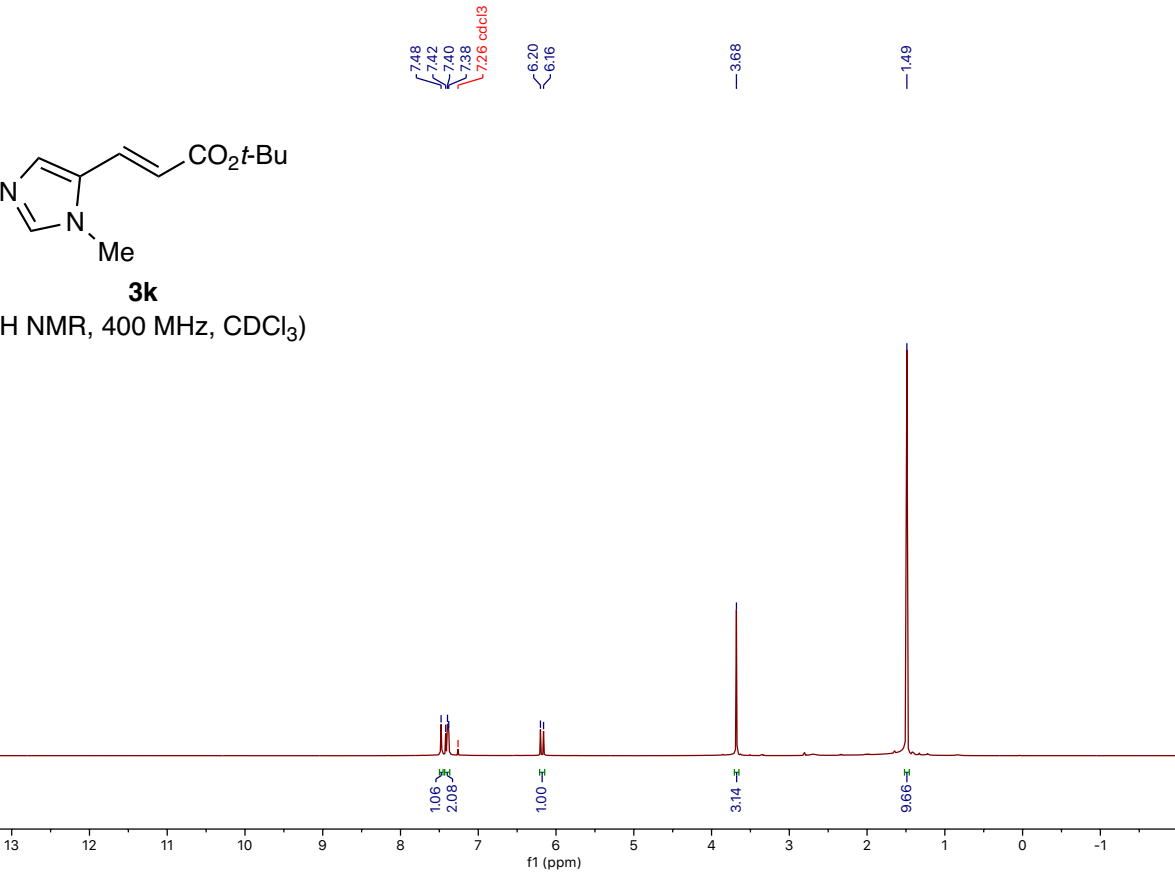


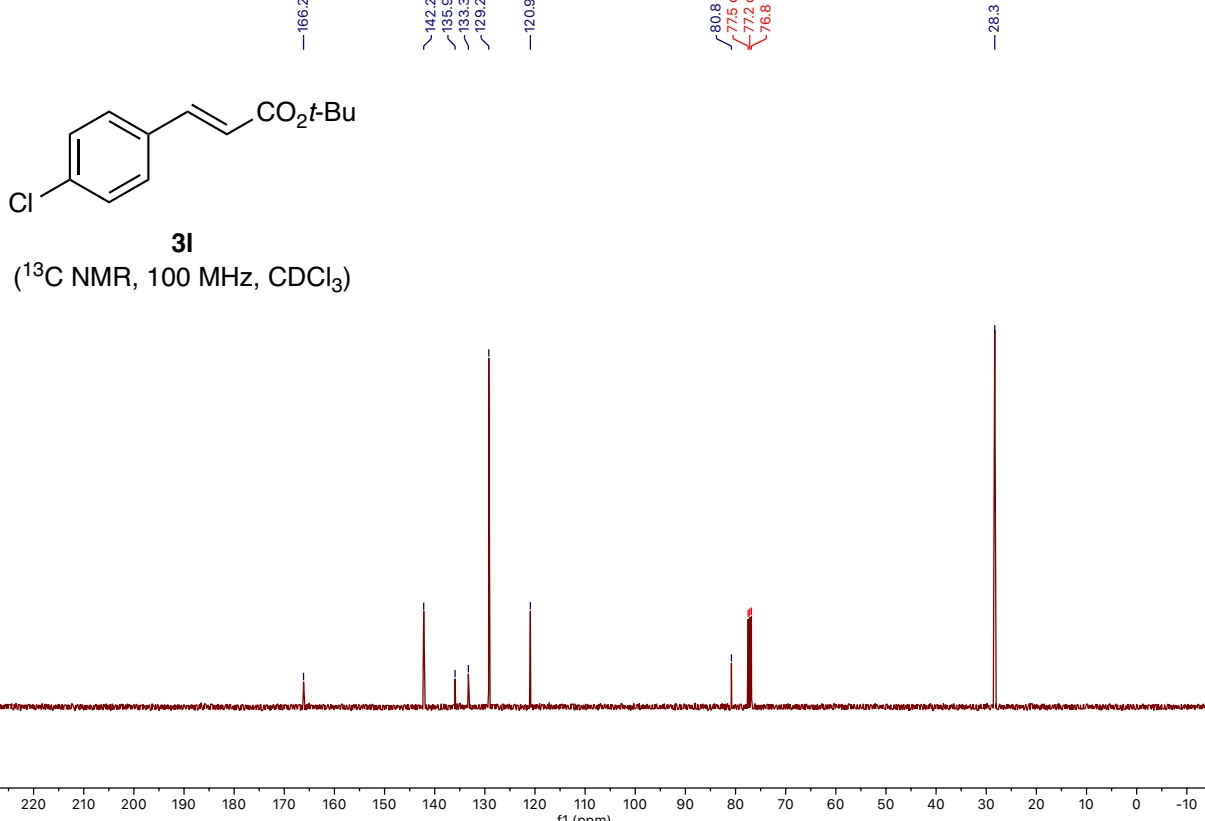
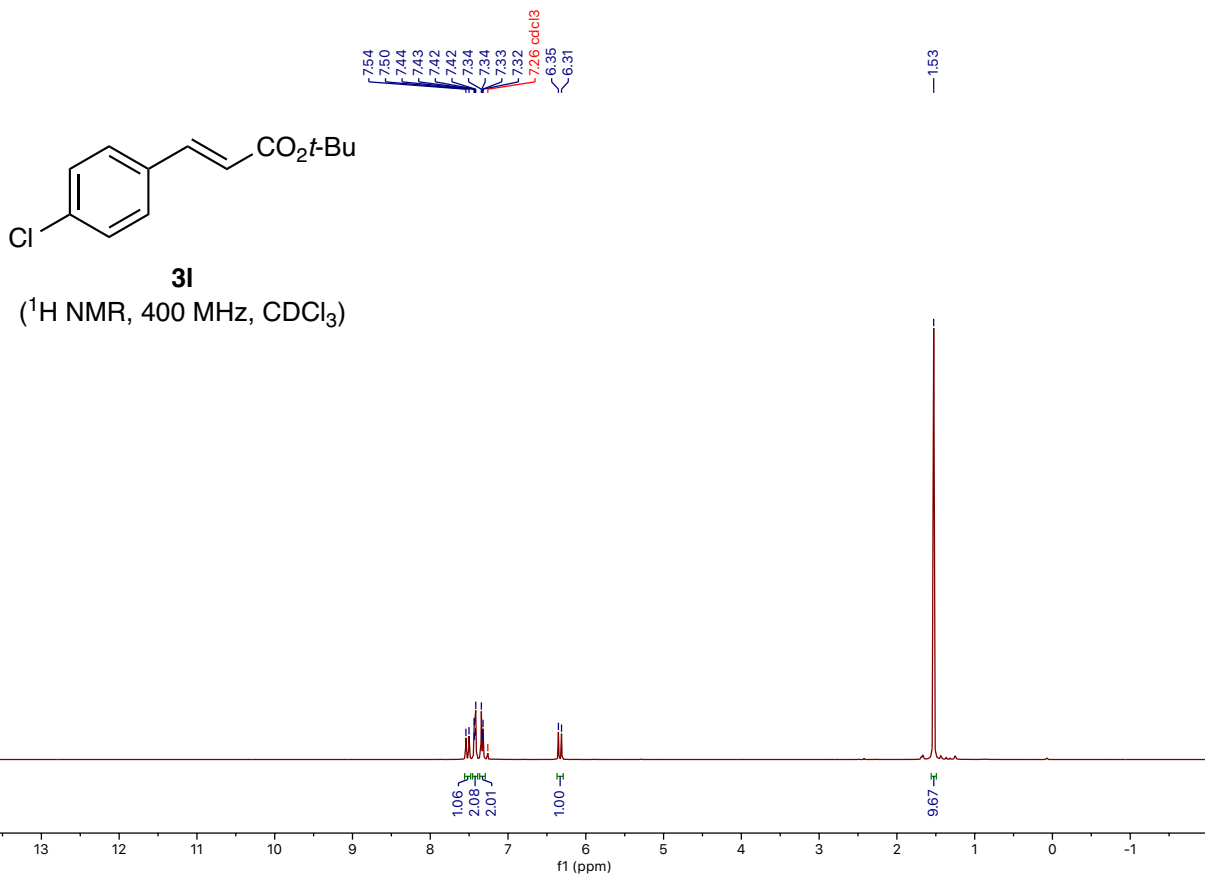
3j

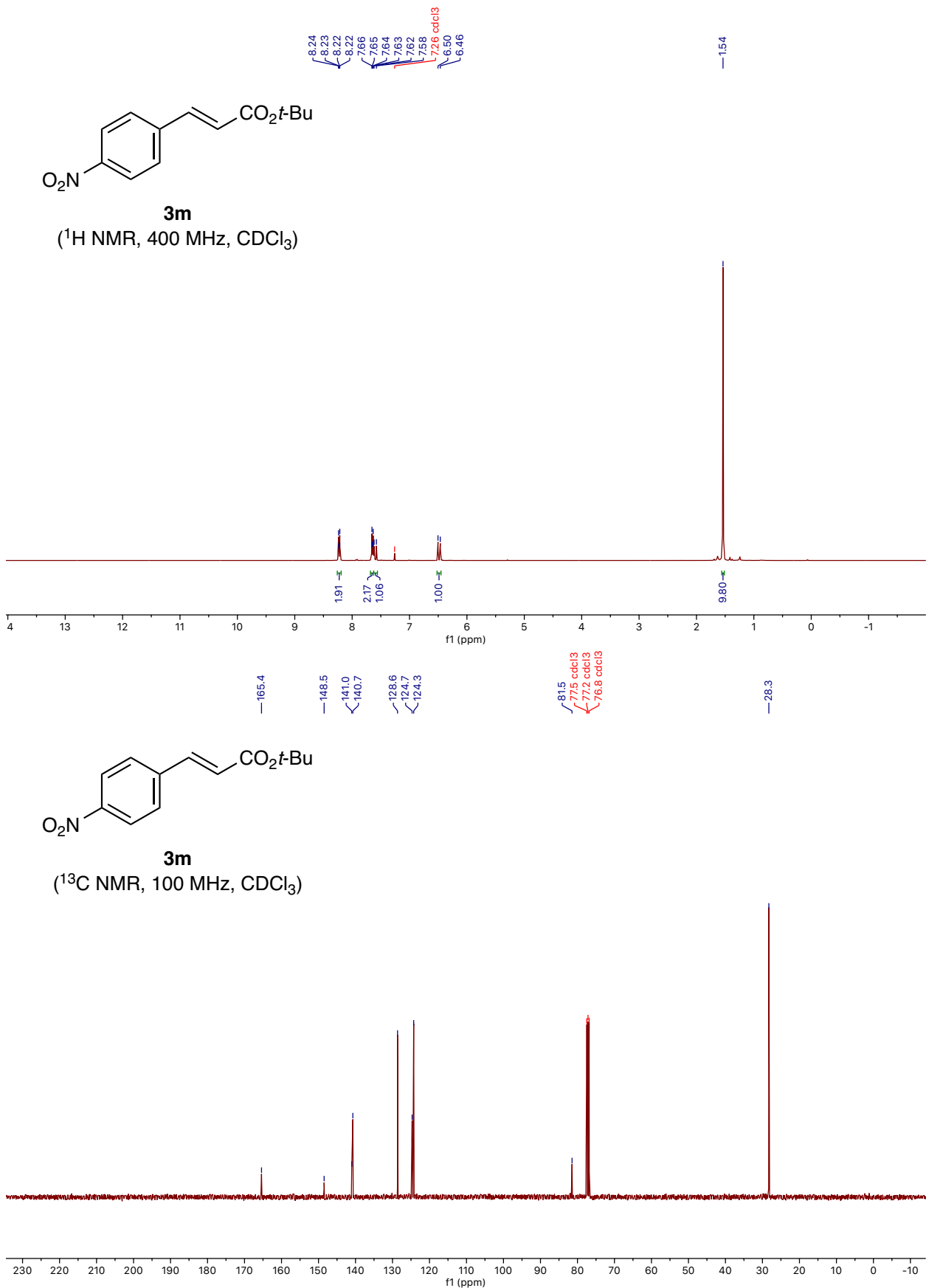


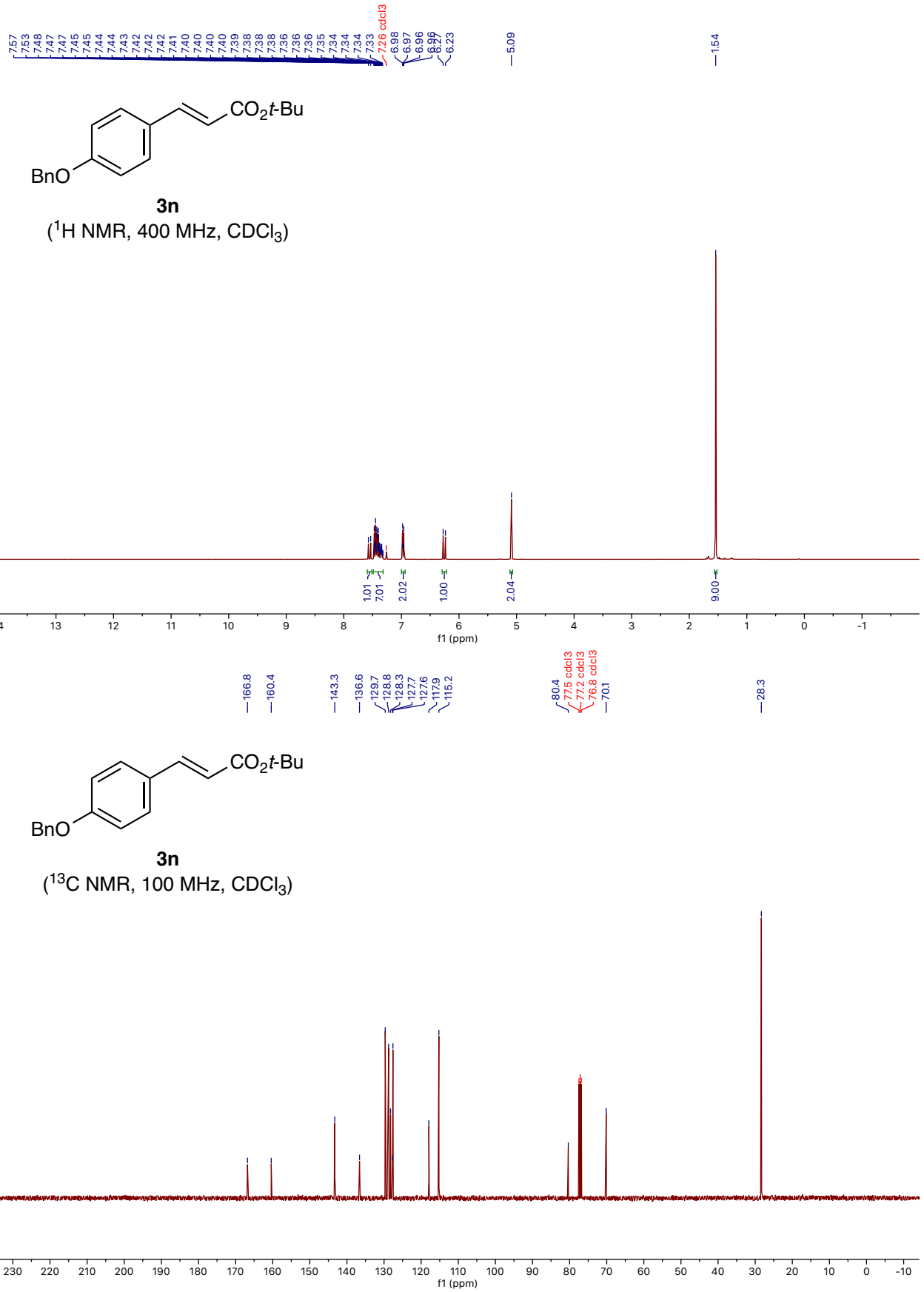
3j
(^{13}C NMR, 100 MHz, CDCl_3)

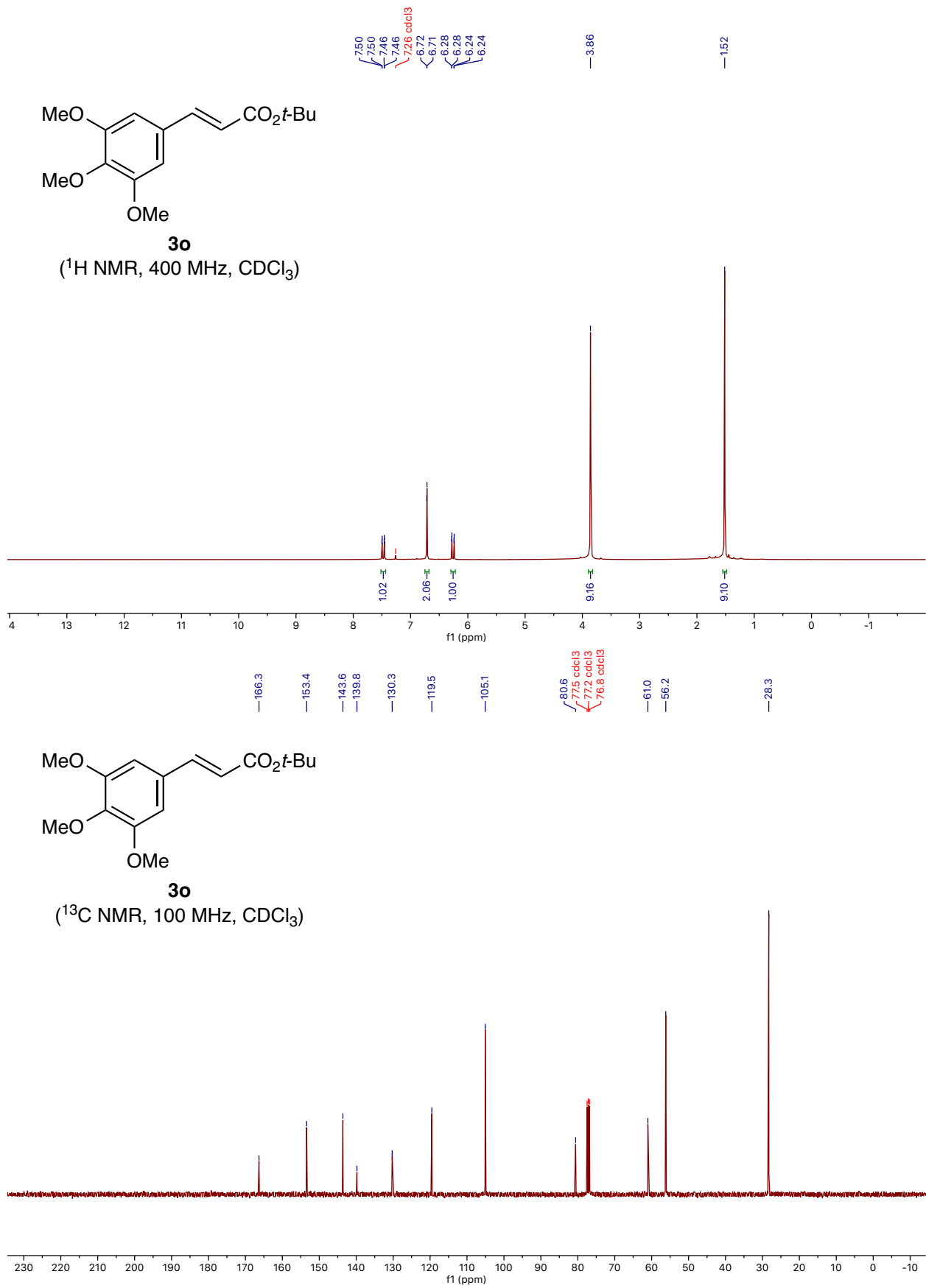


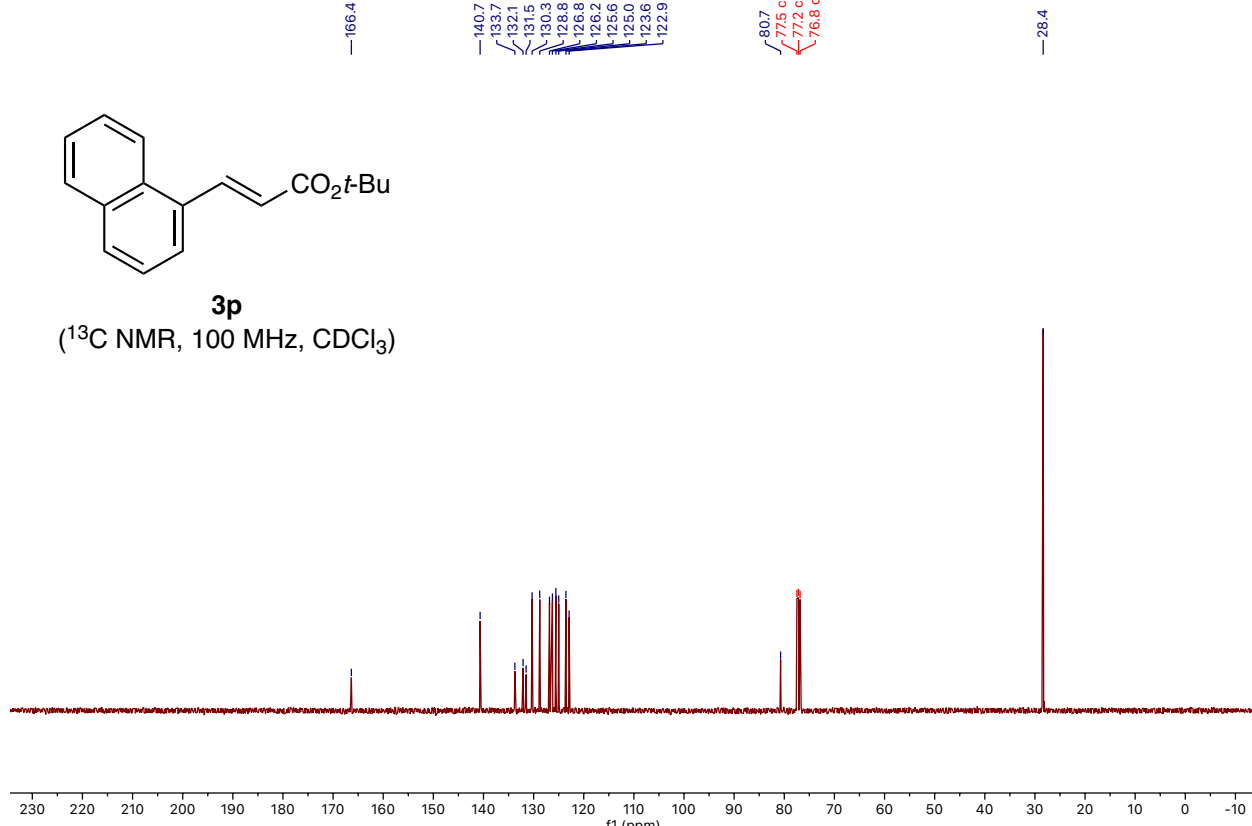
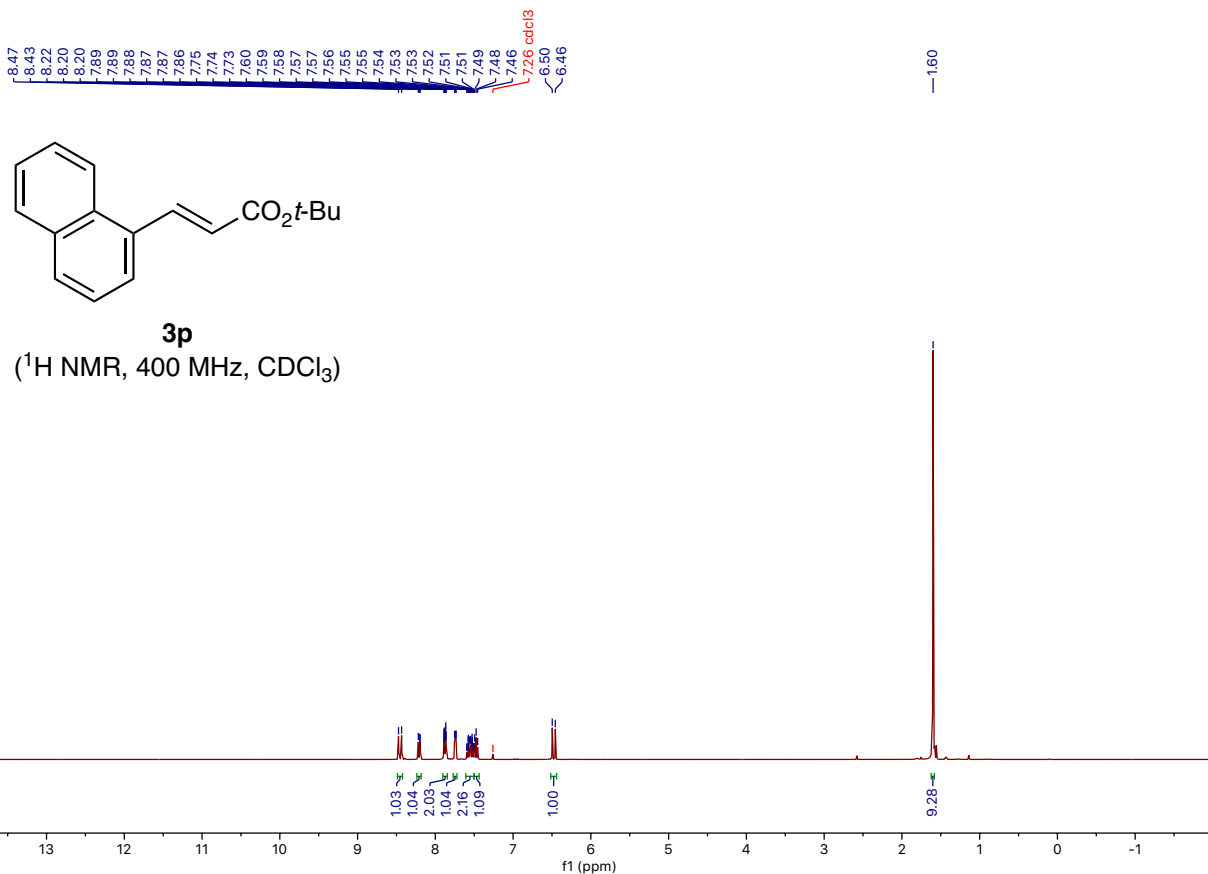


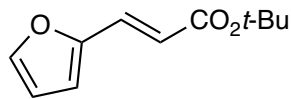




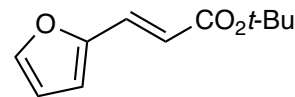
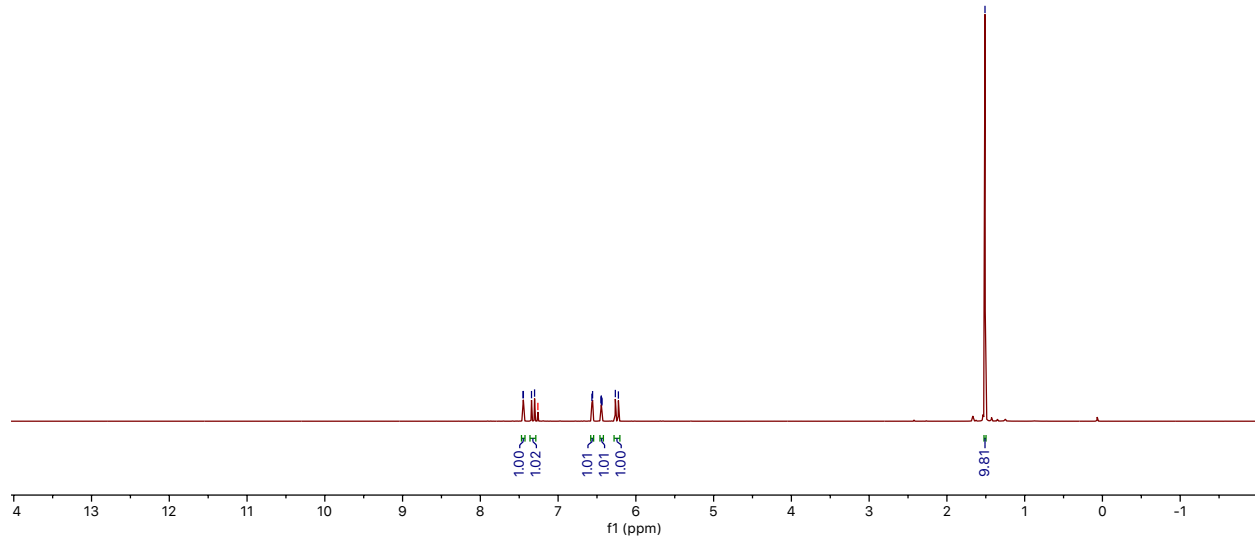




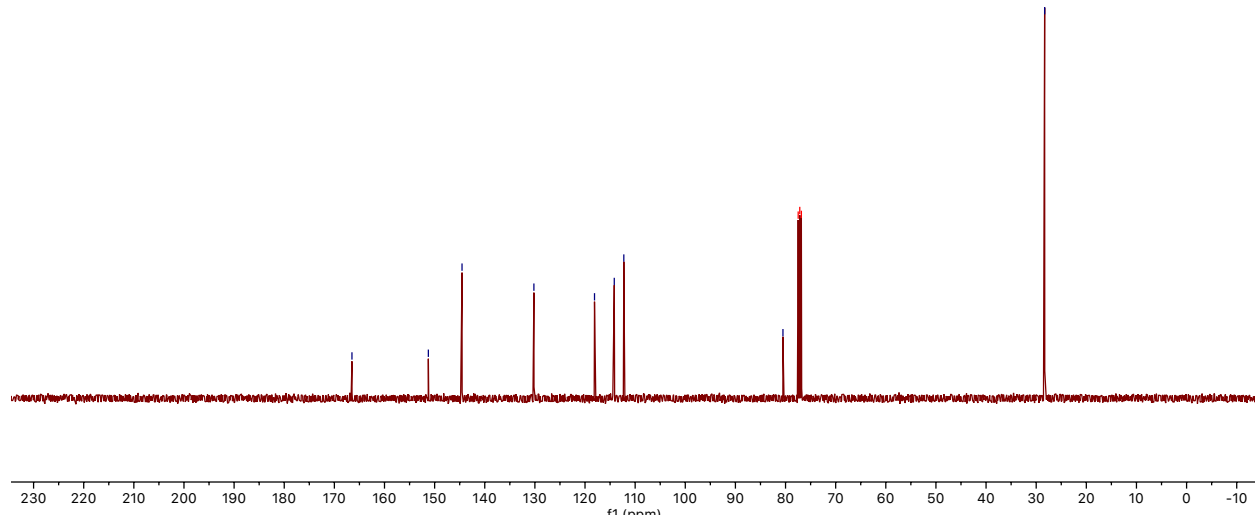


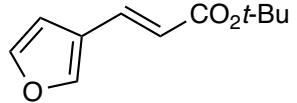


(^1H NMR, 400 MHz, CDCl_3)



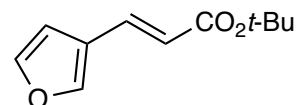
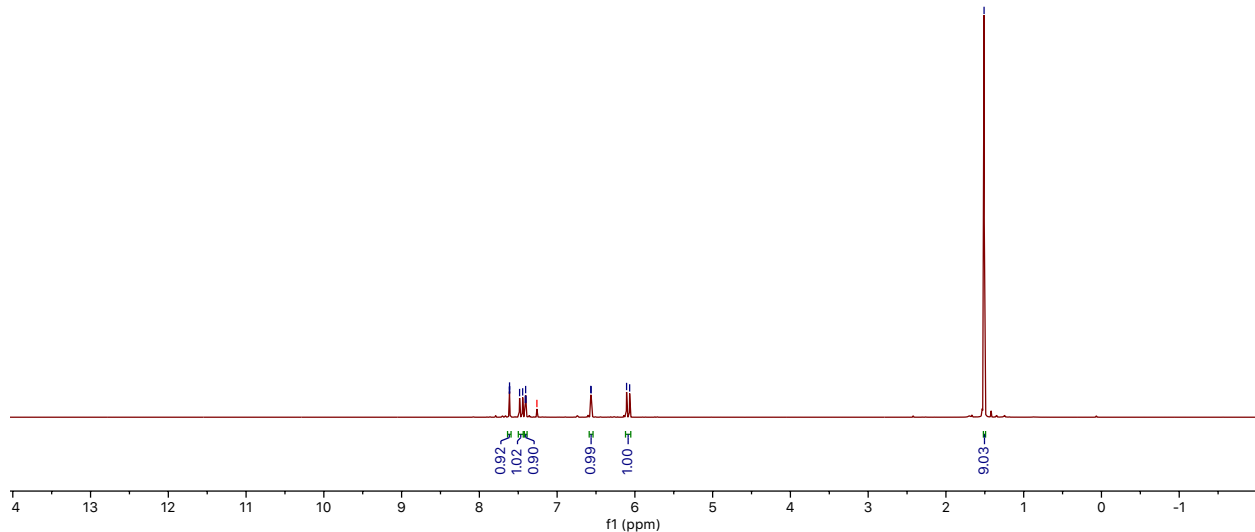
(^{13}C NMR, 100 MHz, CDCl_3)





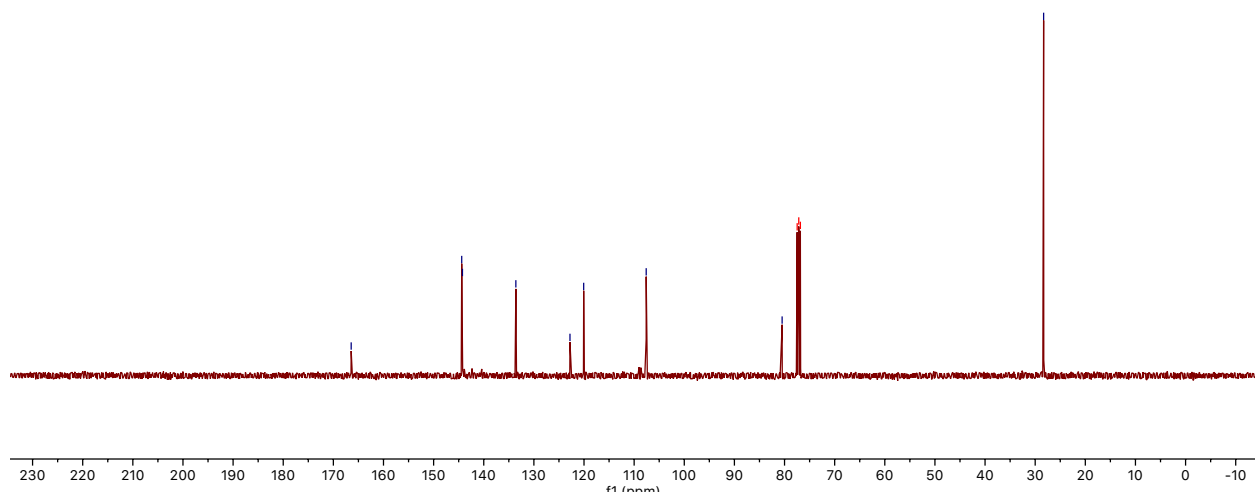
3r

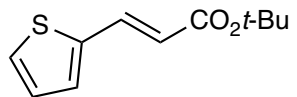
(^1H NMR, 400 MHz, CDCl_3)



3r

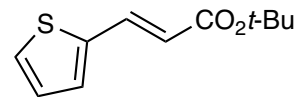
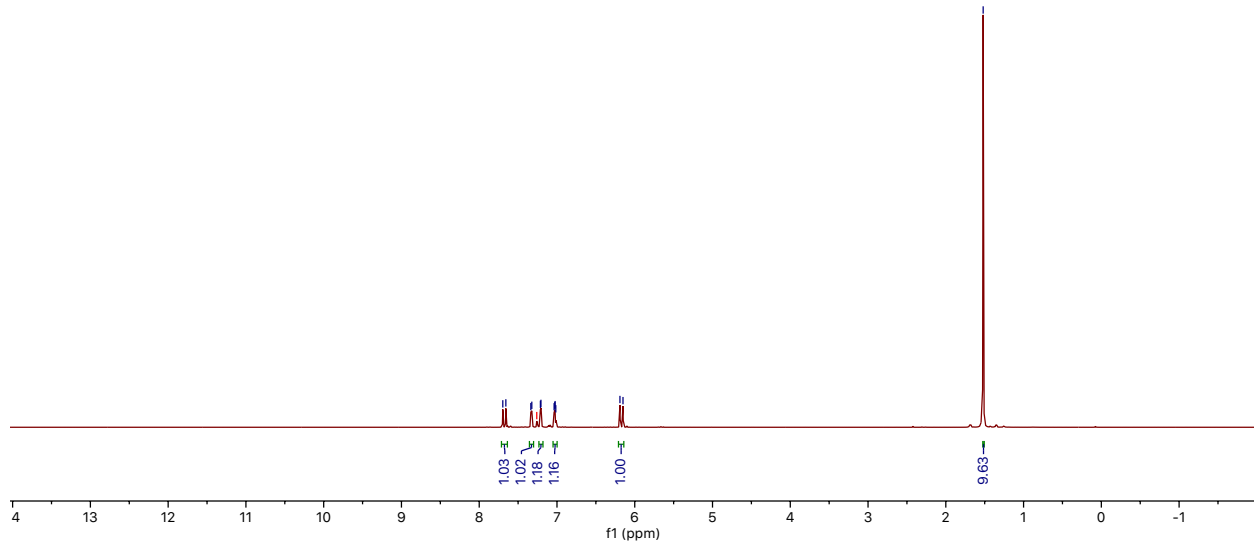
(^{13}C NMR, 100 MHz, CDCl_3)





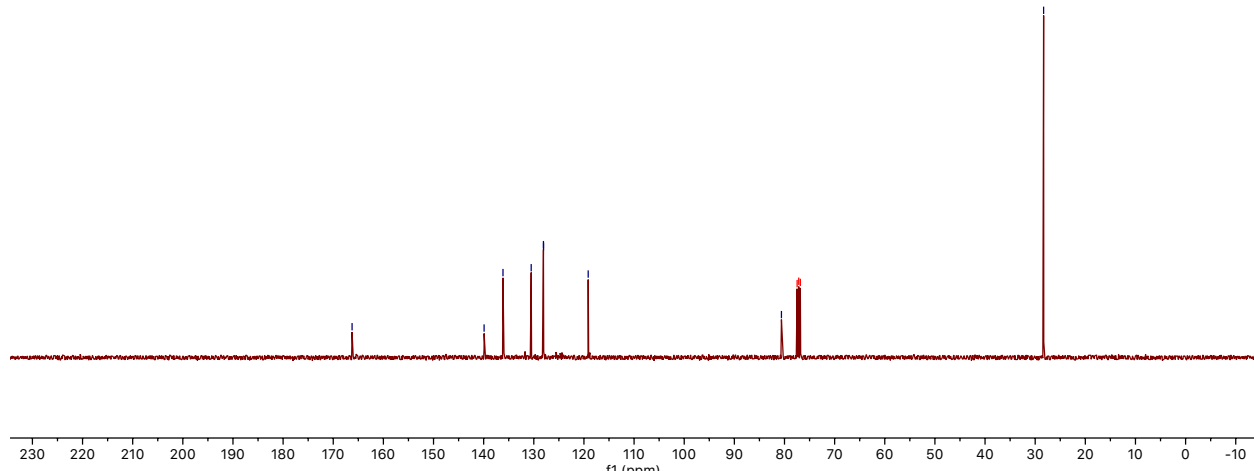
3s

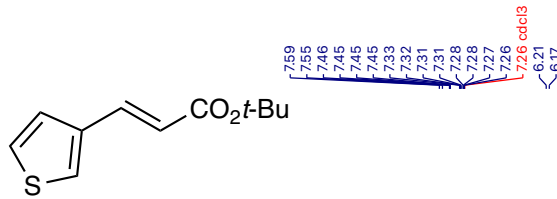
(^1H NMR, 400 MHz, CDCl_3)



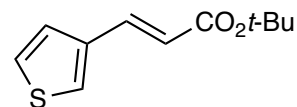
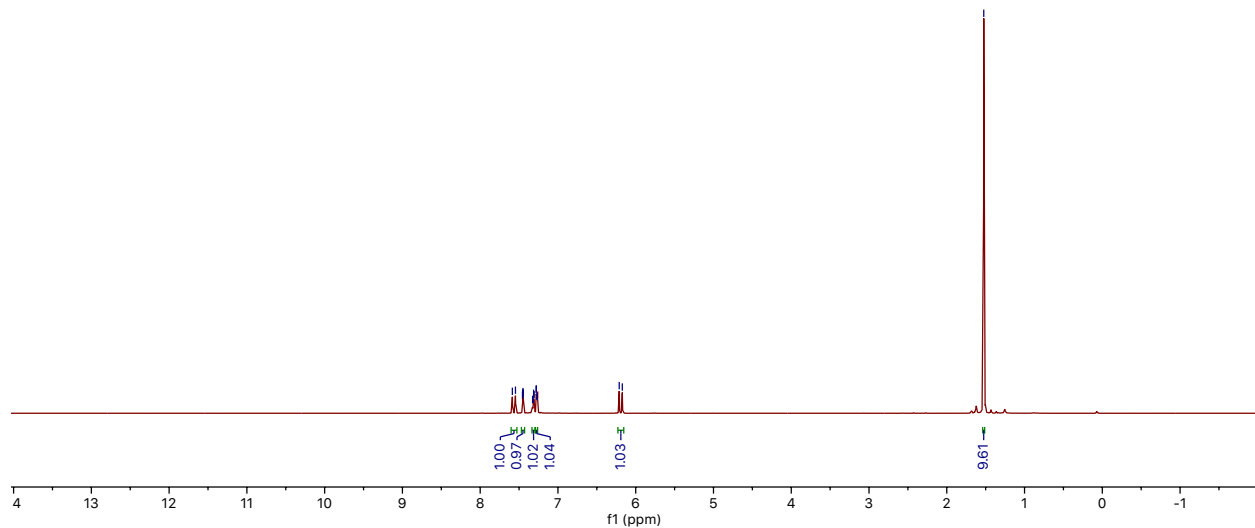
3s

(^{13}C NMR, 100 MHz, CDCl_3)

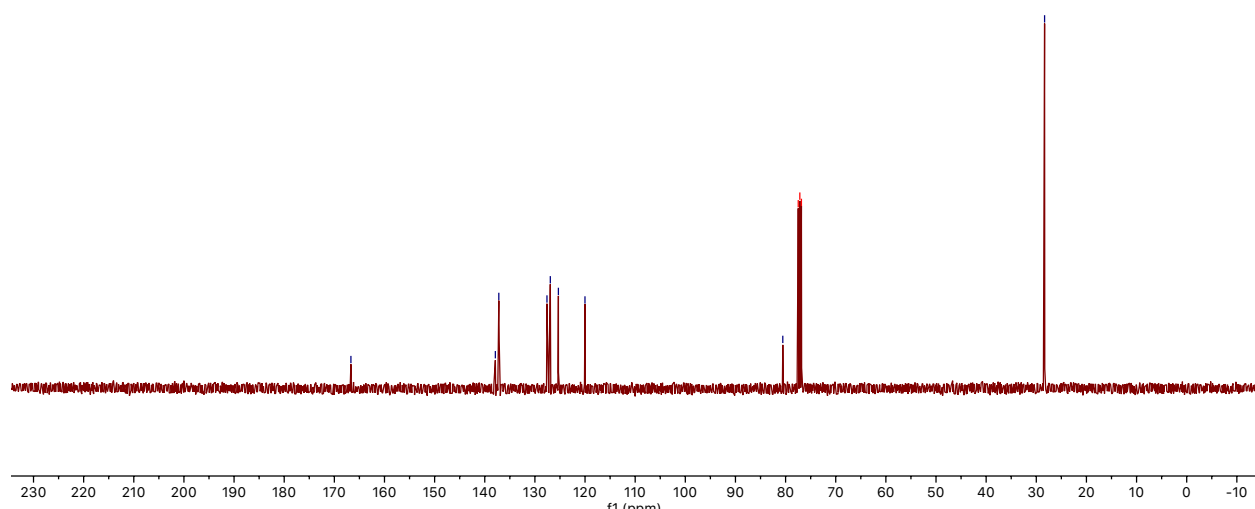


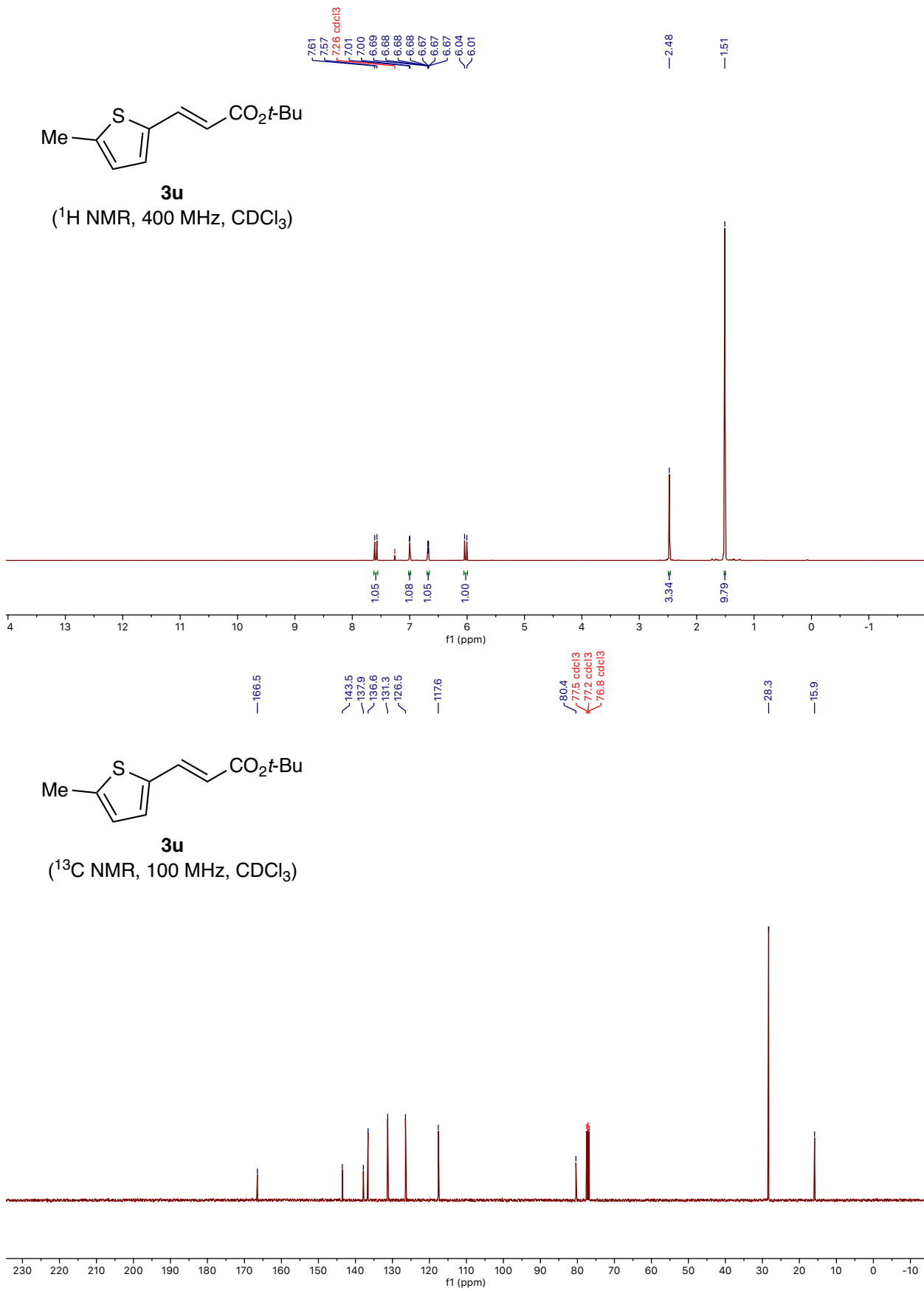


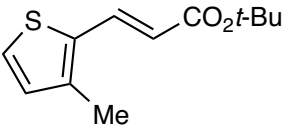
(^1H NMR, 400 MHz, CDCl_3)



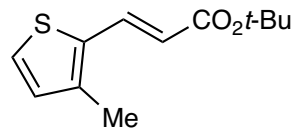
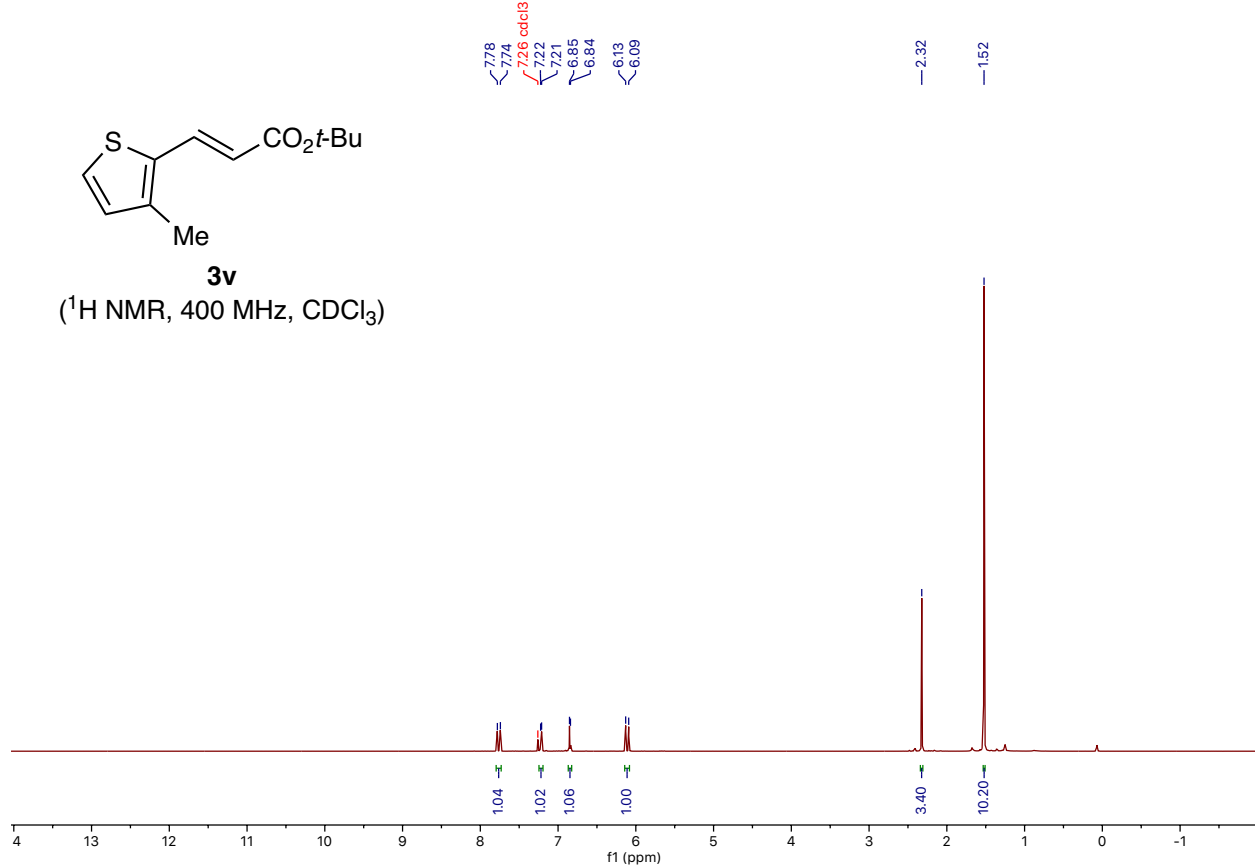
(^{13}C NMR, 100 MHz, CDCl_3)



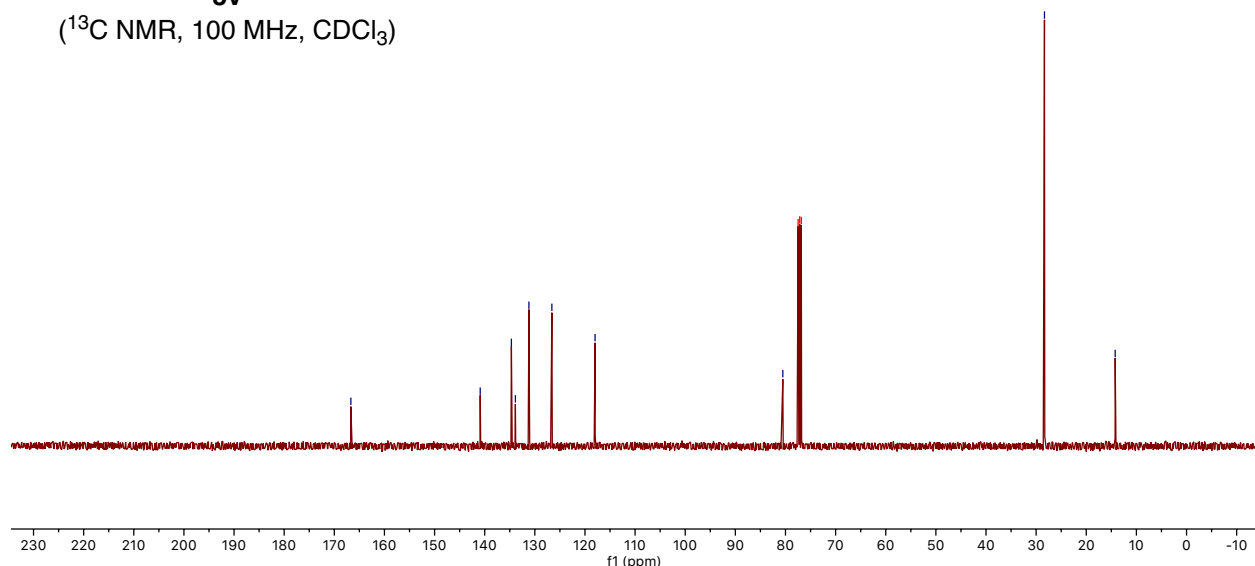


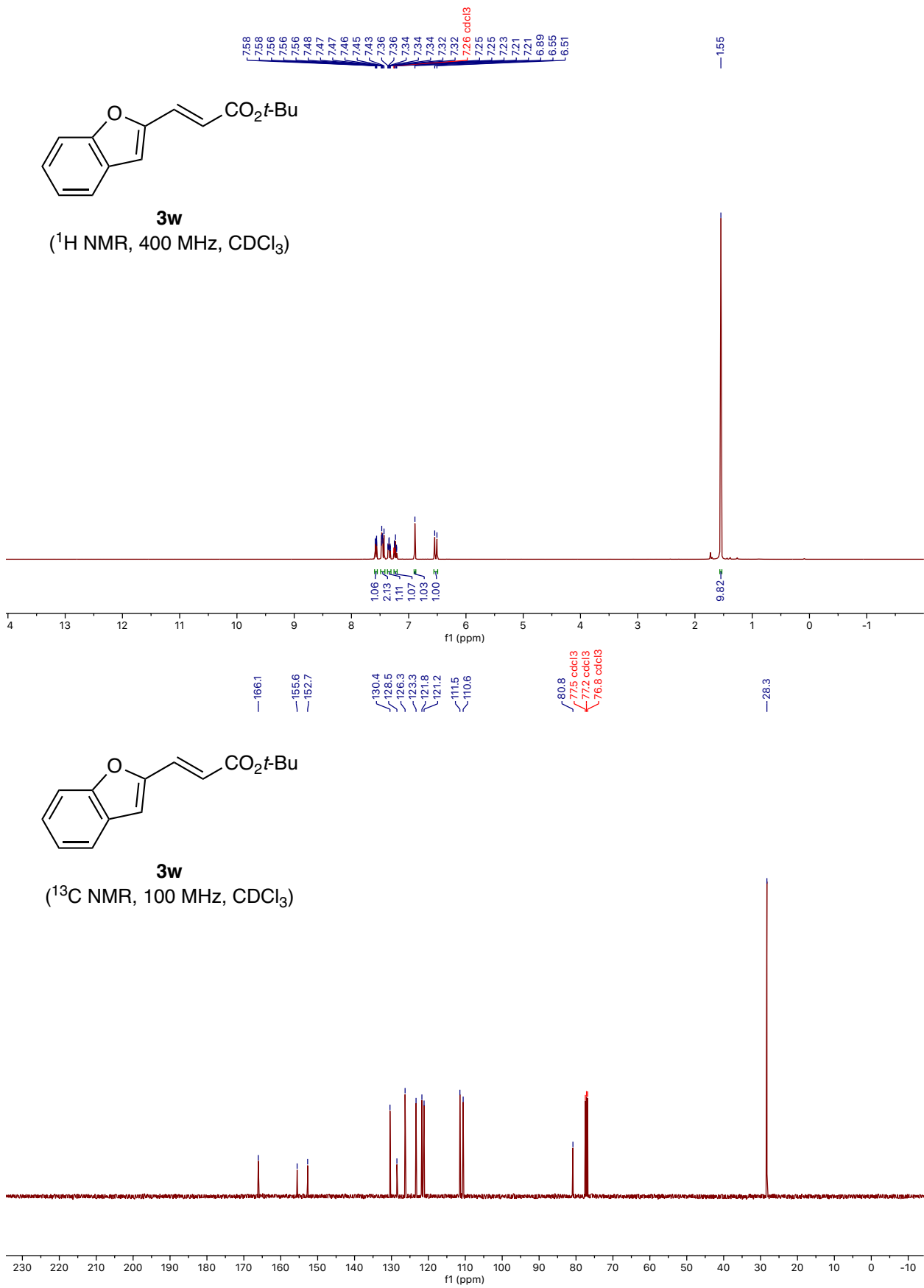


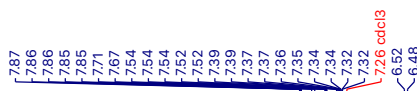
(^1H NMR, 400 MHz, CDCl_3)



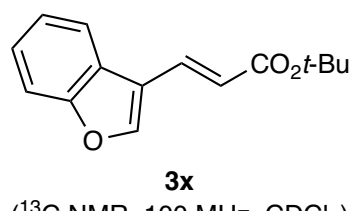
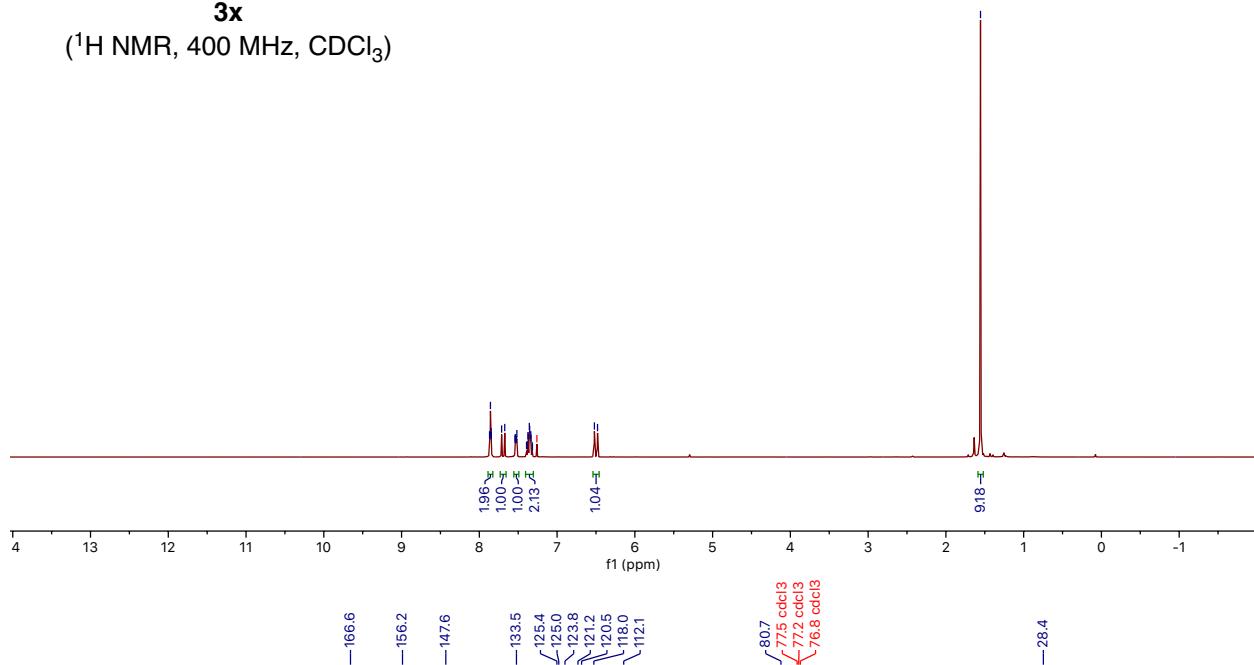
(^{13}C NMR, 100 MHz, CDCl_3)



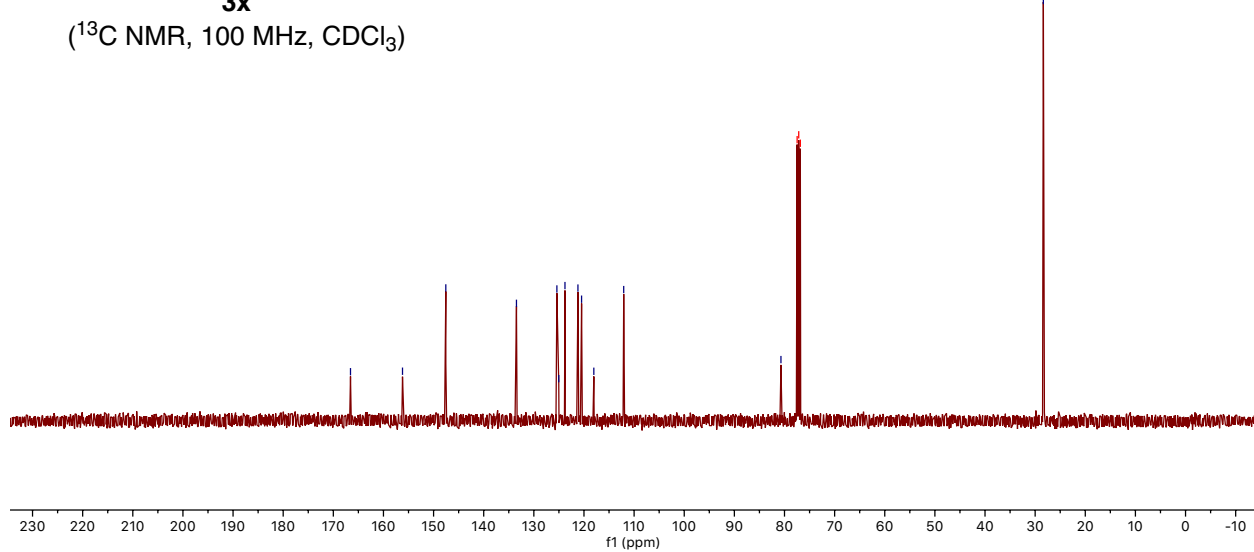


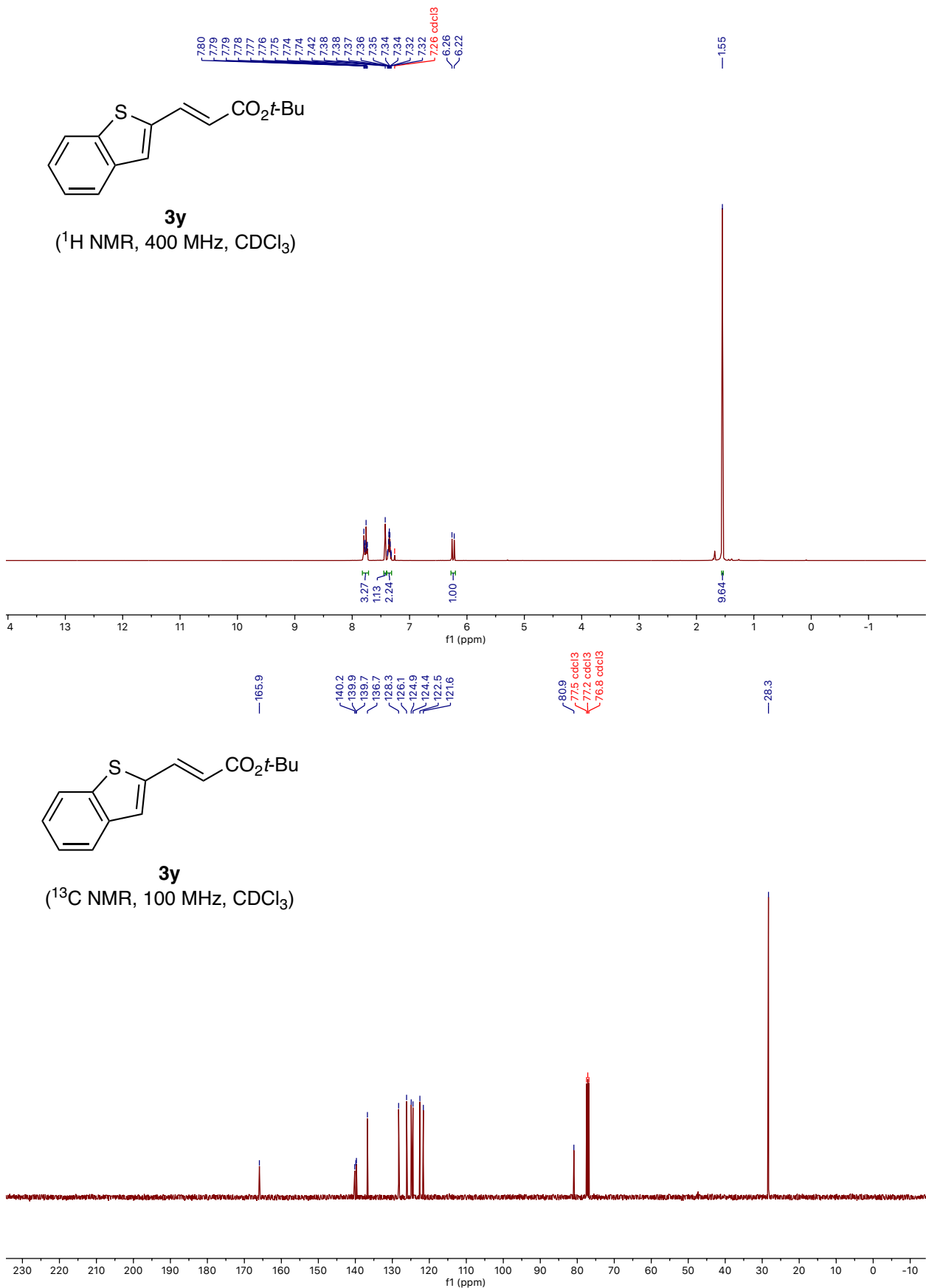


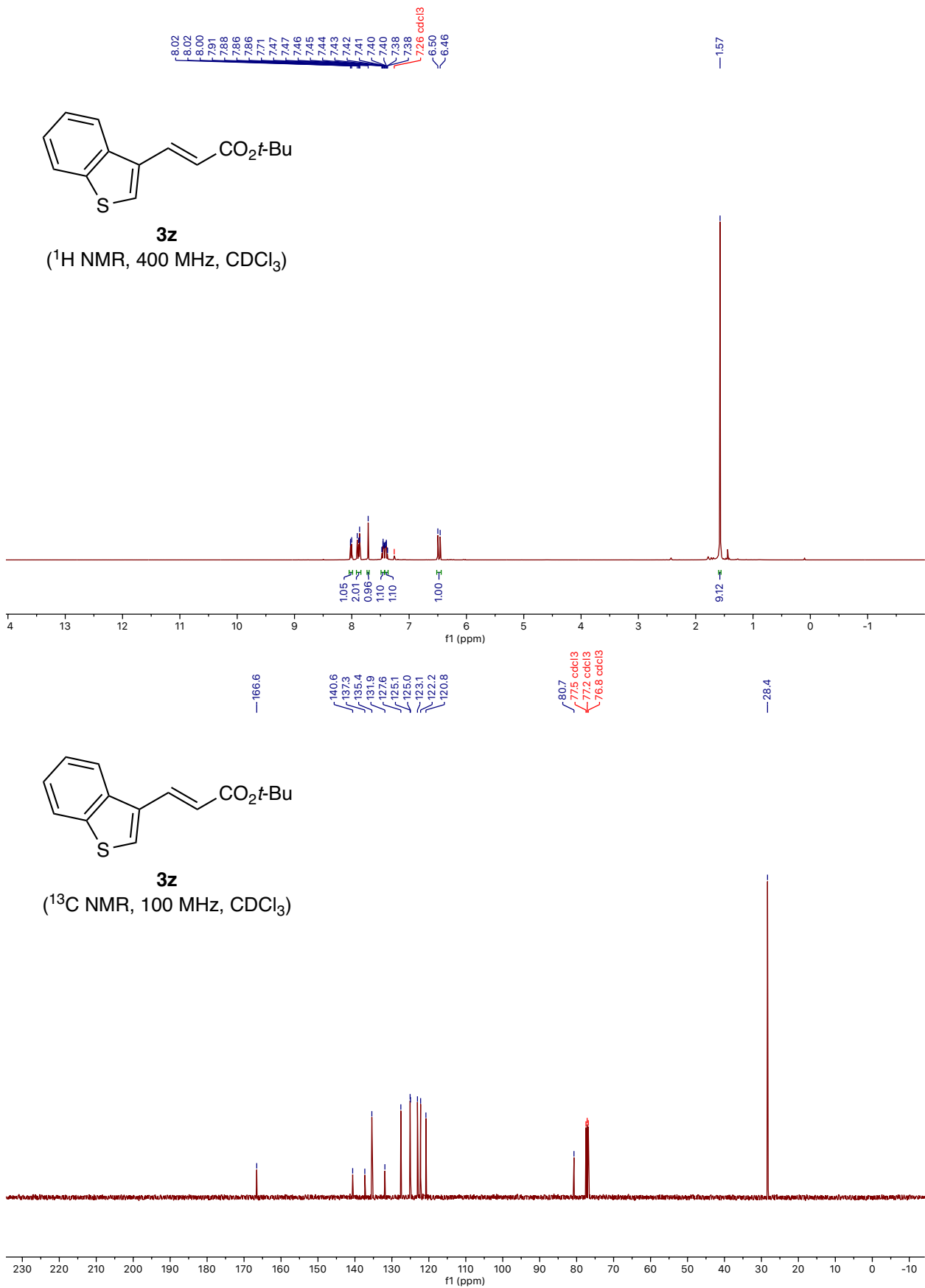
3x
(^1H NMR, 400 MHz, CDCl_3)

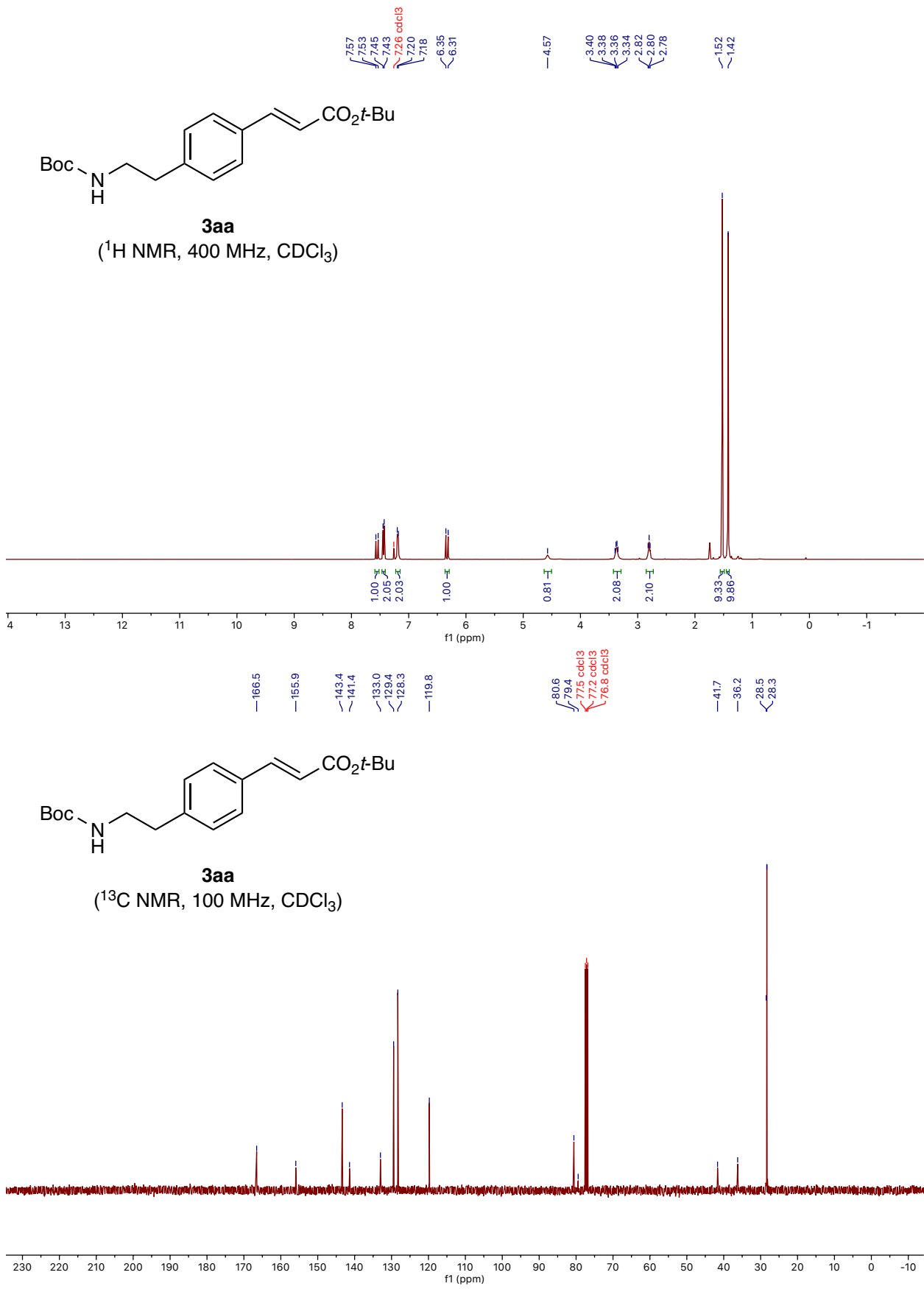


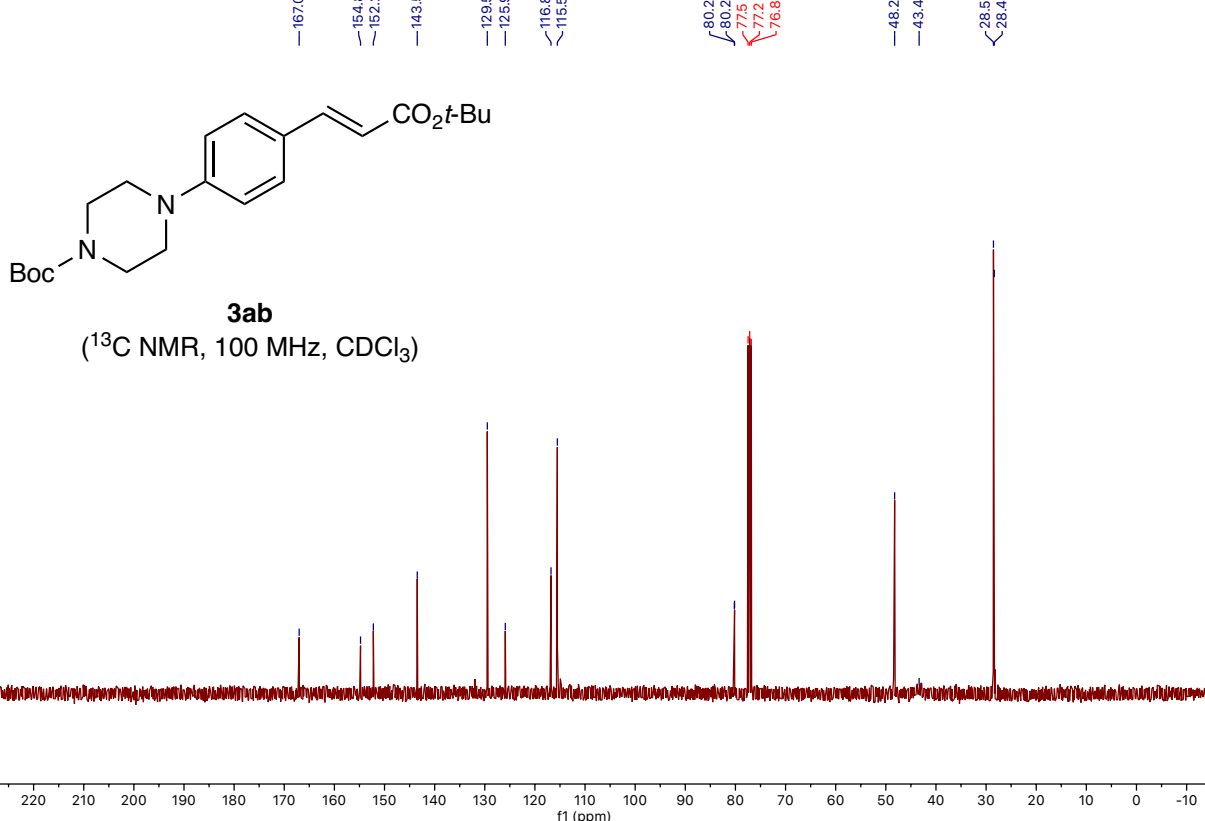
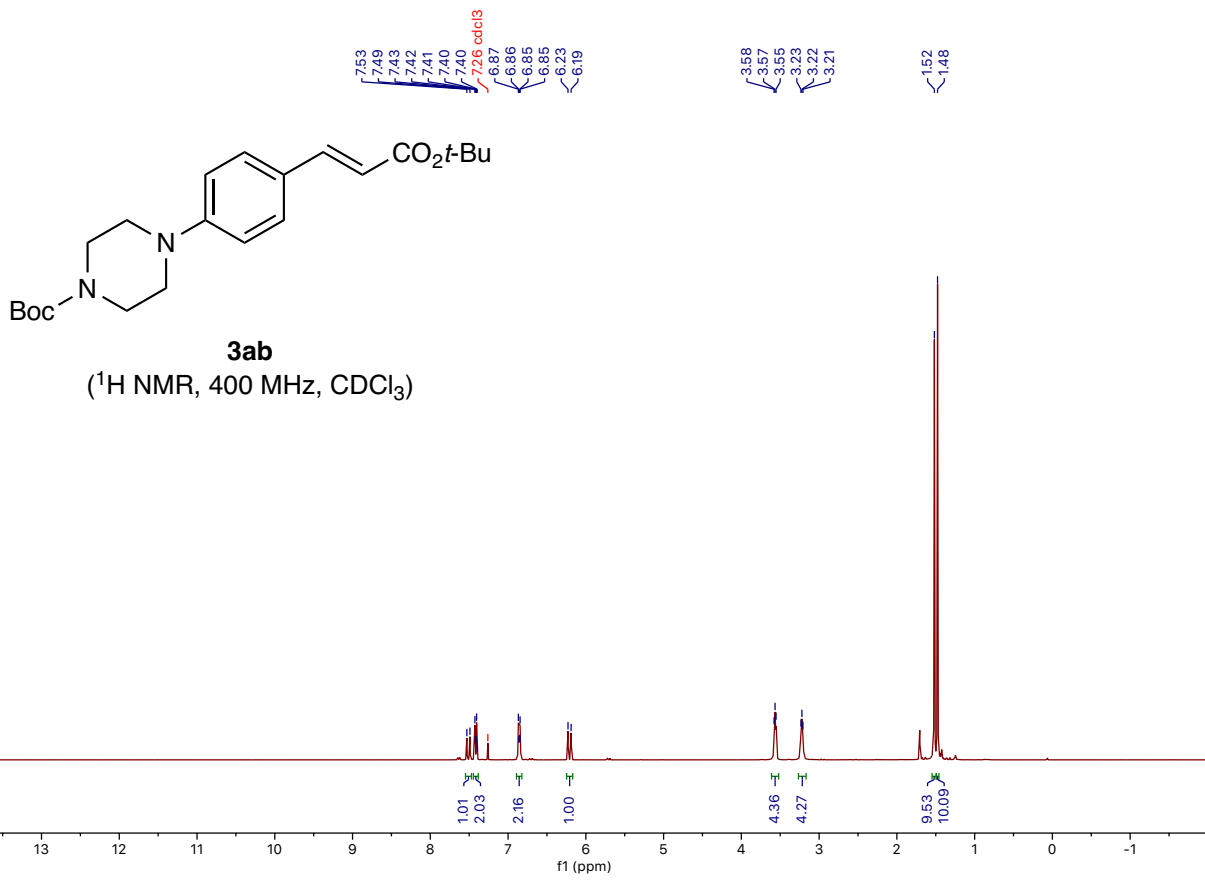
3x
(^{13}C NMR, 100 MHz, CDCl_3)

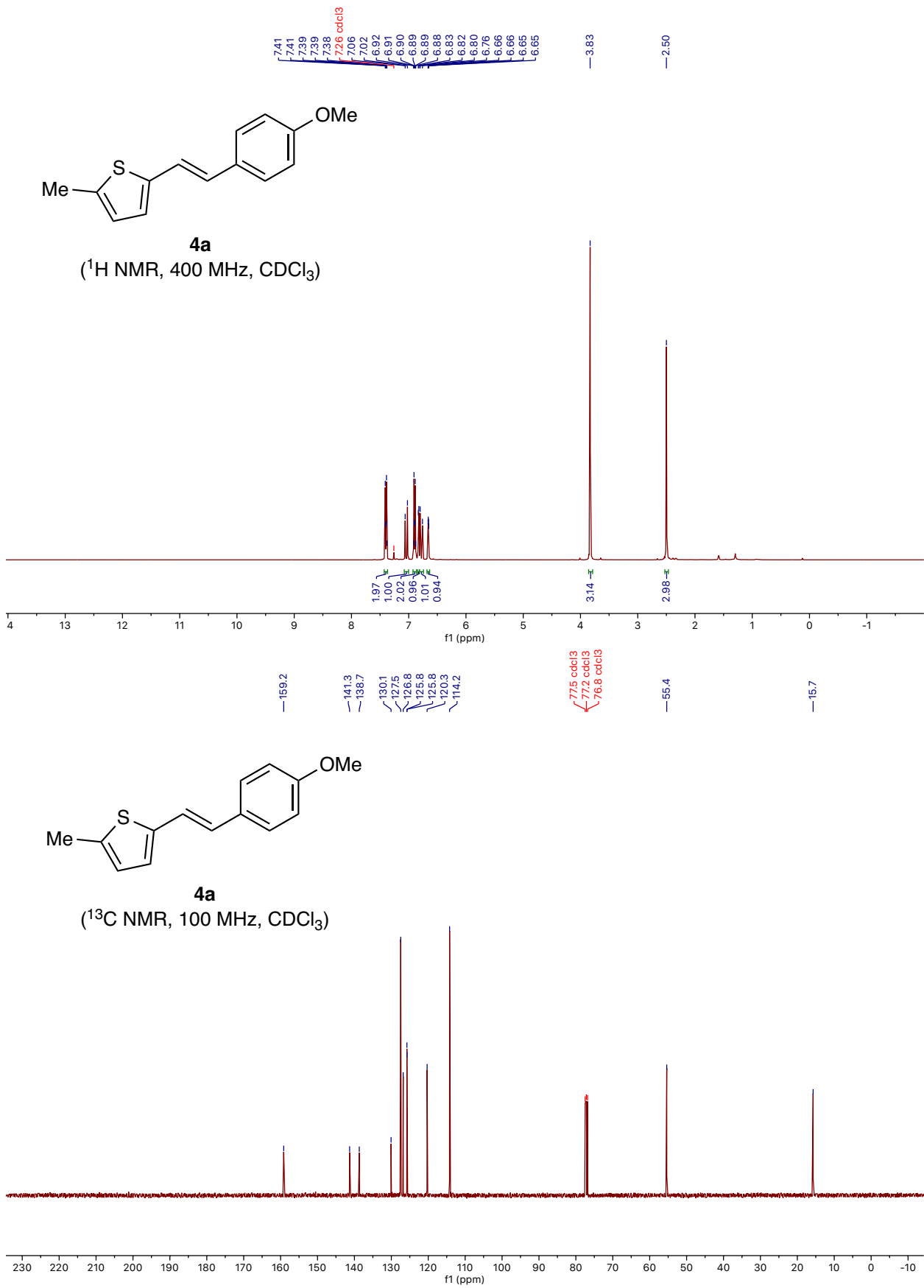


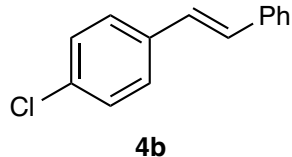




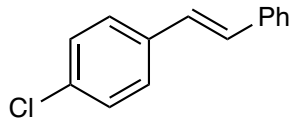
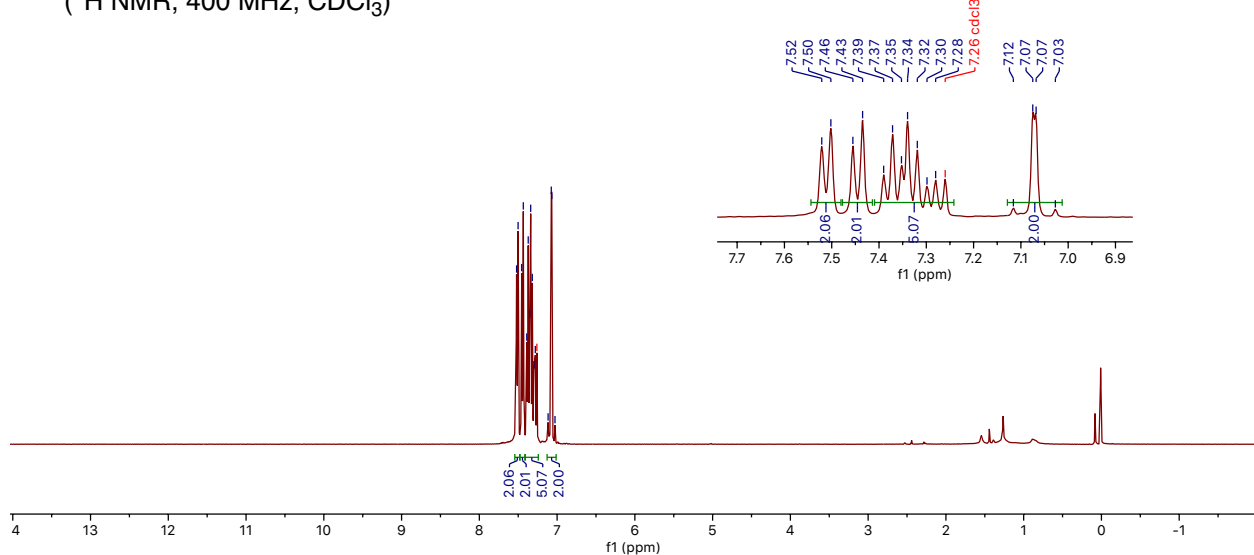




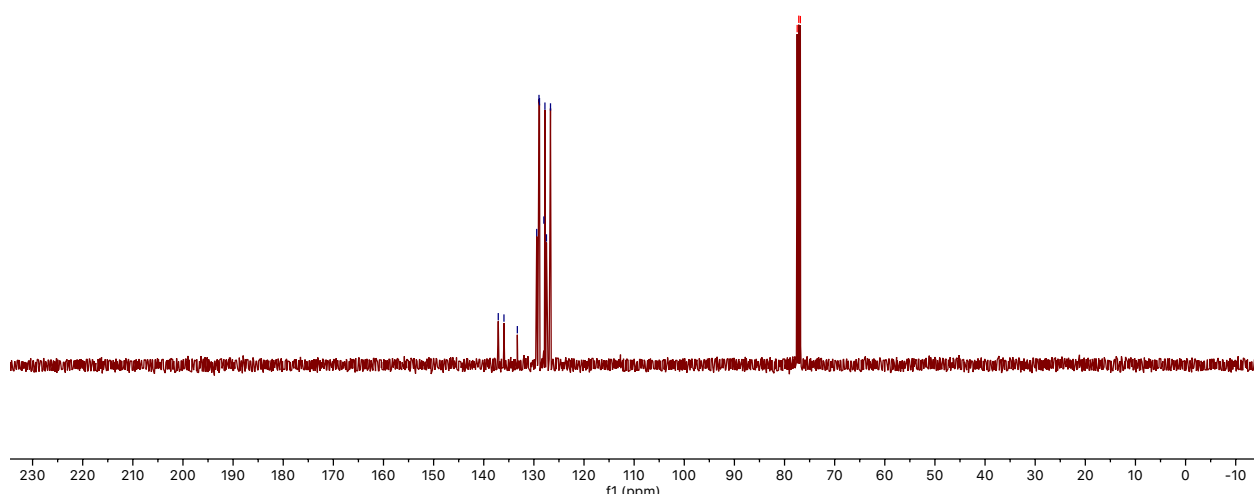


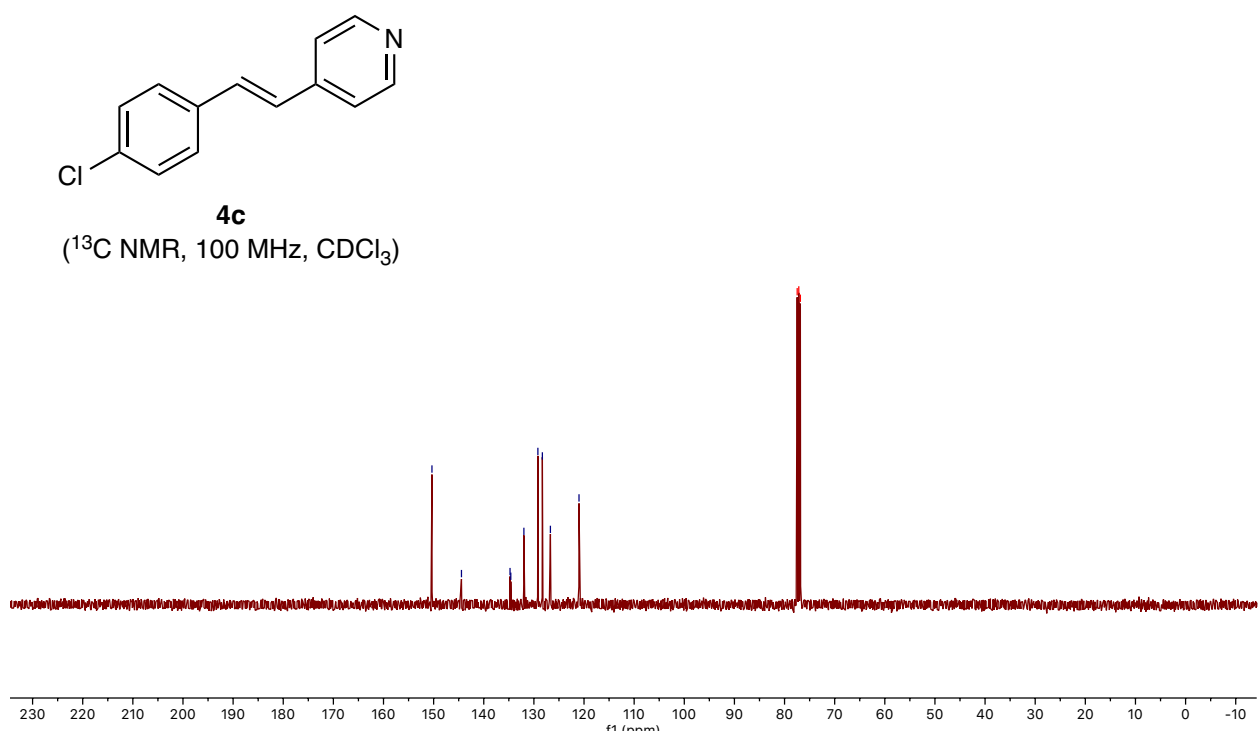
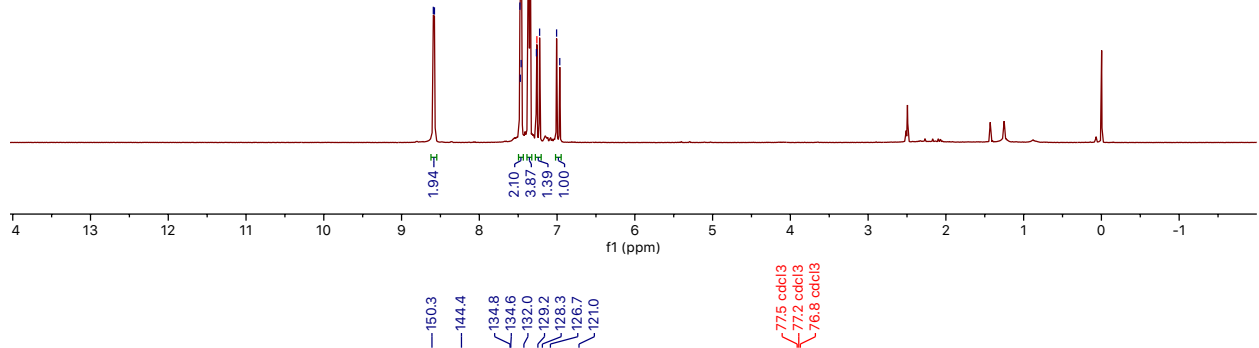
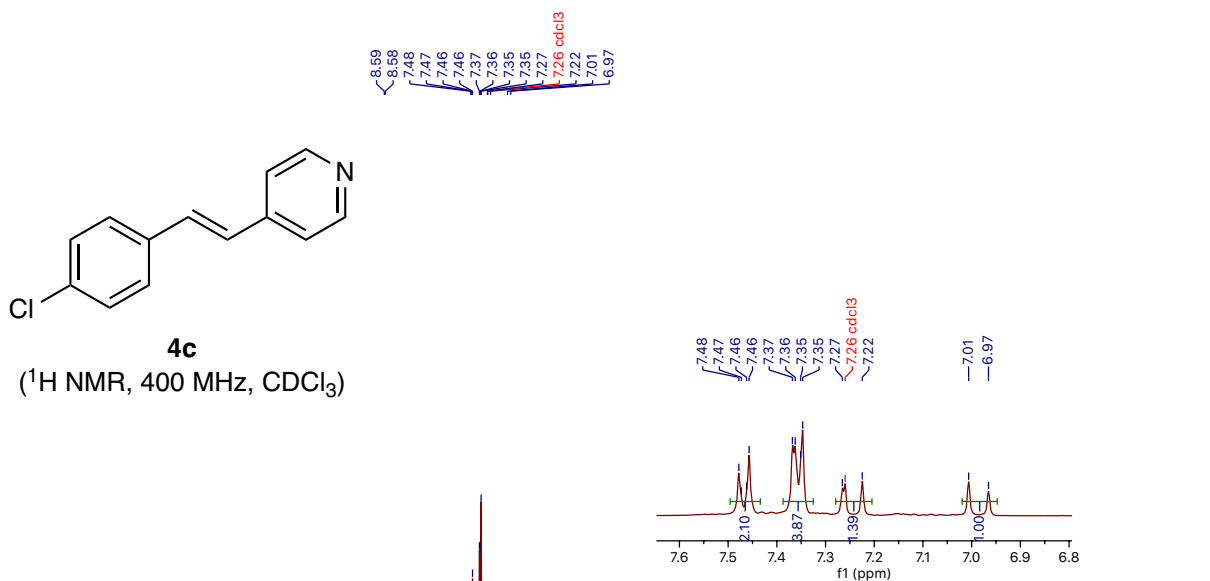


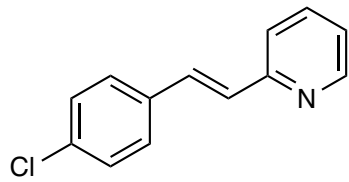
(^1H NMR, 400 MHz, CDCl_3)



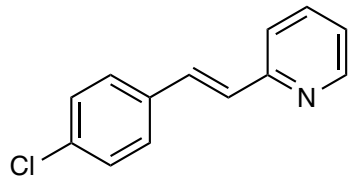
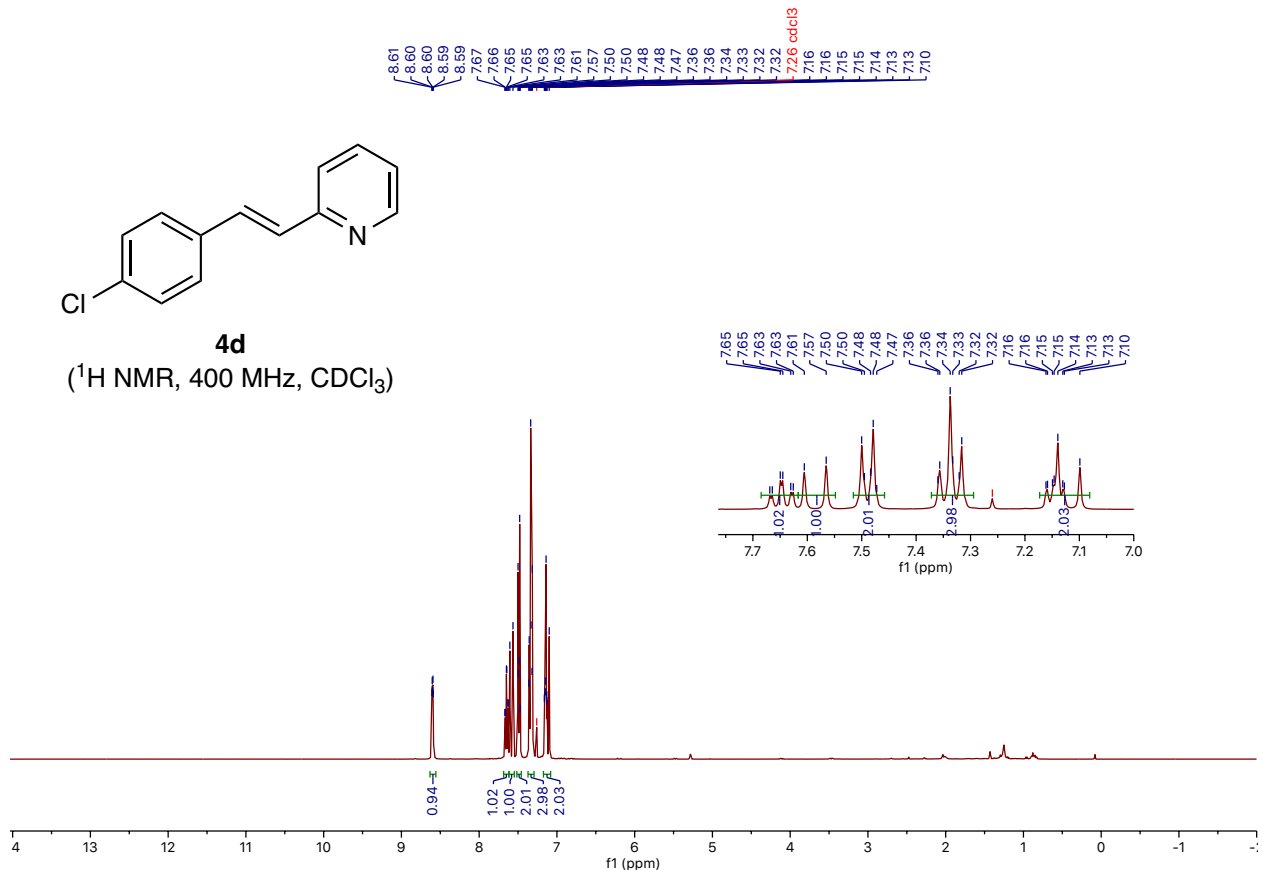
4b



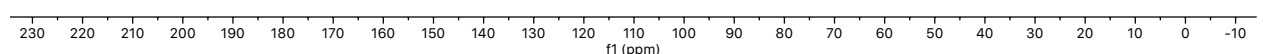


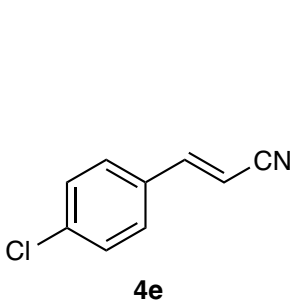


4d

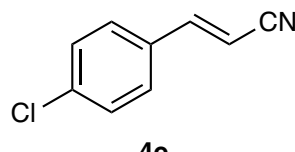
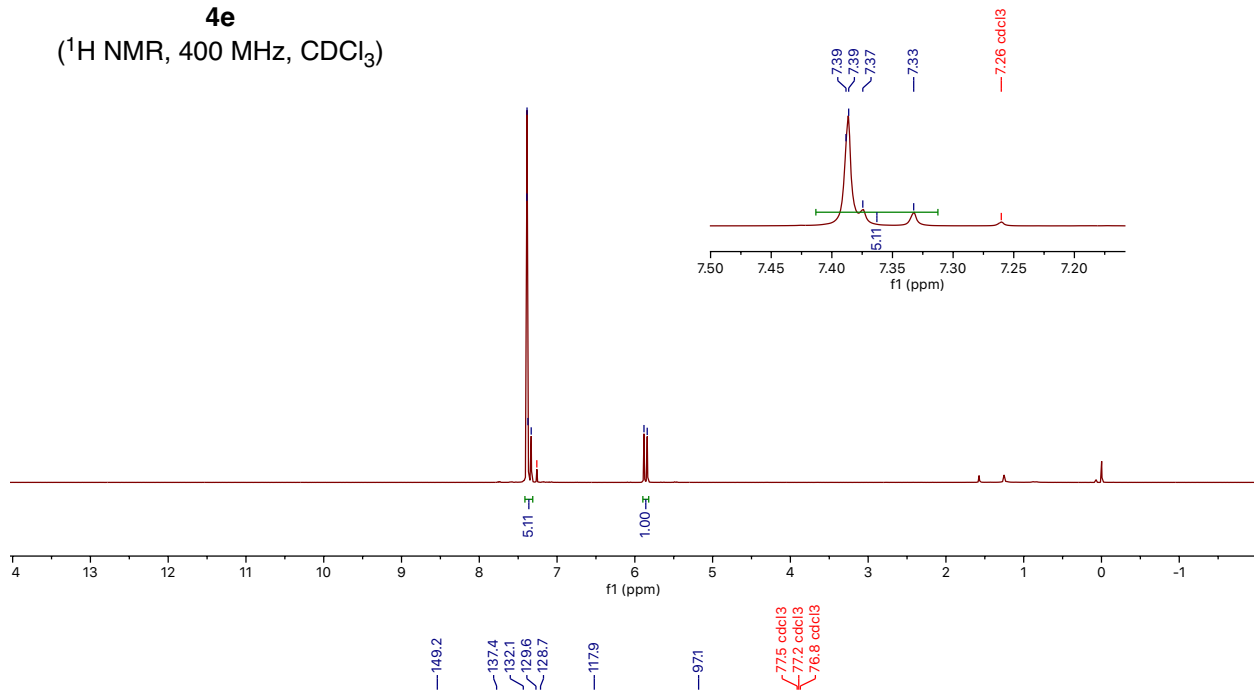


4d
(^{13}C NMR, 100 MHz, CDCl_3)

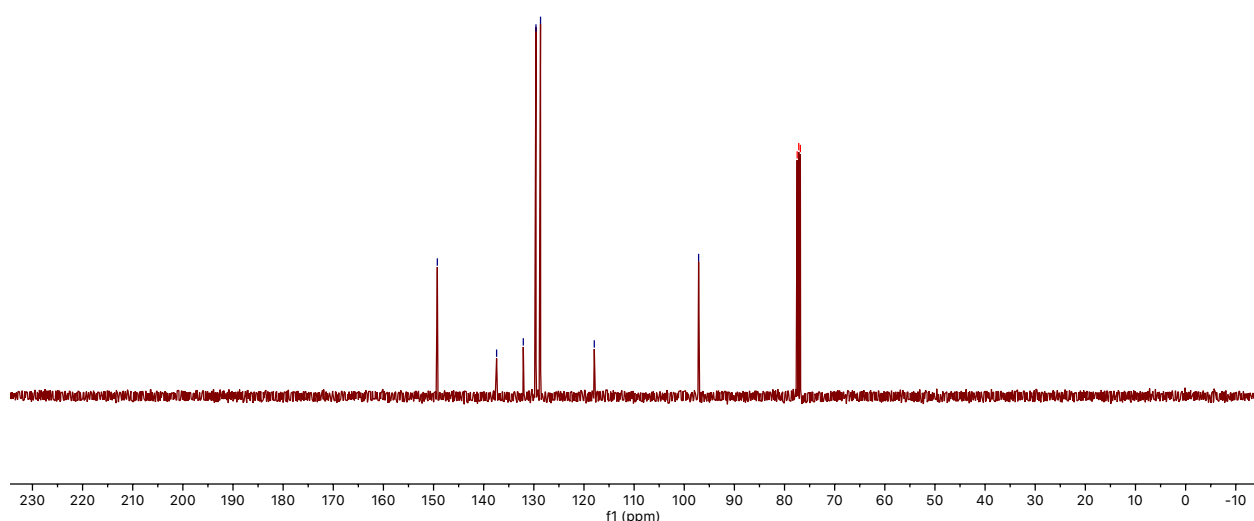


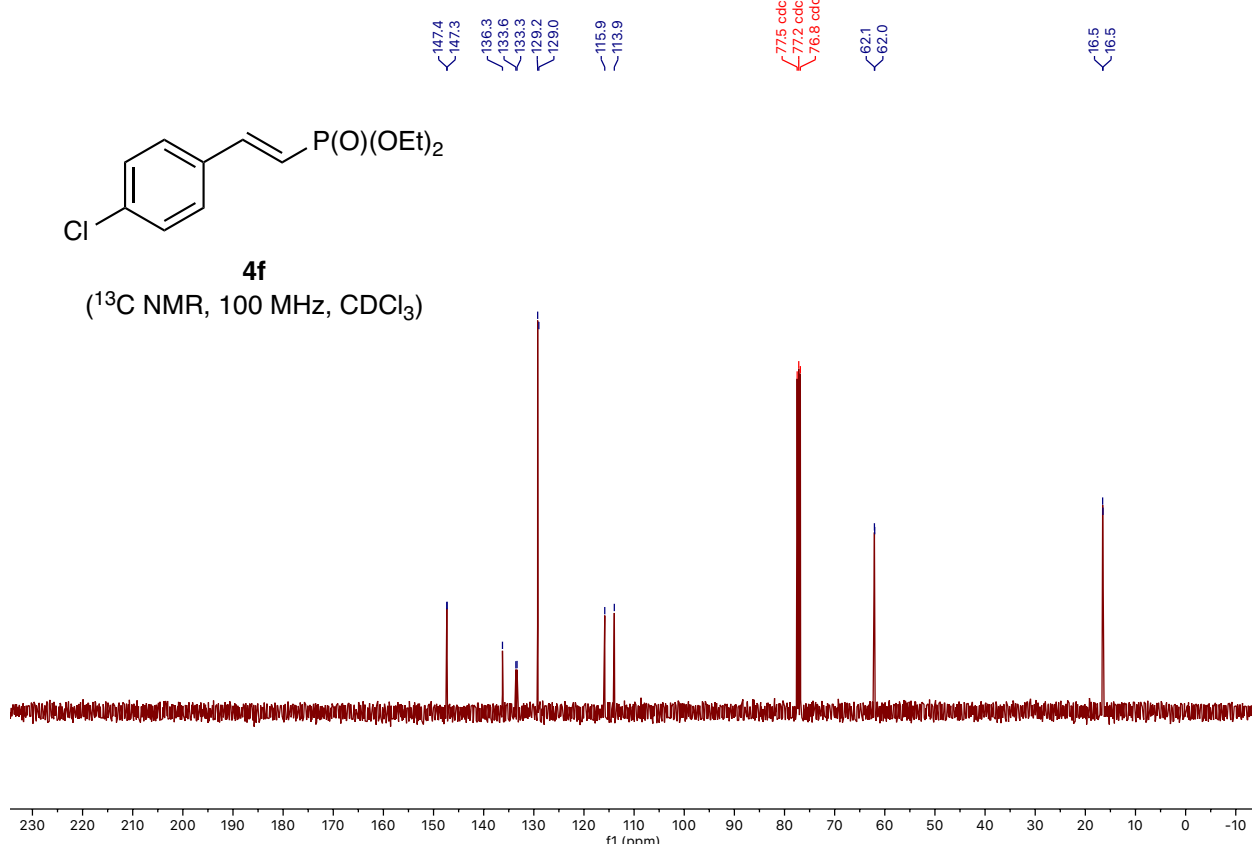
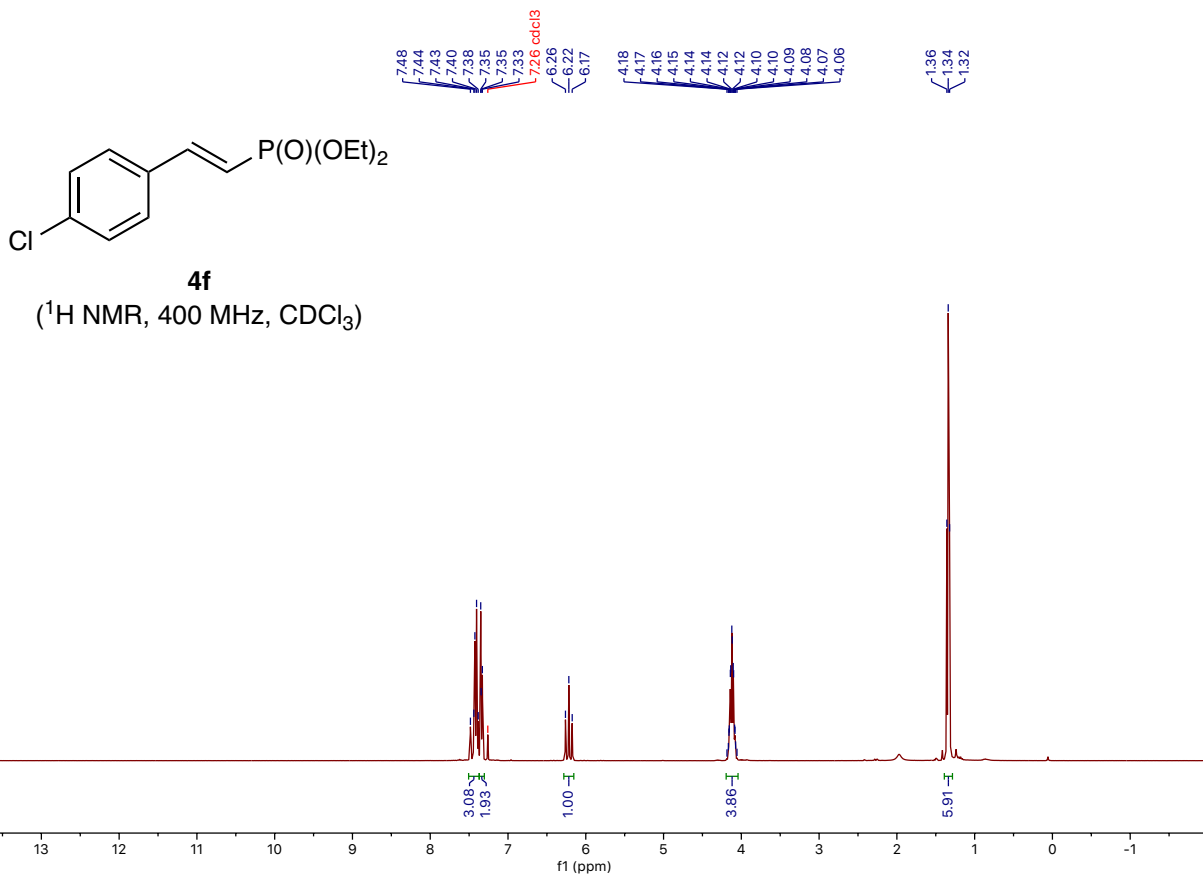


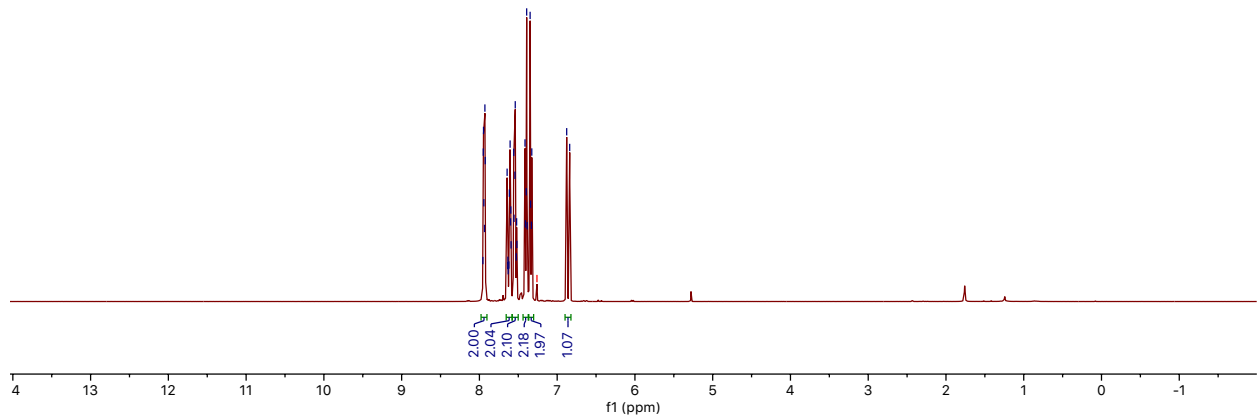
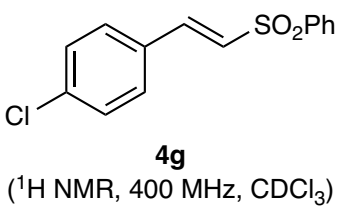
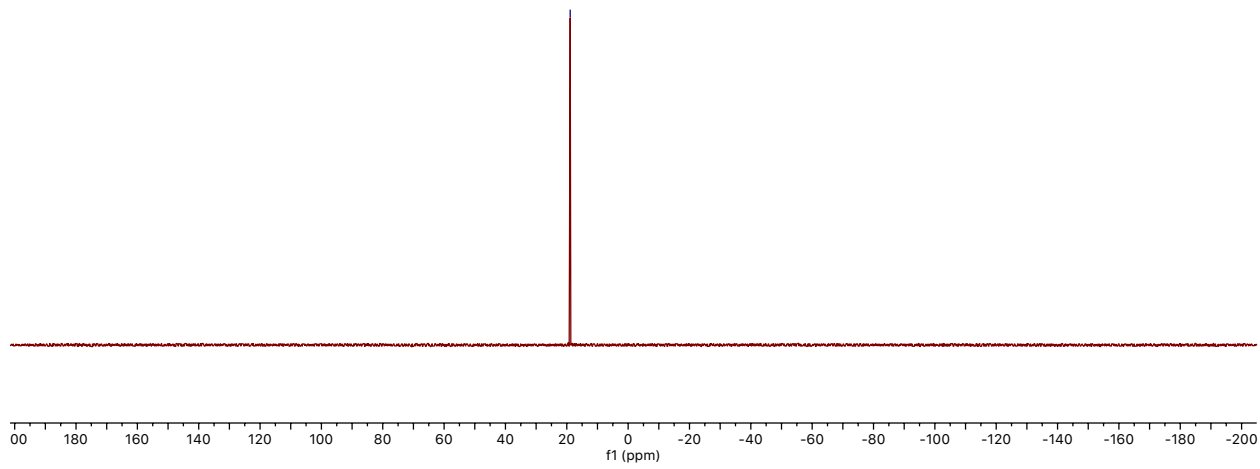
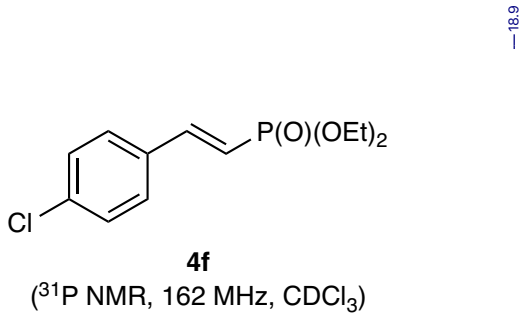
(^1H NMR, 400 MHz, CDCl_3)

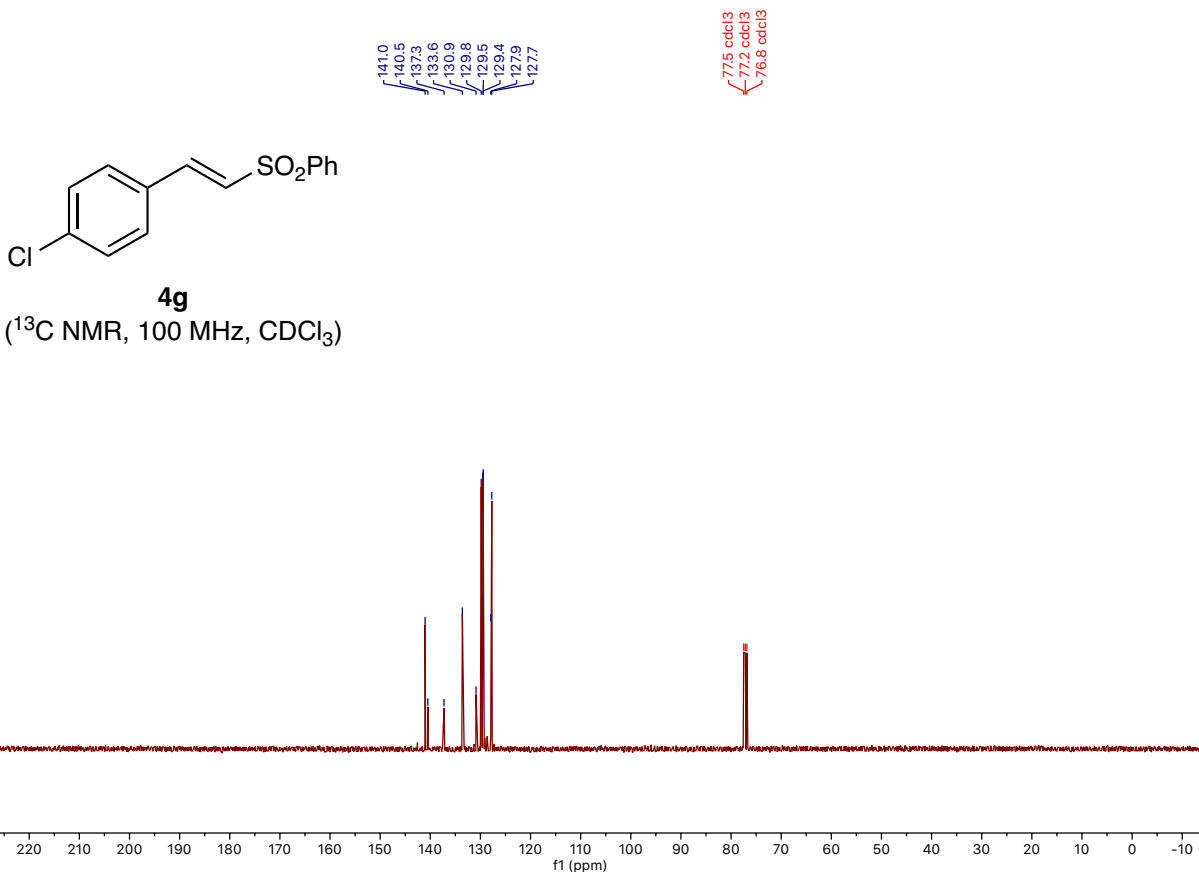


(^{13}C NMR, 100 MHz, CDCl_3)









References

51. M. J. Frisch, G. W. Trucks, H. B. Schlegel, G. E. Scuseria, M. A. Robb, J. R. Cheeseman, G. Scalmani, V. Barone, G. A. Petersson, H. Nakatsuji, X. Li, M. Caricato, A. V. Marenich, J. Bloino, B. G. Janesko, R. Gomperts, B. Mennucci, H. P. Hratchian, J. V. Ortiz, A. F. Izmaylov, J. L. Sonnenberg, D. Williams-Young, F. Ding, F. Lipparini, F. Egidi, J. Goings, B. Peng, A. Petrone, T. Henderson, D. Ranasinghe, V. G. Zakrzewski, J. Gao, N. Rega, G. Zheng, W. Liang, M. Hada, M. Ehara, K. Toyota, R. Fukuda, J. Hasegawa, M. Ishida, T. Nakajima, Y. Honda, O. Kitao, H. Nakai, T. Vreven, K. Throssell, J. A. Montgomery, Jr., J. E. Peralta, F. Ogliaro, M. J. Bearpark, J. J. Heyd, E. N. Brothers, K. N. Kudin, V. N. Staroverov, T. A. Keith, R. Kobayashi, J. Normand, K. Raghavachari, A. P. Rendell, J. C. Burant, S. S. Iyengar, J. Tomasi, M. Cossi, J. M. Millam, M. Klene, C. Adamo, R. Cammi, J. W. Ochterski, R. L. Martin, K. Morokuma, O. Farkas, J. B. Foresman, and D. J. Fox, Gaussian 16, Revision C.01, Gaussian, Inc., Wallingford CT (2016).
52. Y. Zhao, D. G. Truhlar, The M06 suite of density functionals for main group thermochemistry, thermochemical kinetics, noncovalent interactions, excited states, and transition elements: two new functionals and systematic testing of four M06-class functionals and 12 other functionals. *Theor. Chem. Account* **120**, 215–241 (2008).
53. F. Bobrowicz, W. Goddard III, “The Self-Consistent Field Equations for Generalized Valence Bond and Open-Shell Hartree-Fock Wave Functions” in *Methods of Electronic Structure Theory*, H. F. Schaefer, Ed., (Springer US, Boston, MA, 1977) vol. 3, pp. 79–127.

54. W. J. Hehre, R. Ditchfield, J. A. Pople, Self—Consistent Molecular Orbital Methods. XII. Further Extensions of Gaussian—Type Basis Sets for Use in Molecular Orbital Studies of Organic Molecules. *J. Chem. Phys.* **56**, 2257–2261 (2003).
55. S. Grimme, J. Antony, S. Ehrlich, H. Krieg, A consistent and accurate ab initio parametrization of density functional dispersion correction (DFT-D) for the 94 elements H-Pu. *J. Chem. Phys.* **132**, 154104 (2010).
56. J.-D. Chai, M. Head-Gordon, Long-range corrected hybrid density functionals with damped atom–atom dispersion corrections. *Phys. Chem. Chem. Phys.* **10**, 6615–6620 (2008).
57. A. V. Marenich, C. J. Cramer, D. G. Truhlar, Universal Solvation Model Based on Solute Electron Density and on a Continuum Model of the Solvent Defined by the Bulk Dielectric Constant and Atomic Surface Tensions. *J. Phys. Chem. B* **113**, 6378–6396 (2009).
58. J. H. Harenberg, N. Weidmann, K. Karaghiosoff, P. Knochel, Continuous Flow Sodiation of Substituted Acrylonitriles, Alkenyl Sulfides and Acrylates. *Angew. Chem. Int. Ed.* **60**, 731–735 (2021).
59. T. Sperger, C. K. Stirner, F. Schoenebeck, Bench-Stable and Recoverable Palladium(I) Dimer as an Efficient Catalyst for Heck Cross-Coupling. *Synthesis* **49**, 115–120 (2016).
60. E. A. B. Kantchev, G.-R. Peh, C. Zhang, J. Y. Ying, Practical Heck–Mizoroki Coupling Protocol for Challenging Substrates Mediated by an N-Heterocyclic Carbene-Ligated Palladacycle. *Org. Lett.* **10**, 3949–3952 (2008).
61. R. Beesam, D. R. Nareddula, Pd and Ni complexes of a novel vinylidene β -diketimine ligand: Their application as catalysts in Heck coupling and alkyne trimerization. *Appl. Organometal. Chem.* **31**, e3696 (2017).
62. S. D. Bull, S. G. Davies, David. J. Fox, M. Gianotti, P. M. Kelly, C. Pierres, E. D. Savory, A. D. Smith, Asymmetric synthesis of β -pyridyl- β -amino acid derivatives. *J. Chem. Soc., Perkin Trans. 1*, 1858–1868 (2002).
63. A. Maji, O. Singh, S. Singh, A. Mohanty, P. K. Maji, K. Ghosh, Palladium-Based Catalysts Supported by Unsymmetrical XYC–1 Type Pincer Ligands: C5 Arylation of Imidazoles and Synthesis of Octinoxate Utilizing the Mizoroki–Heck Reaction. *Eur. J. Inorg. Chem.* **2020**, 1596–1611 (2020).
64. F. Villalba, A. C. Albéniz, Non-Chelate-Assisted Palladium-Catalyzed Aerobic Oxidative Heck Reaction of Fluorobenzenes and Other Arenes: When Does the C–H Activation Need Help? *Adv. Synth. Catal.* **363**, 4795–4804 (2021).
65. A. Gupta, M. L. Condakes, Thermodynamic Understanding of an Aza-Michael Reaction Enables Five-Step Synthesis of the Potent Integrin Inhibitor MK-0429. *J. Org. Chem.* **86**, 17523–17527 (2021).
66. X. Wang, L. Sun, M. Wang, G. Maestri, M. Malacria, X. Liu, Y. Wang, L. Wu, C–I Selective Sonogashira and Heck Coupling Reactions Catalyzed by Aromatic Triangular Tri-palladium. *Eur. J. Org. Chem.* **2022**, e202200009 (2022).
67. I. Peñafiel, I. M. Pastor, M. Yus, Heck–Matsuda Reactions Catalyzed by a Hydroxyalkyl-Functionalized NHC and Palladium Acetate. *Eur. J. Org. Chem.* **2012**, 3151–3156 (2012).
68. S. G. Davies, A. W. Mulvaney, A. J. Russell, A. D. Smith, Parallel synthesis of homochiral β -amino acids. *Tetrahedron: Asymmetry* **18**, 1554–1566 (2007).
69. D. A. Evans, S. P. Tanis, D. J. Hart, Convergent total synthesis of (\pm)-colchicine and (\pm)-desacetamidoisocolchicine. *J. Am. Chem. Soc.* **103**, 5813–5821 (1981).
70. R. M. Archer, M. Hutchby, C. L. Winn, J. S. Fossey, S. D. Bull, A chiral ligand mediated aza-conjugate addition strategy for the enantioselective synthesis of β -amino esters that contain hydrogenolytically sensitive functionality. *Tetrahedron* **71**, 8838–8847 (2015).

71. J.-F. Paquin, C. R. J. Stephenson, C. Defieber, E. M. Carreira, Catalytic Asymmetric Synthesis with Rh–Diene Complexes: 1,4-Addition of Arylboronic Acids to Unsaturated Esters. *Org. Lett.* **7**, 3821–3824 (2005).
72. W. Fu, Y. Feng, Z. Fang, Q. Chen, T. Tang, Q. Yu, T. Tang, Zeolite Y nanosheet assembled palladium catalysts with high catalytic activity and selectivity in the vinylation of thiophenes. *Chem. Commun.* **52**, 3115–3118 (2016).
73. J. Qu, C.-T. Cao, C. Cao, Determining the excited-state substituent constants of furyl and thienyl groups. *J. Phys. Org. Chem.* **31**, e3799 (2018).
74. Y. Wang, J. Chen, J. Yang, Z. Jiao, C.-Y. Su, Elaborating E/Z-Geometry of Alkenes via Cage-Confining Arylation Catalysis of Terminal Olefins. *Angew. Chem. Int. Ed.* **62**, e202303288 (2023).
75. C.-T. Cao, L. Yan, C. Cao, Determination and application of the excited-state substituent constants of pyridyl and substituted phenyl groups. *J. Phys. Org. Chem.* **34**, e4246 (2021).
76. P. J. Black, M. G. Edwards, J. M. J. Williams, Borrowing Hydrogen: Indirect “Wittig” Olefination for the Formation of C–C Bonds from Alcohols. *Eur. J. Org. Chem.* **2006**, 4367–4378 (2006).
77. Y. Xu, M. T. Flavin, Z.-Q. Xu, Preparation of New Wittig Reagents and Their Application to the Synthesis of α,β -Unsaturated Phosphonates. *J. Org. Chem.* **61**, 7697–7701 (1996).
78. Y. Fang, D. Xu, Y. Yu, R. Tang, S. Dai, Z. Wang, W. Zhang, Controlled Synthesis of β -Keto Sulfones and Vinyl Sulfones under Electrochemical Oxidation. *Eur. J. Org. Chem.* **2022**, e202200091 (2022).
79. G. Cristalli, E. Camaioni, S. Vittori, R. Volpini, P. A. Borea, A. Conti, S. Dionisotti, E. Ongini, A. Monopoli, 2-Aralkynyl and 2-Heteroalkynyl Derivatives of Adenosine-5'-N-Ethyluronamide as Selective A2a Adenosine Receptor Agonists. *J. Med. Chem.* **38**, 1462–1472 (1995).
80. V. D. Möschwitzer, B. M. Kariuki, J. E. Redman, Asymmetric synthesis of aminopyrimidine and cyclic guanidine amino acids. *Tetrahedron Letters* **54**, 4526–4528 (2013).
81. N. Robert, C. Hoarau, S. Célanire, P. Ribéreau, A. Godard, G. Quéguiner, F. Marsais, Efficient and fast Heck vinylation of 2-bromo-6-methyl pyridines with methylacrylate. Application to the synthesis of 6-methyl cyclopenta[b]pyridinone. *Tetrahedron* **61**, 4569–4576 (2005).
82. Y. Akita, T. Noguchi, M. Sugimoto, A. Ohta, Cross-coupling reaction of chloropyrazines with ethylenes. *J. Heterocyclic Chem.* **23**, 1481–1485 (1986).
83. D. S. Palacios, E. Meredith, T. Kawanami, C. Adams, X. Chen, V. Darsigny, E. Geno, M. Palermo, D. Baird, G. Boynton, S. A. Busby, E. L. George, C. Guy, J. Hewett, L. Tierney, S. Thigale, W. Weihofen, L. Wang, N. White, M. Yin, U. A. Argikar, Structure based design of nicotinamide phosphoribosyltransferase (NAMPT) inhibitors from a phenotypic screen. *Bioorg. Med. Chem. Lett.* **28**, 365–370 (2018).
84. Á. P. Molnár Attila, Efficient Heterogeneous Palladium-Montmorillonite Catalysts for Heck Coupling of Aryl Bromides and Chlorides. *Synlett* **2006**, 3130–3134 (2006).
85. K. L. Wilson; J. Murray, H. F. Sneddon, C. Jamieson, A. J. B. Watson, Dimethylisosorbide (DMI) as a Bio-Derived Solvent for Pd-Catalyzed Cross-Coupling Reactions. *Synlett* **29**, 2293–2297 (2018).
86. J. P. Perdew, K. Burke, M. Ernzerhof, Generalized Gradient Approximation Made Simple. *Phys. Rev. Lett.* **77**, 3865–3868 (1996).
87. C. Adamo, V. Barone, Toward reliable density functional methods without adjustable parameters: The PBE0 model. *J. Chem. Phys.* **110**, 6158–6170 (1999).